# Balancing water availability and water demand in the Blue Nile: A case study of *Gumara* watershed in Ethiopia

**Dissertation**

Zur

Erlangung des Doktorgrades (Dr. rer. nat.)

Der

Mathematisch-Naturwissenschaftlichen Fakultät

Der

Rheinischen Friedrich-Wilhelms-Universität Bonn

vorgelegt von

*Sisay Demeku Derib*

*Aus*

*Arsi-Sire, Ethiopia*

Bonn, Dezember 2013

Angefertigt mit Genehmigung der Mathematisch-Naturwissenschaftlichen Fakultät der Rheinischen Friedrich-Wilhelms-Universität Bonn

1. Gutachter: Prof. Dr. B. Diekkrüger

2. Gutachter: Prof. Dr.  J. Bogardi

Tag der Promotion:  31.03.2014

Erscheinungsjahr: 2014

**DEDICATION**

- The well-being of the Nile basin society
- The wise females that are always at my side: my wife (*Hiwot Yirgu*), my mother (*Zewude Gashu*) and my little daughters (*Meklit and Etsubdink*).

**SUMMARY**

Ethiopia suffers from economic water scarcity that makes its water utilization difficult. In-depth understanding of the hydrological processes is important for balancing availability and demand. As part of this basin-wide and national concern, this study examines the water balance and water availability on farm and watershed scales in different scenarios. The objectives of the study were (1) to evaluate water use and water productivity of a small-scale irrigation scheme, (2) to evaluate methods for filling gaps in climatic data, (3) to adopt the Soil and Water Assessment Tool (SWAT) hydrological model for modeling hydrological processes using different modeling setups, and (4) to simulate water demand and water stress status for a period up to 2050 using different land-use and demographic scenarios. The *Gumara* watershed (1520 $km^2$), a tributary of Lake *Tana* and source of the Blue Nile in Ethiopia, was selected for this study.

A case study at a small-scale irrigation scheme shows that there was high water loss during water conveyance and application. At the same time, water stress was observed during irrigation at the scheme level, as the applied water did not match the water needs of different crops.

Environmental modeling requires complete climate data sets, which are rarely available. Therefore, different gap-filling methods were applied and tested. Considering data from neighboring climate stations, the methods arithmetic mean and coefficient of correlation weighting methods gave better daily rainfall estimation than the normal ratio and inverse distance weighting methods. Multiple linear regression methods performed well when filling daily air temperature gaps using data from neighboring stations. After seasonal categorization of daily data and optimization of parameters, procedures using maximum and minimum temperature for simulating solar radiation and relative humidity gave promising performances.

For process analysis, SWAT was applied for the watershed with an acceptable performance when simulating river flow. The effect of data availability on model performance was analyzed using different numbers of climate stations. Using four and six stations resulted in better SWAT water flow modeling performance as compared to two stations. Penman-Monteith and Hargreaves procedures for potential evaporation calculation resulted in comparable river flow modeling in SWAT. Therefore, the Hargreaves method that needs only air temperature can be used for modeling when other climatic data are not available.

Selected watershed management practices shift surface runoff to sub-surface and groundwater flows. An irrigation project planned in the watershed and the watershed management practices shift surface discharge to base flow and evapotranspiration. It will be hard to satisfy the basic human water requirements in 2050 if the existing water management and water productivity conditions pertain. Better green water management and non-consumptive water use options (e.g. hydro power, fishery) can minimize the blue water stress at the Nile basin level.

## Zusammenfassung

Äthiopien leidet unter ökonomischer Wasserknappheit, was die Wassernutzung erschwert. Dieses stellt sowohl für das untersuchte Wassereinzugsgebiet als auch für das Land ein großes Problem dar. Aus diesem Grund ist ein vertieftes Verständnis der hydrologischen Prozesse für die Abwägung der Wasserverfügbarkeit mit dem Wasserbedarf von hoher Bedeutung. Vor diesem Hintergrund untersucht diese Studie den Wasserhaushalt und die Wasserverfügbarkeit von der lokalen (Farm) bis zur Wassereinzugsskala unter Berücksichtigung verschiedener Szenarien mit folgenden Zielen: (1) Bewertung der Wassernutzung und -produktivität in einem kleinbäuerlichen Bewässerungssystem, (2) Bewertung von Methoden zur Ergänzung von Lücken in Klimadaten, (3) Anwendung des hydrologischen Soil and Water Assessment Tool (SWAT) für die Modellierung der hydrologischen Prozesse des Einzugsgebiets unter Berücksichtigung verschiedener Modellkonfigurationen und (4) Simulation von Wasserbedarf und Wasserstress für den Zeitraum bis 2050 mit verschiedenen Landnutzungs- und demographischen Szenarien. Das *Gumara*-Einzugsgebiet (1520 $km^2$), ein Zufluss zum *Tanasee* und Ursprung des Blauen Nils in Äthiopien, wurde für diese Studie ausgewählt.

Eine Fallstudie in einem kleinbäuerlichen Bewässerungssystem zeigt einen hohen Wasserverlust während des Wassertransports und der Wassernutzung. Gleichzeitig wurde Wasserstress während des Bewässerungszeitraums beobachtet, da die ausgebrachte Wassermenge dem Wasserbedarf der verschiedenen Anbaupflanzen nicht entsprach.

Umweltmodellierung bedarf vollständiger Datensätze, die jedoch selten verfügbar sind. Daher wurden verschiedene Methoden angewandt und getestet mit denen die Datenlücken geschlossen werden können. Die Methoden arithmetisches Mittel sowie Korrelationskoeffizienten mit Gewichtung ergaben bessere tägliche Niederschlagsprognosen als die Methoden gewichtete Mittelwerte (normal ratio) und inverse Distanzgewichtung (inverse distance weighting). Lücken in Temperaturdaten können gut aus den Daten benachbarter Stationen mittels multipler linearer Regressionsmethoden geschlossen werden. Mit einer saisonalen Parametrisierung kann aus den Maximum- und Minimumtemperaturen die Solarstrahlung und die relativer Luftfeuchtigkeit abgeleitet werden.

Für die Simulation der hydrologischen Prozesse und des Abflusses wurde SWAT erfolgreich eingesetzt. Die Auswirkung der Datenverfügbarkeit auf die Modellgüte wurde untersucht, indem unterschiedliche Anzahlen von Klimastationen berücksichtigt wurden. Vier bzw. sechs Stationen ergeben eine bessere Simulation des Abflusses verglichen mit zwei Stationen. Der Vergleich der Berechnung der potentiellen Verdunstung nach Penman-Monteith und nach Hargreaves resultiert in vergleichbaren Simulationen des Abflusses mit SWAT. Daher kann die Hargreaves Methode, die nur Lufttemperaturdaten benötigt, zur Modellierung eingesetzt werden wenn andere Klimadaten nicht verfügbar sind.

Bestimmte Bewirtschaftungsverfahren im Einzugsgebiet verändern das Verhältnis des Oberflächen- zu unterirdischem und Grundwasserabfluss. Ein geplantes Bewässerungsprojekt sowie die vorhandenen Bewirtschaftungsverfahren verändern

den Oberflächenabfluss zu Basisabfluss und zur Verdunstung. Unter den derzeitigen Wasserbewirtschaftungsverfahren und der derzeitigen Wasserproduktivität wird es schwer sein, den Wasserbedarf der Bevölkerung im Jahre 2050 zu erfüllen. Ein besseres Management des grünen Wassers sowie Optionen für die nicht konsumtive Wassernutzung (Wasserenergie, Fischerei, etc.) können die Knappheit an blauem Wasser auf der Skala des Nileinzugsgebietes minimieren.

# ማጠቃለያ

ኢትዮጵያ ያላትን የውኃ ሃብት በብቃት ለመጠቀም እንዳትችል የኢኮኖሚ እና የቴክኖሎጂ ክህሎት ተግዳሮቶች ወስነዋታል። በአሁኑ ወቅት በተሻለ መልኩ የውኃ መሰረተ-ልማት እየታየ ቢሆንም ዘላቂነት ያለው ልማት ለማከናወን በተሻለ እውቀት ላይ መመስረት አስፈላጊ ነው። የውኃ ፍሰት ዑደት ምጣኔን እና ለመሰረታዊ ፍላጎት ተደራሽ የሆነን የውኃ አካል መጠን በጊዜ እና በቦታ ወሰን በጥልቀት መረዳት የሚፈለገውን ክህሎት ያዳብራል፤ የሚሰሩ ሥራዎችን በመረጃ ይደግፋል። ይህንን አጠቃላይ አስፈላጊነት መሰረት በማድረግ በእዚህ ጥናት የውኃ ፍሰት ዑደትንና ለጥቅም የሚውል የውኃ ልክን በእርሻ መሬት፣ በተፋሰስና በተለያዩ የመሬት አጠቃቀምና የመሰረታዊ የውኃ ፍላጎት አማራጮች መሰረት የውኃ ምጣኔን ለመተንተን ተሞክሯል። ጥናቱ ያተኮረባቸው አላማዎች፤ (፩) የውኃ አጠቃቀምንና የውኃ ምርታማነትን በናሙና በተመረጠ አነስተኛ የመስኖ አውታር ላይ መገምገም፣ (፪) የተጓደሉ የሚትሪዮሎጂ መረጃዎችን ማምዋያ የተለያዩ ቀመሮችን ማስላት፣ (፫) የውኃ ዑደትን መተንተን የሚያስችል ሞዴል ለጥናቱ ቦታ እንዲያገለግል መሰረታዊ መስፈርቶቹን ማስተካከል እና (፬) ሞዴሉን በመጠቀም የውኃ ፍሰት ምጣኔ ድርሻና የፍላጎት ጫናን በተለያዩ አማራጮች ማስላት ናቸው። በአባይ ወንዝ መነሻ በሆነው በጣና ሃይቅ ተፋሰስ ውስጥ የሚገኝ 1520 እስኩየር ኪሎ ሜትር ስፋት ያለው የጉማራ ንዑስ ተፋሰስ ለጥናቱ ቦታ ተመርጧል።

ዳንታ በተባለ በተፋሰሱ ውስጥ በሚገኝ አነስተኛ የመስኖ አውታር (90 ሄክታር) ላይ በተደረገው ጥናት ውኃን ከወንዝ ጠልፎ ወደተፈለገው ማሳ በማጓጓዝና በማሳ ላይ በሚደረግ የውኃ አጠቃቀም ሂደት ውኃ በብዛት እንደሚባክን፣ ይህ የሚባክነው ውኃ ባልተፈለገ መልኩ ማሳዎችን በማጥለቅለቅና በመስረግ የመስኖ ማሳዎችን ከጥቅም ውጪ ማድረጉ፣ የመስኖ ቦዮች ጥገና እና ፅዳት በወቅቱ ባለመደረጉ ውኃ በተፈለገው ጊዜ፣ መጠንና ቦታ ማድረስ አለመቻሉና በታችኛው የመስኖ ማሳዎች የውኃ እጥረት መከሰቱ ዋና ዋና የሚታዩ ችግሮች ናቸው። በዚህና በተያያዥ ምክንያቶች የሰብሎች የማሳና የውኃ ምርታማነት ከሌሎች ቦታዎች ጋር ሲወዳደር ዝቅተኛ ነው። በመስኖ ቦዮችና ማሳዎች ዳርቻ ላይ የሚገኝ የሳር ምርት በስርገት የሚባክነውን የተወሰነ ውኃ ለከብቶች መኖ ምርት እንዲሰጥ በማድረጉ፣ የበጋ ወቅት የመኖ እጥረትን በመቅረፍና ጥምር የሰብልና እንስሳት ግብርናን በመደገፍ ተጨማሪ ጠቀሜታ አለው፤ የመስኖ ውኃውንም ምርታማነት ከተለመደው የሰብል ምርታማነት ስሌት የበለጠ ያደርገዋል። የምሽት ውኃ ማጠራቀሚያ ጊዜያዊ ኩሬዎች በተለያዩ አመቺ ቦታዎች በመስራት ውኃን በለሊት ለመስኖ መጠቀምን ማስቀረት፣ ገበሬዎች መስኖውን እንዲቆጣጠሩ ማብቃት፣ ለመስኖ ቦታዎች የተሻሉ ምርታማ የሰብልና የመኖ ዝርያዎችን ለይቶ ማቅረብ፣ አዋጭ የሰብሎችን የውኃ ፍላጎት መወሰንና በገበሬዎች አቅም ውኃን የመለኪያ ዘዴዎችን ማቅረብ የውኃ ብክነትን ለመቀነስና ምርታማነትን ለመጨመር ያስችላል።

የተሟላ የሚትሪዮሎጂ መረጃ ለውኃ አጠቃቀም ጥናትና ውሳኔ አሰጣጥ ወሳኝ ነው። በጥናቱ አካባቢ በመሳሪያዎች አለመሟላትና ብልሽት፣ በሰለጠነ የሰው ሃይል እጦትና በመሳሰሉት ምክንያቶች ከየሚትሪዮሎጂ ጣቢያዎቹ ያልተሟላ መረጃ ማግኘት የተለመደ ነው። ዘላቂ መፍትሄ የሚሰጡ ጥናቶችና የውኃ አጠቃቀም ሥራዎችን ለማድረግ እነዚህን መረጃዎች ጥቅም እንዲሰጡ በማድረግ የመረጃ ክፍተትን መሙላት ያስፈልጋል። በዚህ ጥናት አምስተኛ ምእራፍ ላይ የዝናብ፣ የአየር ሙቀት፣ የፀሐይ ሃይልንና የአየር እርጥበት መረጃ ክፍተቶችን ለመሙላት የተለያዩ አማራጭ ዘዴዎች ተገምግመው የተሻሉት ዘዴዎች ተመርጠዋል። የአንድን መረጃ ማሰባሰቢያ ጣቢያ ክፍተት ከአጎራባች ጣቢያዎች መረጃ በመነሳት ለመሙላት የሚያስችሉ ዘዴዎችን መጠቀሙ የተወሳሰበ ካለመሆኑም በተጨማሪ በውሃ ፍሰት ትንታኔ ላይ የተሻለ ተአማኒ ትንታኔ ለመስጠት አስችሎዋል። የፀሐይ ሃይልን እና የአየር እርጥበት መረጃን በቀላሉ መለካት ከሚቻል የአየር ሙቀት መረጃ መቀመር በተወሰነ መጠን ተችሎዋል። መልክዓ ምድሩን መሰረት ያደረገ ቀጣይ ጥናት የተሻለ ግንዛቤ ሊያስገኝ ይችላል።

በአሜሪካን ሃገር ተዋቅሮ በተለታዩ የአለማችን ተፋሰሶች ለብዙ ጊዜ ሥራ ላይ የዋለ የውሃ ፍሰት ምጣኔ ሞዴል (Soil and Water Assessment Tool-SWAT) ተመርጦ የሞዴሉ የውስጥ መሰረታዊ መስፈርቶች ከአካባቢው መረጃ ጋር ተቀባይነት ባለው መልኩ እንዲሰራ ተደርጓል። በጉማራ ተፋሰስ የተደረጉ ጥናቶች በአብዛኛው የሚጠቀሙት የባህር ዳር ሚትሪዮሎጂ መረጃ መመዝገቢያ ጣቢያን መረጃና ከላይ በተገለፀው ዘዴ የተሟላን በተፋሰሱ አቅራቢያ የሚገኝን መረጃን በመጠቀም የሚገኘው የውሃ ፍሰት ምጣኔ ትንተና ከፍተኛ ልዩነት አለው። በአዲስ መልክ መረጃዎችን አድራጅቶና አሟልቶ መጠቀሙ የተሻለ የትንተና ብቃትና ተአማኒነት አለው። ወደፊት ለሚሰሩ የውኃ አጠቃቀም ጥናቶችና ሥራዎች በመልክዓ ምድሩ ገፅታ ወካይነት መሰረት በማድረግ ተጨማሪ የመረጃ መሰብሰቢያ ጣቢያዎችን ማቋቋምና እስካሁን በአካባቢው ከተመዘገበው መረጃ ጋር በዚህ ጥናት የተገለፀውን ስልትና ሌላም በመጠቀም አንናቦ መተንተን የተሻለ የውኃ ምጣኔ ግንዛቤ ለማዳበር ይረዳል። እስከ ቀበሌ ድረስ የተዋቀሩ የመጀመሪያ ደረጃ ትምህርት ቤቶችን እና የጤና ኬላዎችን ለተጨማሪ የሚትሪዮሎጂ መረጃ ማሰባሰቢያነት መጠቀሙ በትንሽ ወጪና በነበረ የተማረ የሰው ሃይል መረጃን በተሻለ ዋስትና እና ጥራት ለማሰባሰብ ያስችላል።

የሃገሪትዋ የመሬት አጠቃቀም ፖሊሲ ተደነገገው መሰረት እንደ እርከን እና የደን ልማት ሥራዎችን በአማራጭነት በመጠቀም፣ መሰረታዊ የውኃ ፍላጎትን በ2000ዎቹና በ2050ዎቹ የህዝብ ብዛት አንፃር በማስላት የውኃ ምጣኔንና ጥቅም ላይ ሊውል የሚችል የውኃ ድርሻን ለመተንተን ተሞክርዋል። የእርከንና የደን ልማት የውኃ ፍሰት ምጣኔን የተወሰነውን ከጎርፍነት ወደ ከርሰምድር ውኃ ፍስትና ለተክሎች እድገት ወደሚውል ትነት መቀየር ያስችላል። በታችኛው የተፋሰሱ ክፍል የሚከሰትን ደራሽ ውኃ ከማማከሉም በተጨማሪ የውኃውን ጠቃሚነት ይጨምራል። ጥናቱ የተጠናቀቀው የጉማራ መስኖ ፕሮጀክት ወደ ጣና የሚፈሰውን ውኃ በብዙ ጥናቶች ከሚፈቀደው ተፈጥሮአዊ የውኃ ፍሰትን ሳይገታ የጎርፍ ውኃን እና ያለጥቅም ሲተን

የነበረን የበጋ ወቅት መጠነኛ የዝናብ ውኃን ተጨማሪ የመስኖ ምርት እንዲሰጥ ያስችለዋል። አሁን ባለው አነስተኛ ዝናብ ተኮር የግብርና ምርታማነትና የህዝብ ብዛት እድገት መሰረት በ2050ዎቹ የሚኖረውን መሰረታዊ የውኃ ፍላጎት ማሟላት እንደማይቻል የጥናቱ ውጤት ያሳያል። ሁሉንም የወንዝ ፍሰት ወደ ግብርና ሥራ በመጥለፍ የወደፊት የውሃ ፍላጎትን ማሟላት ቢቻልም ተፋሰሱ ከጣና ሐይቅ ጀምሮ እስከ ሜዴትራኒያን ባህር የናይል ጫፍ ድረስ ላለው አኗኗር መሰረት በመሆኑ የማይቻል ነገር ነው።የቤተሰብ ምጣኔን ማስተካከል፣ የውኃ ምርታማነትን ማሳደግ እና ውኃ ፈጅ ያልሆኑ የውኃ ጥቅሞችን (የአሳ ምርት፣ መጓጓዣ፣ መዝናኛና ቱሪዝንምን) ማስፋፋት፣ በግብርና ላይ ብቻ ጥገኛ የሆነውን አኗኗር ማከፋፈል ወደፊት የሚገጥመውን የውኃ እጥረት ማቃለል ያስችላል። የጉማራ ተፋሰስ ከሃገሪትዋም ሆነ ከክልሉ አማካይ የህዝብ እፍግታ (ከ200 ሰው በላይ በካሬ ኪሎ ሜትር) በላይ በመሸከሙና ውኃና የእርሻ መሬት የበለጠ ያላቸው የአባይ የታችኛው ተፋሰስ አካባቢዎች ደግሞ በአንፃሩ እስከ 20 ሰው በካሬ ኪሎ ሜትር አነስተኛ የህዝብ ስብጠር አላቸው። እነዚህን ቆላማ ቦታዎች ለኑሮና ለሥራ ምቹ በማድረግ የህዝብ ስብጥርን በሃገር አቀፍ ደረጃ እንዲመጣጠን ማድረጉም ሌላውና ወደፊት ሊደርስ የሚችል መሰረታዊ የውኃ እጥረትን ማቃለያ ገፀ-በረከት ነው። አሁን ሃገሩቱዋ የጀመረችው ታላቁ የህዳሴ ግድብ እንደግብርና ውኃ ፈጅ ያልሆኑ ኢኮኖሚያዊ ጥቅሞችን በመስጠት ወደፊት ሊከሰት የሚችለውን የውኃ እጥረት ሊያቃልል ይችላል። የሚያመነጨው የኤለክትሪክ ሃይል ከናይል ተፋሰስ ውጪ ባሉ ቦታዎች ሃገሪቱዋ ያላትን የገፀ-ምድርና የከርሰ-ምድር ውኃ ከማልማቱም በተጨማሪ ለኑሮ ምቹ ያልሆነውን የአባይ ሸለቆን ለመጓጓዣ፣ ለአሳ ምርት፣ ለመዝናኛ፣ ለንግድና ለቱሪዝም ምቹና ተመራጭ ቦታ በማድረግ የህዝቦችን አኗኗር የተሻለ ያደርጋል።

**TABLE OF CONTENTS**

**LIST OF ACRONYMS**

| | |
|---|---|
| AET | Actual evapotranspiration |
| ALPHA_BF | Baseflow alpha factor |
| AM | Arithmetic mean |
| ARARI | Amhara Region Agricultural Research Institute |
| ARBIDMPP | *Abbay* River Basin Integrated Development Master Plan Project |
| ASTER | Advanced Space borne Thermal Emission and Reflection Radiometer |
| AWC | available soil water content |
| BMZ | German Federal Ministry for Economic Development Cooperation (Bundesministerium Für Wirtschaftliche Zusammenarbeit) |
| CCW | Coefficient of correlation weighting |
| CSA | Central Statistics Authority |
| DEM | Digital Elevation Model |
| DM | Dry matter |
| EEPC | Ethiopian Electric Power Corporation |
| ENMA | Ethiopian National Meteorological Agency |
| EPLAUA | Environmental Protection, Land Administration and Use Authority |
| ESCO | Soil evaporation compensation factor |
| EWNHS | Ethiopian Wildlife and Natural History Society |
| FAO | Food and Agriculture Organization of the United Nations (UN) |
| FC | Field capacity |
| GDEM | Global Digital Elevation Model Ethiopian |
| GERDP | Grand Ethiopian Renaissance Dam Project |
| GIP | *Gumara* irrigation Project |
| GIS | Geographical Information System |
| GPS | Geographical Positioning System |
| GW_DELAY | Groundwater delay |
| GW_REVAP | Groundwater revap coefficient |
| GWQMN | Threshold water depth in the shallow aquifer for flow |
| HRU | Hydrologic response unit |
| IDW | Inverse distance weighting |
| ILRI | International Livestock Research Institute |
| ITCZ | Inter-tropical convergence zone |
| IWMI | International Water Management Research Institute |
| LAI | Leaf area index |
| MEDaC | Ministry of Economic Development and Co-operation |
| MoFED | Ministry of Finance and Economic Development |
| MoWR | Ministry of Water Resources |
| NBI | Nile Basin Initiative |
| NMSA | National Meteorological Services Agency |
| NR | Normal ratio |

| | |
|---|---|
| NSE | Nash-Sutcliffe efficiency |
| PBIAS | Percent bias |
| PET | Potential evapotranspiration |
| PW | Permanent wilting |
| RCHRG_DP | Deep aquifer percolation fraction |
| REVAPMN | Threshold water depth in the shallow aquifer for revap |
| RMSE | Root mean square error |
| RSR | Ratio of root mean square error to observation standard deviation |
| SCS-CN | Soil Conservations Service curve number |
| SM | soil moisture |
| SMEC | Snowy Mountains Engineering Corporation |
| SPOT | Satellite Pour l'Observation de la Terre |
| SUFI | Sequential Uncertainty Fitting |
| SURLAG | Surface runoff lag coefficient |
| SWAT | Soil and Water Assessment Tool |
| TAW | Total available water |
| TLU | Tropical livestock unit, (where 1 TLU is 250 kg live weight) |
| USBR | United States Bureau of Reclamation |
| WAPCOS | Water and Power Consultancy Service |
| WCD | World Commission on Dams |
| WXGEN | Weather generator |

# 1 GENERAL INTRODUCTION

Water is vital for life. On a global scale, it is abundant in quantity, but spatial and temporal availability of fresh water is a problem. Water scarcity is considered one of the major challenges for livelihoods and the environment in sub-Saharan Africa (SSA; Amede et al. 2011). After Nigeria, Ethiopia has the highest population in Africa with 80 million people (Awulachew et al. 2005). Although the country has abundant water supplies and arable land, food insecurity due to the occurrence of frequent droughts and famines is one of the main challenges (Ministry of Water Resources, MoWR 2007). Water availability is erratic in space and time due to the seasonal variation in rainfall and a lack of structures regulating water flow (Awulachew et al. 2005).

## 1.1 Problem definition

Effective water resources development is very important for the Ethiopian Nile in particular and for the Nile Basin in general. It is widely recognized as being crucial for sustainable economic growth and poverty reduction in developing countries (World Bank 2004; Grey and Sadoff 2006). In 2007, MoWR (2007) concluded that promotion and expansion of irrigation was urgent in order to increase food and raw materials production for agro-industries, thus increasing employment opportunities and foreign exchange earnings (MoWR 2007). However, according to Molden et al. (2007), Ethiopia is grouped under the countries with economic and technological water scarcity. The authors considered Ethiopia a country with a high water availability per capita, but this availability may be different at finer space and time scales. It needs to be understood when, where and how much water is available and how an intervention plan will be suitable both now based on existing weather and land-use variables and in future with the expected land-use and climate changes. Meteorological data are generally too scarce for detailed analysis of the water balance at the local level where water development is to be implemented. These information gaps need to be filled.

The study area is characterized by a mixed crop-livestock system (Haileslassie et al. $2009_{a;b}$), and water is important for both crop and livestock components to optimize productivity. Peden et al. (2007) proposed a concept of livestock water productivity (LWP), a factor not considered previous productivity analyses. It is defined as the ratio of the total net livestock products and services over the total water depleted and degraded in the process of obtaining these products and services (Descheemaeker et al. 2009). Crop-livestock water productivity is strongly affected by the depleted water for each component. Understanding the spatial and temporal distribution of the water balance is very important to control water depletion in order to improve water productivity. Therefore, a joint project was proposed by the International Livestock Research Institute (ILRI) and the International Water Management Research Institute (IWMI): "Improving water productivity of crop-livestock systems of sub-Saharan Africa". The project was funded by the German Federal Ministry for Economic Development Cooperation (Bundesministerium Für Wirtschaftliche Zusammenarbeit-BMZ). Its overall objective was the development and promotion of options for enhancing water productivity. Evaluating the water balance of a pilot site and addressing the percentage of water lost as unproductive evaporation and/or runoff and that of productive transpiration were two of the six specific objectives. Potential improvement of water productivity will be driven based on the vapor shifts for supporting decision making by local and regional development planning officers. This research output of the project is the basis of this study, which aims to fill information gaps existing for decision making in water development in the area such as information on water use for small-scale irrigation schemes and methods to improve database development, and to fill missing data. It also evaluates modeling approaches and water balance and water availability in the study area.

## 1.2 Research objectives

The main research objective of this study was to evaluate the water balance and water availability of the *Gumara* watershed, northwest Ethiopia, on spatial and temporal scales. Although spatial and temporal scales can be refined into smaller units, data availability at smaller scales is a problem in the area. For example, density of the meteorological stations and land-use and soil data can determine the spatial scale of the water balance modeling. Since the studied watershed is an agricultural area, rainy and dry season time scales can provide meaningful water balance results to identify gaps for development intervention. Therefore, the specific research objectives of the research were:

1) To evaluate the water use and water productivity of a small-scale irrigation scheme in the study area. This addresses the water use and water productivity in the area in the dry seasons and at irrigation scheme scales.
2) To evaluate different techniques for filling missing meteorological data so that the existing database of the area can be exploited better for improved hydrological modeling than in previous studies.
3) To assess the effect of meteorological station density, potential evapotranspiration calculation methods and missing data on the performance of the hydrological model Soil and Water Assessment Tool (SWAT).
4) To assess the effect of land-use/water-use changes on the water balance and water availability in the study area.

Each specific objective is presented in the following chapters of this dissertation.

## 1.3 Outline of the dissertation

Chapter 1 comprises general introduction, problem definition and objectives of the study. Chapter 2 highlights the study area and water resources of Ethiopia while Chapter 3 introduces the theoretical background of water balance modeling and the SWAT model. A case study on water balance and water productivity in a small-scale irrigation scheme is presented in Chapter 4. Methods for filling spatial and temporal missing data are presented in Chapter 5. Effects of meteorological station density and potential evaporation methods on SWAT model performance are discussed in Chapter 6. Chapter 7 presents the results of the study on the effect of land-use and demographic changes on water balance and water availability. Chapter 8 summarizes the overall findings of the study.

# 2 STUDY AREA

## 2.1 Location, topography and demography

Ethiopia is classified into three physiographic regions: northwestern plateau, southeastern plateau and the Rift Valley (Woldemariam 1972). The study area, the *Gumara* watershed, is located on the northwestern plateau in the Lake *Tana* Basin (Figure 2-1). This is considered as the source of Blue Nile River and is located on 10°57′-12°47′N latitude and 36°38′-38°14′E longitude (Tessema 2006). The basin includes the *Gojam-Gondor* escarpment and the lower plains *Dembiya, Fogera* (part in the study area) and *Kunzila* surrounding the lake, which are wetlands in the rainy season*.* About 40 rivers drain into the lake (Kebede 2006). Lake *Tana* is the biggest natural water body in Ethiopia. It obtains 93% of its water from four rivers: *Gilgel-Abbay, Reb, Gumara* and *Megetch* (Kebede 2006); *Gumera* River is in the study area. The topography ranges from 1780 m at the lakeshore to 4080 m asl at the top of the *Guna* mountain in the east of the study watershed (Figure 2-2).

The area is one of the most highly populated highland parts of Ethiopia. The Lake *Tana* Basin has about three million inhabitants (CSA, 2011), where 256,000 live in the largest city on the lakeshore, Bahir Dar. About 15,000 people are estimated to live on the 37 islands in the lake (CSA, 2003).

## 2.2 Climate and soil

The climate is tropical highland monsoon where the seasonal rainfall distribution is controlled by the movement of the inter-tropical convergence zone and moist air from the Atlantic and Indian Ocean in the summer (June-September) (Kebede 2006). Mean annual rainfall over the Lake *Tana* Basin is 1,326 mm and the average annual evaporation of the lake surface is approximately 1,675 mm (SMEC 2008). Rainfall distribution is highest in the southern part of the *Gilgel Abbay* watershed and lowest in the northern part of the *Megech* watershed. In the *Gumara* watershed, annual rainfall varies from 1100 mm to 1600 mm per year (Figure 2-3).

The area is composed of sedimentary, effusive and intrusive rocks (Woldemariam 1972). Alisols, Fluvisols, Leptosols, Luvisols, Nitisols, Regosols and

Vertisols are the main soil types found with chromic, eutric, heplic and lithic horizon modifiers in the Lake *Tana* Basin (BCEOM 1998).

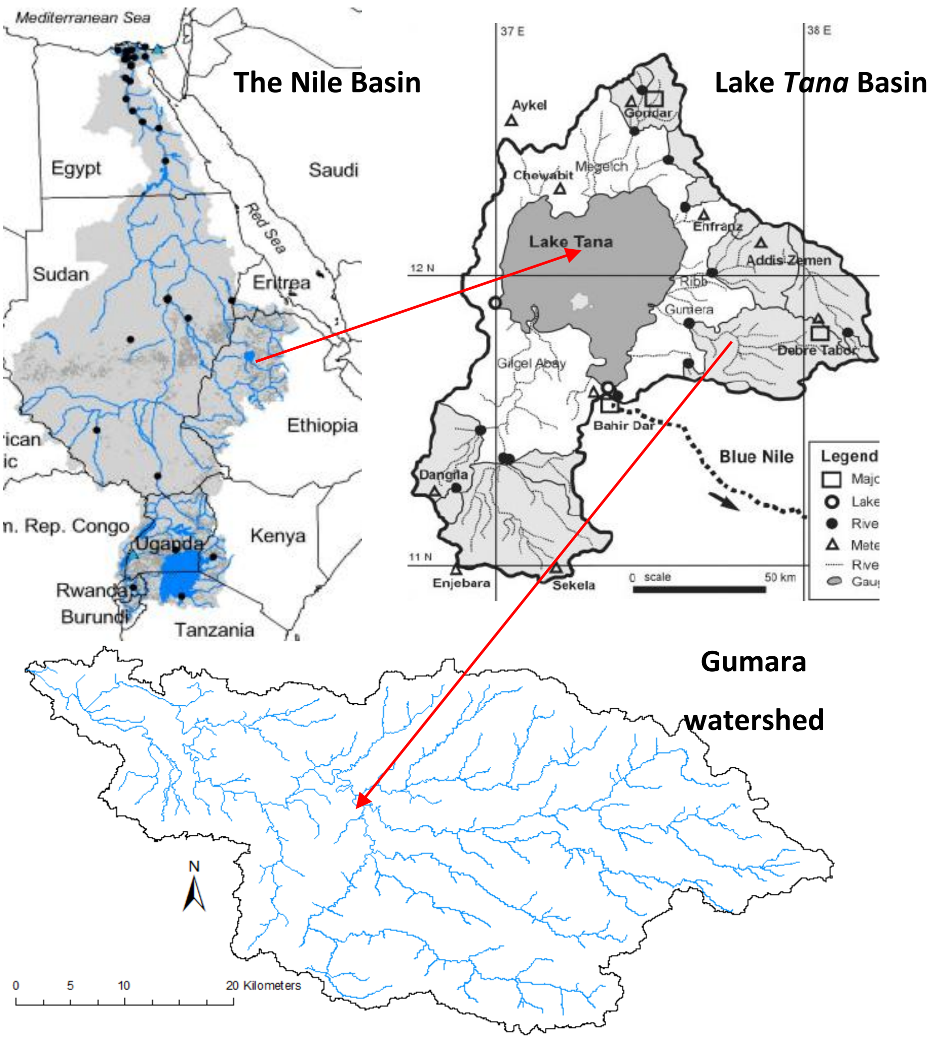


Figure 2-1 Location of study area: Nile Basin, Lake Tana Basin and *Gumara* watershed. Sources: Wale et al. (2009) and World Resources Institute, http://earthtrends.wri.org/text/map_lg.php?mid=299

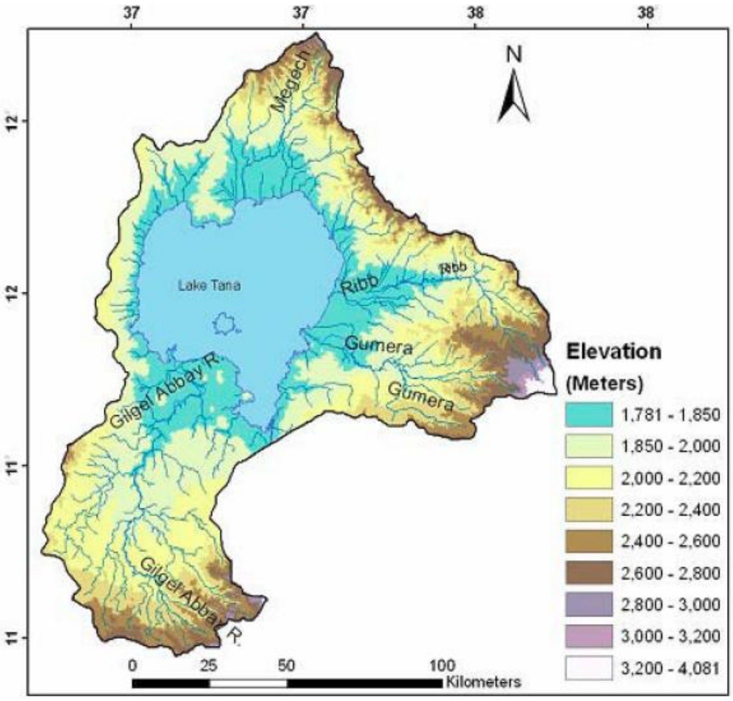


Figure 2-2 Topography and hydrography of Lake Tana Basin
*Source: (Yilma and Awulachew 2009), where Gumera is synonomus to Gumara in the dissertation*

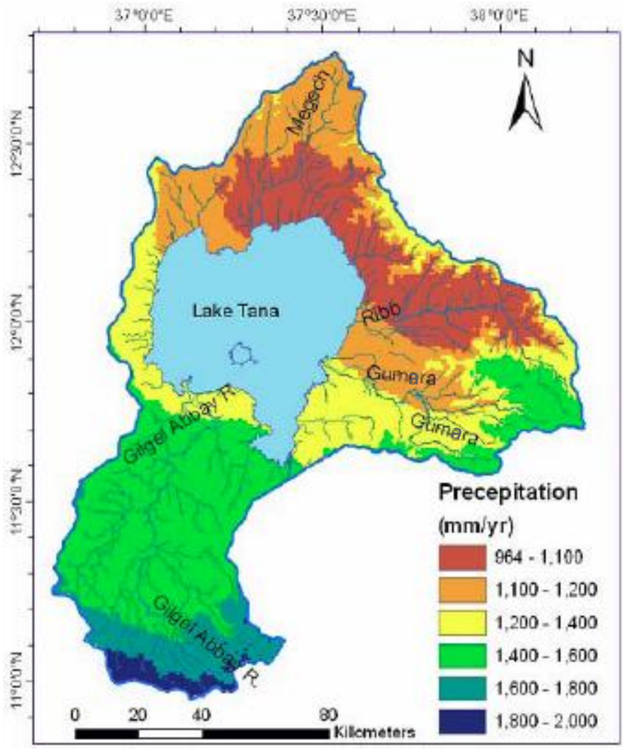


Figure 2-3 Annual rainfall distribution in Lake Tana Basin
*Source: (Yilma and Awulachew 2009), where Gumera is synonomus to Gumara in the dissertation*

## 2.3 Land-use, agriculture and biodiversity

About 10.1% of the country is covered by arable land, 0.65% by permanent crops and 1% is covered by water (MoWR 2002). Haileslassie et al. ($2009_a$) classified the farming system of the *Gumara* watershed into rice-based cash crops, maize-small cereals and cereal-pulses. Rainfed mixed farming with a wide range of food crops like cereals, pulses and vegetables is the main land-use of the study area, where livestock production is also an important component of the livelihoods (Johnston and McCartney, 2010). The area is characterized by low crop production (783 to 1234 kg $ha^{-1}$) with fragmented farmland holdings less than 1 ha per household (Erkossa et al. 2009).

The economic resources in the study area have great potential. It is the home of the well-known *Fogera* cattle, which are used for milk production. Lake *Tana* has an estimated fish production of 10,000 to 15,000 ton/year (IPMS, 2005). The lake and the surrounding wetlands are endowed with rich biodiversity and cultural heritages. The lake contains 18 species of barbus fish (Cyprinidae family) and the only large cyprinid species flock in Africa (LakeNet 2004). At least 217 bird species are to be found in the area, and the lake is estimated to hold a minimum of 20,000 water birds (EWNHS 1996). Twenty monasteries dating from the sixteenth and seventeenth century are located on the lake islands with many cultural and natural assets. The *Tis Issat* Falls, one of Africa's largest waterfalls, is located on the Blue Nile approximately 35 km downstream of the Lake *Tana* outflow. Around 30,000 domestic and foreign tourists visit the area each year (EPLAUA 2006).

## 2.4 Water resources and development in Ethiopia

Ethiopia has 12 river basins (Figure 2-4) with a total surface water volume of 122 $km^3$ and 2.6 to 6.5 $km^3$ groundwater potential (MoWR 2002). The Nile River has three sub-watersheds in Ethiopia: Blue Nile*, Baro-Akobo* and *Tekeze*. The Blue Nile (called *Abbay* in Ethiopia) watershed is the main sub-watershed starting from the Lake *Tana* Basin. The *Baro Akobo* sub-watershed is located to the south of the Blue Nile. The country has abundant renewable water resources with 1300 and 2500 $m^3$ per year per capita at national and Blue Nile Basin levels, respectively (Johnston and McCartney 2010).

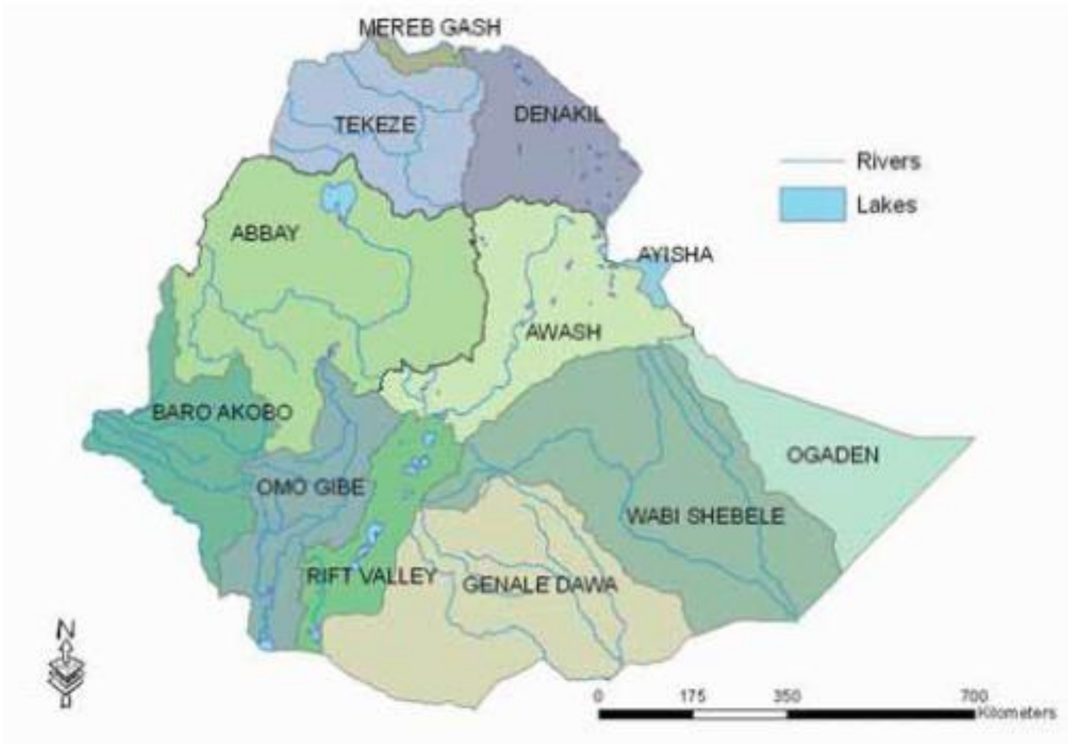


Figure 2-4 River basins of Ethiopia

***Source: (Awulachew et al. 2007)***

Most of the surface water resources of the country are shared with neighboring nations, which makes water resources development complicated. Figure 2-5 shows the shares of annual flows and irrigable land potential of the transboundary rivers and internal water systems of Ethiopia. More than 90% of the annual water flow and the irrigable land potential of the country are located along transboundary river basins. About 30% of the area in the Nile Basin contributes 70% and 60% of the annual flow and irrigable land, respectively.

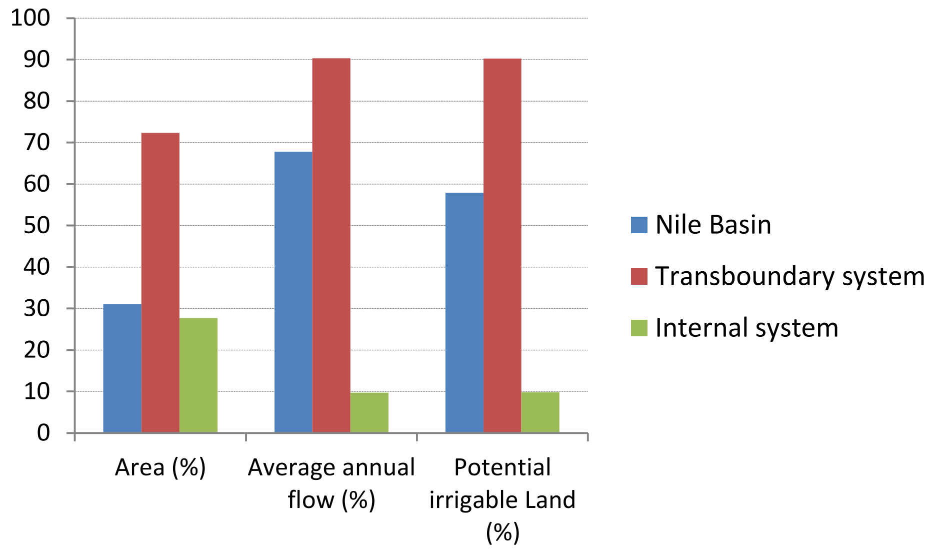


Figure 2-5 Relative potential of Nile Basin, total transboundary and internal watercourse systems with respect to whole Ethiopia

***Source: secondary data taken from (Arsano 2007 )***

Frequent and sever water shortages due to rainfall variability (CA 2007) are one of the factors of the low land productivity in the country. The contribution of per capita reservoir water has been very low (about 100 $m^3$) as compared to that of South Africa (750 $m^3$) and North America (6150 $m^3$) (World Bank 2006). The World Bank (2006) recommended the development of water storage infrastructures as an economic priority, since hydrological variability costs 30% of the country's economic development in GDP due to crop failure and livestock deaths. Hence, water shortage and other related problems lead to food insecurity, so that 46% of the population was undernourished in 2008 (von Grebmer et al. 2008). Rainfed agricultural production is vulnerable to seasonal water shortage (Johnston and McCartney 2010), and 75-80% of the rainfed production is consumed at the household level (World Bank 2006; Block et al. 2007) even in good rainfall seasons and wet years with low surplus production for the market. Moreover, the drinking water supply is very low (38% at country level and 26% in rural areas) (WHO-UNICEF 2010). People in rural areas travel more than a kilometer to search for and to fetch drinking water (UN Water 2006).

There are indications that water development is one of the best entry points to avert these problems. Smallholder irrigation can generate higher household incomes (U$ 323 per ha) than rainfed systems (U$147 per ha) (Johnston and

McCartney 2010). According to recommendations in studies and based on evidence, water resources development has taken place throughout the country. The Ethiopian government has been developing the water resources infrastructure since the 1980s. About 5-6% of the 3.7 million ha potentially irrigable land of the country is covered by irrigation. In 2005, this area covered only 30 $m^2$ per capita. This is very low as compared to the global level of 450 $m^2$ (Awulachew et al. 2005).

Therefore, due to frequent droughts and extreme poverty, the Ethiopian government is working to develop the water resources of the country to attain economic growth and to reduce poverty through the construction of additional infrastructure, particularly hydropower and irrigation schemes (MoFED 2006; Awulachew et al. 2008; Block et al. 2007; McCartney et al. 2009).

Water resources assessment for hydroelectric power generation and irrigation in 1964 by the U.S. Bureau of Reclamation (USBR) identified four main hydropower dam sites along the main Blue Nile River in Ethiopia (USBR 1964). A nationwide study in 1990 by the Water and Power Consultancy Service (WAPCOS 1990) identified 129 potential hydropower sites. The Abbay River Basin Integrated Development Master Plan Project (ARBIDMPP) conducted by the MOWR of Ethiopia proposed more than 20 projects for irrigation, hydropower, and multipurpose dams (MOWR 1998) (Figure 2-6 ).

Lake *Tana* Basin is identified as a priority hydro-infrastructure development area to attain the Millennium Development Goals (McCartney et al. 2010). In 2009, a big multi-functional project was inaugurated that transfers Lake *Tana* water to the nearby *Beles* catchment through a 12 km-long tunnel (7.1 m diameter) (Salini and Mid-day 2006). This project generates 460 MW (2,310 GWh) electric power using 3 $km^3$ water per annum (SMEC 2008). The tail water of this project is planned to be used for irrigation. However, the social and environmental costs overweigh the benefits of transferring water from one catchment to the other (WCD 2000; King and McCartney 2007). Two dams are under construction, and a feasibility study concerning another three dams at the headwater of the lake for irrigation is in its final stage. Two hydropower stations were functioning at the natural outlet of the lake at the time of this study. The Tana-Beles watershed is one of the development corridors of the country, and integrated water resources development programs are thus under implementation there (World Bank 2008).

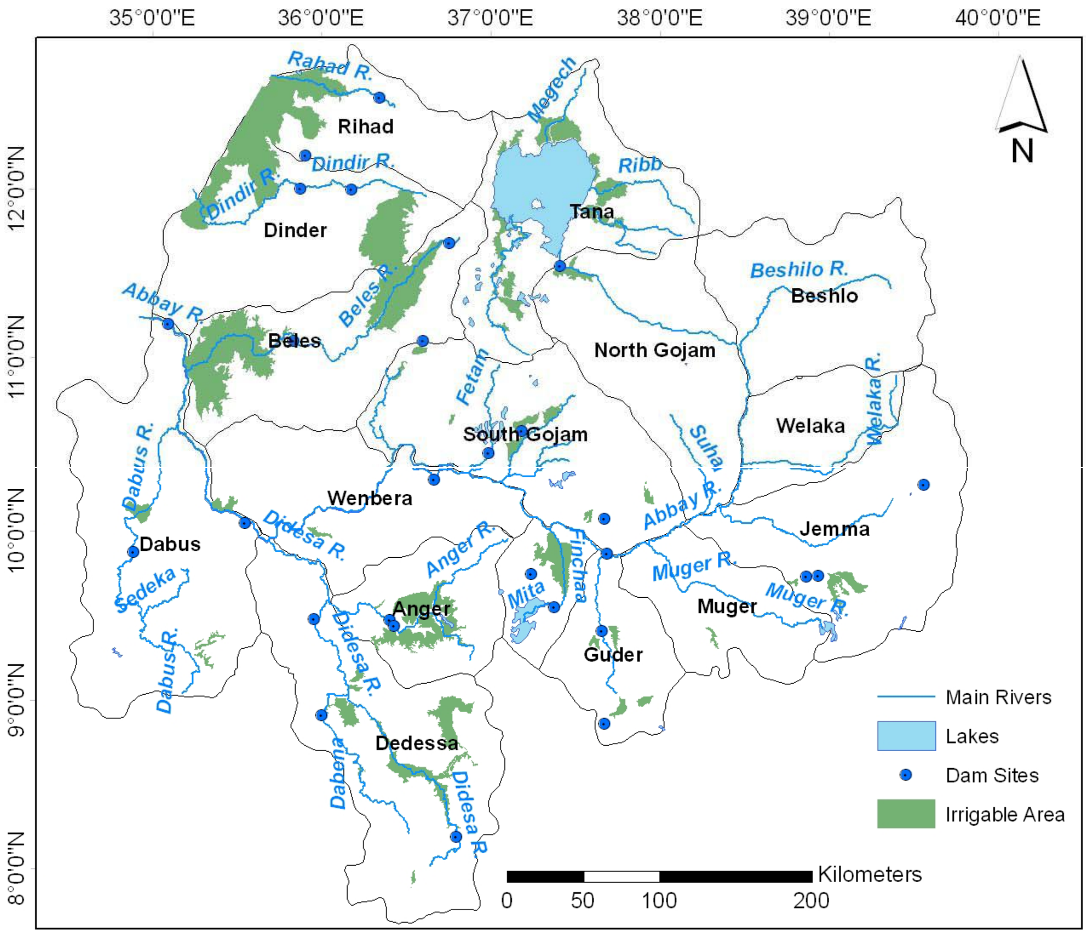


Figure 2-6 Proposed irrigation and dam sites in Basin

***Source: (Yilma and Awulachew 2009)***

This water resource development will result in significant land- and water-use changes that may affect the existence of the fresh water body in the lake and in the river system. Any expected changes in the Nile River water resources may have effects on the economies, production, energy supply and environmental quality of the region (NBI 2001; Hulme et al. 2005). Without considering the impact of climate change, McCartney et al. (2010) estimated that the planned water development projects in the Lake *Tana* watershed will lead to a decrease in the water level of the lake by 0.81 m

(10% of the mean level), and in the lake area by 30-81 $km^2$ (by ca. 1.9-3.6%). According to the authors, the existing water resource development for hydropower generation at *Tis Issat* at the outlet of Lake Tana has modified flows downstream of the lake, reduced water levels of the lake, and significantly decreased the flow over the *Tis Issat* waterfall.

# 3 WATER BALANCE AND MODEL STRUCTURE

## 3.1 Hydrological processes and water balance

Atmospheric, surface and subsurface/groundwater flows and storages are important parts of the hydrological cycle. Water is found in solid, liquid and gaseous states in the hydrological cycle. It can be transformed from one component to another either naturally (runoff, precipitation, seepage, infiltration, evaporation, condensation, deep percolation) or/and artificially (dam, irrigation, diversion, pumping).

The hydrological processes are too complex to illustrate them through exact measurements everywhere and every time. The simplified representation of some of the important hydrological processes can be done to conceptualize the hydrological system in the form of a model (Anderson & Woessner 1992). A hydrological system model approximates the actual system and transforms input variables to hydrological output variables (Chow et al. 1988; Dooge 1968). It can be generally described as in equation 3-1.

$$Q(t) = \Omega I(t) \tag{3–1}$$

where *Q* and *I* are output and input variables, respectively, as a function of time *t*, and $\Omega$ is a function transferring the input to the output. This function can be expressed by an algebraic equation (algebraic operator) or differential equation (differential operator). Parameters in a model are quantities that characterize some parts in the system and attain constant values in time, space and condition.

Chow et al. (1988) classified hydrological models into three categories according to the way they treat randomness, space and time. Stochastic models are models whose variables are probabilistic in nature and random in distribution. If the variables of the models are free from randomness, the models are said to be deterministic. If we consider the spatial nature of models, we can group them as lumped or distributed. Lumped models ignore the spatial variability of hydrological processes, input variables or parameters, while distributed models try to address spatial variability using more input data.

Models are also classified as conceptual/empirical and physical with respect to how they equate the real processes within the hydrological system. Conceptual models express the relationships of processes in the hydrological system based on laboratory or field measurement data as done by using regression models, without understanding the real physical process that is done behind. Physically based models, on the other hand, try to equate and represent the processes based on some understanding of their physics. Since physically based models have different parameters related to one or more space coordinates, they can also be grouped under distributed or semi-distributed models (Beven 1985).

Hydrological processes include canopy interception, infiltration, evaporation, transpiration, overland flow, canal flow, unsaturated subsurface flow and saturated subsurface flow. The processes are generally grouped into storages (surface, subsurface and groundwater), inflows and outflows from the system. These processes can be estimated using a series of empirical and hydraulic equations (Arnold et al. 1998) in the model. These equations have parameters that are dependent on biophysical inputs, measured water outputs and management interventions. Model parameters have to be optimized with respect to input-output data of the area. This is known as parameter optimization (parameterization or calibration). Some parameters influence the output of the model more than the others do. Identification of these parameters will help to select very important parameters for model calibration (Vandenberghe et al. 2002 cited in Alamirew 2006). The identification process is known as sensitivity analysis. Verification is important by comparing the estimated output of the calibrated model with measured data that are not used during the calibration process. Models are calibrated and verified using standard statistical measures like percent difference between measured and simulated values, coefficient of determination ($r^2$) to measure the trends of fitness of both measured and simulated results, and Nash-Suttcliffe efficiency (Nash and Suttcliffe 1970) to compare how much similar the average simulated result is to the average measured value within a given period. Santhi et al. (2001) assumed an acceptable calibration for hydrology at percent difference less than 15%, coefficient of determination greater than 0.6 and Nash-Sutcliffe efficiency greater than 0.5.

### 3.2 Hydrological models for data-scarce areas

Model selection is determined by the availability of data, purpose of application and the accuracy of the output needed. Physically based distributed models need more data to calibrate a watershed. However, they are good for ungauged watersheds, effectively saving time for measuring every parameter of the watershed once they are calibrated. Studies advise to take care when using these models for data-scarce areas (Legesse et al. 2003; Andersen et al. 2001). Lumped models are quite robust for these areas although they result in less detailed output for climatic and land-use impacts. Bormann and Diekkrueger (2003 and 2004) applied lumped hydrological models that require less input data. However, they recommend applying detailed models to address the effect of land-use and climate on the environment for relatively better understanding.

### 3.3 Soil and Water Assessment Tool (SWAT)

SWAT is a continuation of about three decades of modeling efforts conducted by the United States Department of Agriculture - Agricultural Research Service (USDA-ARS). It has gained international acceptance as a robust interdisciplinary watershed-modeling tool. More information is available from international SWAT conferences, hundreds of SWAT-related papers presented at numerous scientific meetings, and dozens of articles published in peer-reviewed journals (Gassman et al. 2007). SWAT is a basin-scale, continuous-time model that operates on a daily time step. It is designed to predict the impact of different watershed management on water, sediment, and agricultural chemicals transportation for ungauged watersheds. It is physically based, computationally efficient, and capable of continuous simulation over long periods.

Applications of SWAT have expanded worldwide over the past decade (Gassman et al. 2007). Many of the applications have been driven by the needs of various government agencies, particularly in the United States and the European Union. These applications were done for assessments of anthropogenic, climate change, and other influences on a wide range of water resources or exploratory assessments of model capabilities for potential future applications. SWAT was selected as an important tool for this study for the following reasons.

(1) It considers many components of the hydrologic balance like precipitation, surface runoff, infiltration, evapotranspiration, lateral flow from the soil profile, and return flow from shallow aquifers (Gassman et al. 2007).

(2) It considers sediment yield, crop biomass, crop rotations, grassland/pasture systems, forest growth, planting, harvesting, tillage, nutrient applications, pesticide applications, biomass removal and manure deposition of grazing operations, continuous manure application options to confined animal feeding operations, conservation and water management practices, and pollutants transport (Gassman et al. 2007). These applications of SWAT can be used in the future once its hydrological application to the area is verified.

(3) It has automated sensitivity, calibration, and uncertainty analysis components, data generator and Geographic Information System (GIS) interface (Gassman et al. 2007). The weather generator routine of SWAT considers the problem of missing data for the area.

(4) It is physically based and can model ungauged watersheds that have no monitoring data and can quantify the impact of changes in management practices (Neitsch et al. 2011).

(5) It is computationally effective and can simulate processes in very large basins or a variety of management strategies without excessive investment in time and money (Neitsch et al. 2011).

(6) It enables users to study long-term impacts to address gradual impacts on downstream water bodies (Neitsch et al. 2011).

In SWAT, a watershed is divided into multiple sub-watersheds and then into hydrologic response units (HRUs) that consist of homogeneous land-use, management, and soil characteristics (Gassman et al. 2007). The SWAT2009 version (Neitsch et al. 2011) under ArcSWAT2.5 in the ArcGIS interface of ArcGIS9.3 version is used for this study. The *Gumara* River basin was partitioned in sub-watershed, and a refined stream network layer was formed based on the threshold minimum drainage area required to start a stream. These sub-watershed and stream network layers were done using the digital elevation model (DEM). The smallest unit of spatial discretization was produced based on a unique combination of land-use, slope and soil layers overlay. This spatial unit is assumed to respond similarly for hydrological inputs in SWAT (Neitsch et al. 2011). It is called hydrologic response unit (HRU).

### 3.4 Water balance and parameters in SWAT

SWAT simulates the hydrologic cycle using the water balance equation 3-2:

$$SW_t = SW_o + \sum_{i=1}^{t}(R_t - Q_{surf} - E_a - w_{seep} - Q_{gw}) \tag{3–2}$$

where $SW_t$ is the final water content (mm $H_2O$), $SW_0$ is the initial water content in time *i* (mm $H_2O$), *t* is the time (in days, months, or years), $R_t$ is the amount of rainfall in time *i* (mm $H_2O$), $Q_{surf}$ is the amount of surface runoff in time *i* (mm $H_2O$), $E_a$ is the amount of evapotranspiration in time *i* (mm $H_2O$), $w_{seep}$ is the amount of water entering the vadose zone from the soil profile in time *i* (mm $H_2O$), and $Q_{gw}$ is the amount of return or baseflow in time *i* (mm $H_2O$). The time scales depend on the concern of the analysis, since SWAT can simulate at daily, monthly and annual scales. Each term of the water balance equation has detailed physical processes that are interlinked in a harmony related to the atmosphere-vegetation-soil consortium. The details of these processes and physical phenomena are well presented in the SWAT input/output and theoretical documentations and literature (http://swatmodel.tamu.edu/ Cited 27/06/2011). The main terms in the water balance equation 3-2 are discussed below from these documents.

1. **Surface runoff**: Also known as overland flow, the part of the rainfall flowing along the slopes. SWAT uses the Soil Conservations Service (SCS) curve number (*CN*) method to calculate surface runoff. Surface runoff is expressed using the equation 3-3 (SCS, 1972):

$$Q_{surf} = \frac{(R_{day} - I_a)^2}{R_{day} - I_a + S} \text{ and } I_a = 0.2 * S \quad (3–3)$$

where $S$ is soil storage or retention, $R_{day}$ is daily precipitation, and $I_a$ initial surface abstraction that includes surface storage, interception and infiltration to moist soil surface up to runoff generation, all in mm water (mm $H_2O$). Soil storage or retention volume is expressed in terms of curve number *CN* as in equation 3-4:

$$S = 25.4\left(\frac{1000}{CN} - 10\right) \quad (3–4)$$

By substituting $I_a$ and $S$ in equation 3-5, surface runoff is expressed as:

$$Q_{surf} = \frac{(R_{day} - 0.2S)^2}{R_{day} + 0.8S} \quad (3–5)$$

Surface runoff will occur when the amount of rainfall exceeds the initial abstraction and infiltration to the root zone. Therefore, *CN* is a function of land-use, soil and antecedent soil moisture content. These functional relationships and *CN* values are provided in the SWAT manual and user guide (Neitsch et al. 2011).

The soil bulk density ( $\rho_b$ ,) and saturated hydraulic conductivity ( $K_{sat}$ ) of a soil play an important role in the water movement through the soil profile, and also make water accessible for surface runoff and evapotranspiration. The effects of $\rho_b$ and $K_{sat}$ are explained with the relationships of soil-water constants. Field capacity (*FC*), available soil water content (*AWC*) and permanent wilting point (W*P*) are the three constants of soil-water content of a given soil that determine water fluxes in the soil profiles. They are related in the expression given in equation 3-6:

$$FC_{ly} = WP_{ly} + AWC_{ly} \quad (3\text{–}6)$$

where $FC_{ly}$ is the water content of a given soil layer at field capacity, $WP_{ly}$ is the water content of a given soil layer (ly) at permanent wilting point, and $AWC_{ly}$ is the available soil water content of the layer, all expressed as a fraction of the total soil volume. SWAT estimates $PW$ using equation 3-7:

$$PW_{ly} = 0.40 * \frac{m_c * \rho_b}{100} \quad (3\text{–}7)$$

where $m_c$ is the percent clay content (%), and $\rho_b$ is the bulk density of the soil layer (Mg $m^{-3}$). Actual water content of the given soil layer is the forcing input of percolation. Water percolates to the next layer if the water content of the given layer exceeds its field capacity by $SW_{ly,excess}$ as expressed by equations 3-8 and 3-9:

$$SW_{ly,excess} = SW_{ly} - FC_{ly} \quad \text{if} \quad SW_{ly} > FC_{ly} \quad (3\text{–}8)$$

$$SW_{ly,excess} = 0 \quad \text{if} \quad SW_{ly} \leq FC_{ly} \quad (3\text{–}9)$$

where $SW_{ly,excess}$ is the drainable volume of water in a given soil layer on a given day, $SW_{ly}$ is the soil layer water content on a given day, and $FC_{ly}$ is the field capacity water content of the soil layer on the same day, all in mm water (mm $H_2O$). The amount of water that moves from a given soil layer to its underlying layer is calculated using the storage routing equation 3–10:

$$w_{perc,ly} = SW_{ly,excess} * (1 - \exp[\frac{-\Delta t}{TT_{perc}}]) \quad (3\text{–}10)$$

where $w_{perc,ly}$ is the amount of water (mm $H_2O$) that percolates from a given soil layer on a given day, $\Delta t$ is the length of the time steps (hrs) and $TT_{perc}$ is the travel time of percolation in the soil layer (hrs).

The travel time of percolation ($TT_{perc}$) is a function of the saturation water content ($SAT_{ly}$) in mm $H_2O$, and saturated hydraulic conductivity ($K_{sat}$) in mm $h^{-1}$ of the given soil layer as in equation 3-11:

$$TT_{perc} = \frac{SAT_{ly} - FC_{ly}}{K_{sat}} \tag{3–11}$$

Water that percolates in the underlying soil layer can flow to the nearby reach as a subsurface flow and/or percolates to the next soil layer. Water that percolates from the lowest soil layer enters to the vadose zone, i.e., the unsaturated zone between the lowest soil layer and the top of the aquifer (Figure 3-1).

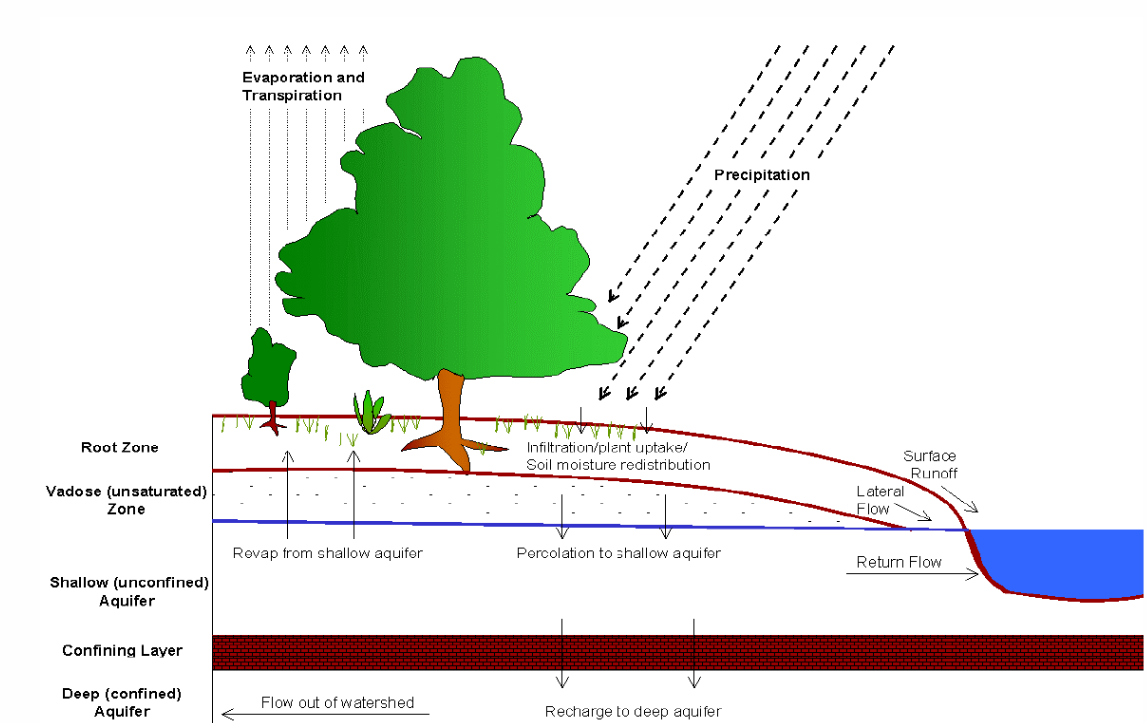


Figure 3-1 Schematic representation of hydrologic cycle.

***Source: Neitsch et al. (2011)***

A portion of the surface runoff will reach the outlet of large watersheds where the time of concentration is greater than one day. The surface storage coefficient (*SURLAG*) in SWAT is incorporated to lag the portion of the runoff for more than a day. The portion of the runoff generated that is calculated using the *CN* procedure and reached at the main channel on a given day is calculated in equation 3-12:

$$Q_{surf} = (Q'_{surf} + Q_{stor,i-1}).\left(1 - \exp\left[\frac{-surlag}{t_{conc}}\right]\right) \quad (3–12)$$

where $Q_{surf}$ is the runoff portion discharged to the main channel on a given day (mm $H_2O$), $Q'_{surf}$ is the portion of runoff generated on that day (mm $H_2O$), $Q_{stor,i-1}$ is the surface runoff lagged from the previous day (mm $H_2O$), and $t_{conc}$ is time of concentration of the sub-watershed (hrs). Time of concentration is the total time needed for a drop of rain from the remotest point in the sub-watershed to the reach. This parameter consists of time of overland flow-$t_{ov}$, i.e., the time needed to take the water upstream to the outlet of the sub-watershed, and time of channel flow-$t_{ch}$, all in hours. It is given by equation 3-13:

$$t_{conc} = t_{ov} + t_{ch} \quad (3–13)$$

**2. Evapotranspiration:** This is a term collectively used for the water in a given watershed that is converted to water vapor. It is the interaction of water from soil-vegetation surface and atmosphere. Evapotranspiration exceeds the runoff generated at continental levels (Dingman 1994). Potential evapotranspiration, *PET*, is defined as the amount of water transpired by a green 30-50 cm high alfalfa crop completely shading the ground with unlimited soil water supply (Thornthwaite 1948; Jensen et al. 1990). This amount is the base to calculate actual evapotranspiration of any given day for a given land-use and soil water supply. Two of the three methods used by SWAT that are used in this study to calculate *PET* are the Penman-Monteith (Monteith 1965; Allen 1986; Allen et al. 1989) and Hargreaves (Hargreaves et al. 1985) methods. The Penman-Monteith method uses the parameters solar radiation, maximum and minimum air temperature, relative humidity and wind speed to calculate potential evapotranspiration, while the Hargreaves method requires only maximum and minimum air temperature. The Hargreaves method can be used in a study area where solar radiation, relative humidity and wind speed data are not available.

The Penman-Monteith method combines energy, aerodynamic and surface resistance terms that account for water vapor removal to the atmosphere. It is given by the equation 3-14:

$$\lambda E = \frac{\Delta.(H_{net} - G) + \rho_{air}.c_p.[e_z^o - e_z]/r_a}{\Delta + \gamma.(1 + r_c/r_a)} \tag{3–14}$$

where $\lambda E$ is the latent heat flux density in MJ m$^{-2}$ d$^{-1}$, *E* is potential evapotranspiration (*PET*) rate in mm d$^{-1}$, $\Delta$ ($d(e)/d(T)$ in kPa °C$^{-1}$) is the slope of the saturation vapor pressure-temperature curve, $H_{net}$ is the net radiation in MJ m$^{-2}$ d$^{-1}$, *G* is the heat flux density to the ground in MJ m$^{-2}$ d$^{-1}$, $\rho_{air}$ is the air density in kg m$^{-3}$, $c_p$ is the specific heat at constant pressure in MJ kg$^{-1}$ $^{\circ}C^{-1}$, $e_z^o$ is the saturation vapor pressure of air at height z in kPa, $e_z$ is the water vapor pressure of air at height z in kPa, $\gamma$ is the psychrometric constant in kPa $^{\circ}C^{-1}$, $r_c$ is the plant canopy resistance in s m$^{-1}$, and $r_a$ is the diffusion resistance of the air layer or aerodynamic resistance in s m$^{-1}$.

The Hargreaves method uses equation 3-15:

$$\lambda E = 0.0023.H_o.(T_{mx} - T_{mn})^{0.5}.(\overline{T}_{av} + 17.8) \tag{3–15}$$

where $\lambda$ is the latent heat of vaporization in MJ kg$^{-1}$, *E* is potential evapotranspiration (*PET*) rate in mm d$^{-1}$, $H_o$ is the extraterrestrial radiation in MJ m$^{-2}$ d$^{-1}$, $T_{mx}$ is the maximum air temperature in $^{\circ}C$, $T_{mn}$ is the minimum air temperature in $^{\circ}C$, and $\overline{T}_{av}$ is the mean air temperature in $^{\circ}C$. Details and relationship of terms given in equations 3-14 and 3-15 are well described in Allen et al. (1998).

After *PET* is calculated, SWAT quantifies the actual evapotranspiration (*AET*) that is composed of surface evaporation and transpiration through plant cells. SWAT first calculates evaporation from the canopy and then evaporation from the soil surface and sublimation from snow, if any, at hydrological response unit (HRU) level. All these components of the actual evapotranspiration are calculated as a function of *PET* with some additional parameters. For example, SWAT uses leaf area index (*LAI*) to calculate transpiration and a soil evaporation compensation coefficient (*ESCO*) to adjust the evaporative demand distribution through soil depth.

**3. Lateral flow:** This is the subsurface water flow for soils with high hydraulic conductivity. The saturated soil zone is formed through water that ponds above a local impermeable soil layer (perched water). This water is under atmospheric or less pressure. SWAT uses the kinematic storage model developed by Sloan and Moore (1984) to simulate subsurface flow in a two-dimensional section along a hillslope. The saturated hydraulic conductivity of the soil plays a role in controlling the lateral flow as indicated in the equation 3-16:

$$Q_{lat} = 0.024.\left(\frac{2.SW_{ly,excess}.K_{sat}.slp}{\phi_d.L_{hill}}\right) \tag{3–16}$$

where $Q_{lat}$ is lateral flow discharged at a hillslope outlet on a given day (mm $H_2O$), $SW_{ly,excess}$ is the volume of drainable water stored in a saturated soil layer for a given day (mm $H_2O$), $K_{sat}$ is saturated hydraulic conductivity of the soil layer (mm $h^{-1}$), *slp* is slope of the soil layer given by $\tan(\alpha_{hill})$, $\alpha_{hill}$ is hillslope segment angle to the horizontal, $\phi_d$ is the drainable porosity of the soil layer (mm/mm), and $L_{hill}$ is the hillslope length (m). The drainable volume of water stored in a saturated soil layer for a given day is calculated as excess soil water from the field capacity as in equation 3-17:

$$SW_{ly,excess} = SW_{ly} - FC_{ly} \text{ if } SW_{ly} > FC_{ly}\ ;\ SW_{ly,excess} = 0 \tag{3–17}$$

where $SW_{ly,excess}$ is the stored portion of drainable water in a saturated soil layer (ly) for a given day (mm $H_2O$), $SW_{ly}$ is soil moisture content of a soil layer at on a given day (mm $H_2O$), and $FC_{ly}$ is the field capacity soil water content of the given soil layer (mm $H_2O$).

**4. Groundwater:** This is water in the saturated zone under a pressure higher than atmospheric pressure (i.e., positive pressure). Water can join the groundwater system by infiltration, percolation or/and seepage from the water bodies. It mainly leaves this system by discharge into rivers or water bodies (return flow or baseflow). It can also move upward to the unsaturated zone and then evapotranspires through the capillary fringe.

Groundwater in SWAT is divided into two aquifer systems. The first is a shallow, unconfined aquifer that contributes return flow to streams (groundwater flow or baseflow). The second is a deep, confined aquifer that does not contribute return flow to streams inside the watershed. Water is deep percolated into the confined aquifer and is assumed lost from the given watershed.

The time needed to recharge the shallow aquifer through the vadose zone through bypass flow or percolation is important to partition water as surface and groundwater flow. The hydraulic properties of the geologic formation determine this value. SWAT uses an exponential decay weighing function (Sangrey et al. 1984) to quantify the time delay of the aquifer recharge. Water passing the soil layer and recharging the two aquifers is given by equation 3-18:

$$w_{rchrg,i} = (1 - \exp[-1/\delta_{gw}]).w_{seep} + \exp[-1/\delta_{gw}].w_{rchrg,i-1} \qquad (3\text{–}18)$$

where $w_{rchg,i}$ is the recharge amount entering the aquifers on $i$ day (mm $H_2O$), $\delta_{gw}$ is the groundwater delay time or drainage time of the overlaying geologic formation (days), $W_{seep}$ is amount of water existing at the bottom of the soil profile on day $i$ (mm $H_2O$), and $w_{rchrd,i-1}$ is the recharge amount entering the aquifers on $i-1$ day (mm $H_2O$).

Part of the recharged water is routed to the deep aquifer as in equation 3-19:

$$w_{deep} = \beta_{deep}.w_{rchrg} \quad (3\text{–}19)$$

where $w_{deep}$ is the water amount passing to the deep aquifer on a given day (mm $H_2O$), $\beta_{deep}$ is the aquifer percolation constant, and $w_{rchrg}$ is the recharge amount entering the aquifers on a given day (mm $H_2O$). The groundwater delay time, $\delta_{gw}$, and the aquifer percolation constant, $\beta_{deep}$, are important parameters (SWAT parameters *GW_DELAY* and *RCHRG_DP*, respectively) and were used to adjust the water balance during the calibration stage of this study. Groundwater delay time is varied with respect to depth of the water table and the hydraulic properties of the soil and geological structure. It is estimated indirectly by simulation of aquifer recharge of a given watershed or optimizing simulation of the groundwater level with measured values. Once the *GW_DELAY* value is calibrated for a given watershed, it can be used for other watersheds within similar geomorphic areas (Sangrey et al. 1984). *GW_DELAY* can shift the hydrograph limbs of simulation to adjust lagging curves.

The Hooghoudt (1940) steady-state ground water response to a given recharge is used to quantify baseflow to a given reach (equation 3-20):

$$Q_{gw} = \frac{8000.K_{sat}}{L_{gw}^{\ 2}}.h_{wtbl} \quad (3\text{–}20)$$

where $Q_{gw}$ is the baseflow into the given reach on a given day (mm $H_2O$), $K_{sat}$ is saturated hydraulic conductivity of the shallow aquifer (mm day$^{-1}$), $L_{gw}$ is the distance from the sub-watershed divide to the reach (m), and $h_{wtbl}$ is the water table height (m). The groundwater discharge during no recharge time can be simplified as given by equation 3-21:

$$Q_{gw} = Q_{gw,o}.\exp[-\alpha_{gw}.t] \quad \text{if } aq_{sh} > aq_{shthr,q} \text{ otherwise } Q_{gw}=0 \quad (3\text{–}21)$$

where $Q_{gw,o}$ is the baseflow into the given reach at the beginning of the recession curve (mm $H_2O$), $\alpha_{gw}$ is the baseflow recession constant (vary from 0 to 1) in days, $aq_{sh}$ is amount of water stored in the shallow aquifer on a given day (mm $H_2O$), and $aq_{shthr,q}$ is the threshold water level in the shallow aquifer for which groundwater starts to contribute baseflow (mm $H_2O$). $\alpha_{gw}$ and $aq_{shthr,q}$ are important parameters in SWAT (*ALPHA_BF* and *GWQMN*, respectively).

Baseflow alpha factor in days (*ALPHA_BF*) is the baseflow recession constant of proportionality between groundwater flow and recharge changes to the aquifer (Smedema and Rycroft 1983). *ALPHA_BF* varies from 0.1 to 0.3 for watersheds that respond slowly to groundwater change and from 0.9 to 1.0 for fast response watersheds. It can be estimated by analyzing the recession curve of the measured discharge hydrograph of a watershed during the no-recharge period.

If the water table in the shallow aquifer exceeds *GWQMN*, baseflow to a reach has occurred, otherwise there is no baseflow. Altering this value can control the amount of water fluxes to baseflow directly, and to *AET* as "revap" flow indirectly. That means that increasing *GWQMN* can decrease baseflow, and vice versa.

When the overlying soil surface is dry and the underlying layer is wet, water will diffuse upward and evaporate. Water is also removed from the shallow aquifer by deep-rooted plants. SWAT models this removal; the process is called "revap". It occurs only if the water content in the shallow aquifer exceeds a certain revap threshold level during a dry period. The maximum amount of water that can pass through the revap process is given by equation 3–22:

$$w_{revap,mx} = \beta_{rev} . E \qquad (3\text{–}23)$$

where $w_{revap.mx}$ is the maximum amount of water moving into the soil zone (mm $H_2O$), $\beta_{rev}$ is the revap coefficient (*GW_REVAP* in SWAT), and *E* is the potential evapotranspiration (*PET*) of the given day (mm $H_2O$). The actual amount of revap is then calculated as in equation 3–24:

$w_{revap} = w_{revap,mx} - aq_{shthr,rvp}$ if $aq_{shthr,rvp} > aq_{sh} < (aq_{shthr,rvp} + w_{revap,mx})$

$w_{revap} = w_{revap,mx}$ *if* $aq_{sh} \geq (aq_{shthr,rvp} + w_{revap,mx})$

Otherwise, $w_{revap} = 0$ (3–25)

where $w_{revap}$ is the actual amount of water moving into the soil zone (mm $H_2O$), $aq_{sh}$ is the amount of water stored in the shallow aquifer for a given day (mm $H_2O$), and $aq_{shthr,rvp}$ (*REVAPMN* in SWAT) is the threshold water level in the shallow aquifer for a revap to take place (mm $H_2O$).

*GW_REVAP* is a coefficient that governs revap flow. There is no revap flow if *GW_REVAP* is zero and revap is equal to *PET* when its value is 1.0. *GW_REVAP* varies from 0.02 to 0.20.

**5. Channel flow:** Effective hydraulic conductivity in the main channel alluvium (mm/hr) (CH_K(2) in SWAT) controls the amount of water lost or gained within a given reach according to whether the type of the reach bed materials is effluent or influent. Values of *CH_K(2)* as initial condition for different bed materials are given in Lane (1983); they can also be obtained during calibration of SWAT. The SWAT parameters discussed above are listed in Table 3-1.

**Table 3-1 SWAT parameters used for calibration**

| Parameter | Code | Description |
|---|---|---|
| 1 | *CN2* | Initial *SCS* curve number value for moisture condition 2 |
| 2 | *ALPHA_BF* | Baseflow alpha factor |
| 3 | *SOL_AWC* | Available water capacity |
| 4 | *SOL_K* | Saturated hydraulic conductivity |
| 5 | *RCHRG_DP* | Deep aquifer percolation fraction |
| 6 | *GWQMN* | Threshold water depth in the shallow aquifer for flow |
| 7 | *GW_REVAP* | Groundwater revap coefficient |
| 8 | *REVAPMN* | Threshold water depth in the shallow aquifer for revap |
| 9 | *ESCO* | Soil evaporation compensation factor |
| 10 | *GW_DELAY* | Groundwater delay |
| 11 | *SURLAG* | Surface runoff lag coefficient |

# 4 WATER USE AND PRODUCTIVITY OF SMALL-SCALE IRRIGATION SCHEME

## 4.1 Summary

In Ethiopia, irrigation is mainly implemented in small-scale irrigation schemes, and these are often characterized by low water productivity. This part of the study analyzes the efficiency and productivity of a typical small-scale irrigation scheme in the highlands of the Blue Nile, Ethiopia. Canal water flows and the volume of irrigation water applied were measured at field level. Grain and crop residue biomass and grass biomass production along the canals were also measured. To triangulate the measurements, irrigation farm management, effects of water logging around irrigation canals, farm water distribution mechanisms, effects of night irrigation, and water losses due to soil cracking created by prolonged irrigation were closely observed. The average canal water loss from the main, secondary and field canals was 2.58, 1.59 and 0.39 l $s^{-1}$ 100 $m^{-1}$, representing 4.5, 4.0 and 26% of the total water flow, respectively. About 0.05% of the loss was attributed to grass production for livestock, while the rest was lost through evaporation and canal seepage. Grass production for livestock feed had a land productivity of 6190.5 kg $ha^{-1}$ and a water productivity of 0.82 kg $m^{-3}$. Land productivity for straw and grain was 2048 and 770 kg $ha^{-1}$, respectively, for tef, and 1864 kg $ha^{-1}$ and 758 kg $ha^{-1}$, respectively, for wheat. Water productivity of the crops varied from 0.2 to 1.63 kg $m^{-3}$. A significant volume of water was lost from the small-scale irrigation systems mainly because farmers' water application did not match crop needs. The high price incurred by pumped irrigation positively affected water management by minimizing water losses, and forced farmers to use deficit irrigation. Improving water productivity of small-scale irrigation requires integrated interventions including night storage mechanisms, optimal irrigation scheduling, and empowerment of farmers to maintain canals and to have proper irrigation schedules.

## 4.2 Introduction

Ethiopia, where recurrent drought affects agriculture, has 12 river basins and 19 natural lakes (see section 2.4). The mean annual surface water flow in Ethiopia is estimated at 122 $km^3$ (MCE 2001; MoWR 1999), and the potential irrigable land is reported to be about 3.7 million ha. Despite the huge potential of water and land resources, only 5% was actually under irrigation (Awulachew et al. 2005). In view of the increasing population and the corresponding demand for food, improvement of irrigation water management and intensification of agricultural practices are important. This has triggered the Ethiopian government to embark on developing small-scale irrigation schemes (Awulachew et al. 2007; MoFED 2006; Lambiso 2005). Different studies (e.g., Turner 1994; Vincent 1994; 2003) have advocated that more emphasis needs to be placed on the design, implementation, performance and hydrology of small-scale irrigation schemes. On the other hand, investments in large-scale irrigation schemes have often failed with regard to their anticipated performance (Faulkner et al. 2008). According to MoWR (1999) small-scale irrigation schemes are defined as those covering less than 200 ha. These constituted 67.5% (5718.7 ha) of the irrigated area in Amhara National Regional State.

In the mixed farming systems of sub-Saharan Africa in general, and of Ethiopia in particular, irrigation farming produces large amounts of livestock feed in the dry season. The feed includes grasses growing near the canals and the field borders as well as crop residues. Crop residue accounts for 60% of the annual feed in the study area (Descheemaeker, personal communication, 2010). Therefore, in mixed farming systems, it is crucial to consider water productivity of irrigation water with respect to both food and feed production.

Studies in different parts of the world have evaluated and monitored irrigation performance using adequacy, efficiency, dependability and equity as indicators (Molden and Gates 1990; Molden et al. 1998; Unal et al. 2004). All these performance indicators are based on the water balance of the system and were used to identify spatial and temporal trends. According to Unal et al. (2004), performance evaluation is used to assess the impact of interventions, to diagnose constraints, to understand factors that increase performance, to compare performance both within and outside the studied irrigation system, and to improve the irrigation system's overall productivity. Perry (1996) also conceptualized the components of the water balance in agricultural systems in terms of inflows (as canal/diverted supplies and rainfall) and outflows (as crop transpiration, non-beneficial evaporation, drainage, and net groundwater flow) and their interactions.

Data on the performance of small-scale irrigation schemes are scarce in Ethiopia in particular (Awulachew et al. 2007) and in Africa in general (Faulkner et al. 2008). This study was designed to establish water depletion and food and feed water productivity, and in order to assess which, where and when interventions could be applied to improve the water productivity of such schemes. Therefore, the objectives of this study were:

(i) To quantify irrigation water loss and water needed and used to produce biomass,

(ii) To quantify feed and food water productivity, and

(iii) To identify opportunities for improving irrigation efficiency and productivity.

### 4.3 Materials and methods

#### 4.3.1 Study area

The study area, the *Guanta* small-scale irrigation scheme, is located in the highlands of the Blue Nile basin 11°50´N and 37°39´E at 1797 m asl in Ethiopia (Figure 4-1; Figure 2-1). It was selected based on accessibility, representativeness of small-scale irrigation in the study watershed, and availability of information. A stone masonry diversion structure and a 1555 m main canal (conveying water from the diversion) were constructed by the local government in 2001; 850 m of the main canal and 1341 m of the secondary canal conveying water from the main canal were not yet lined. The layout of field canals (conveying water from the secondary canals to the individual fields) varied from time to time, and it was difficult to map them. Other land units in the scheme were drainage basins and wetlands. Drainage basins were enclosed gully-like natural flood basins during the main rain rainy season. Farmers released excess irrigation water to these basins after irrigating their plots. On the other hand, wetlands were irrigated lands in the first years of the scheme. These land units were changed to wetlands due to the overflow of water from the secondary canals and drainage basins. In 2009, the irrigation scheme had an area of 90 ha, of which 21 ha were covered by pump irrigation at the upstream side of the main canal.

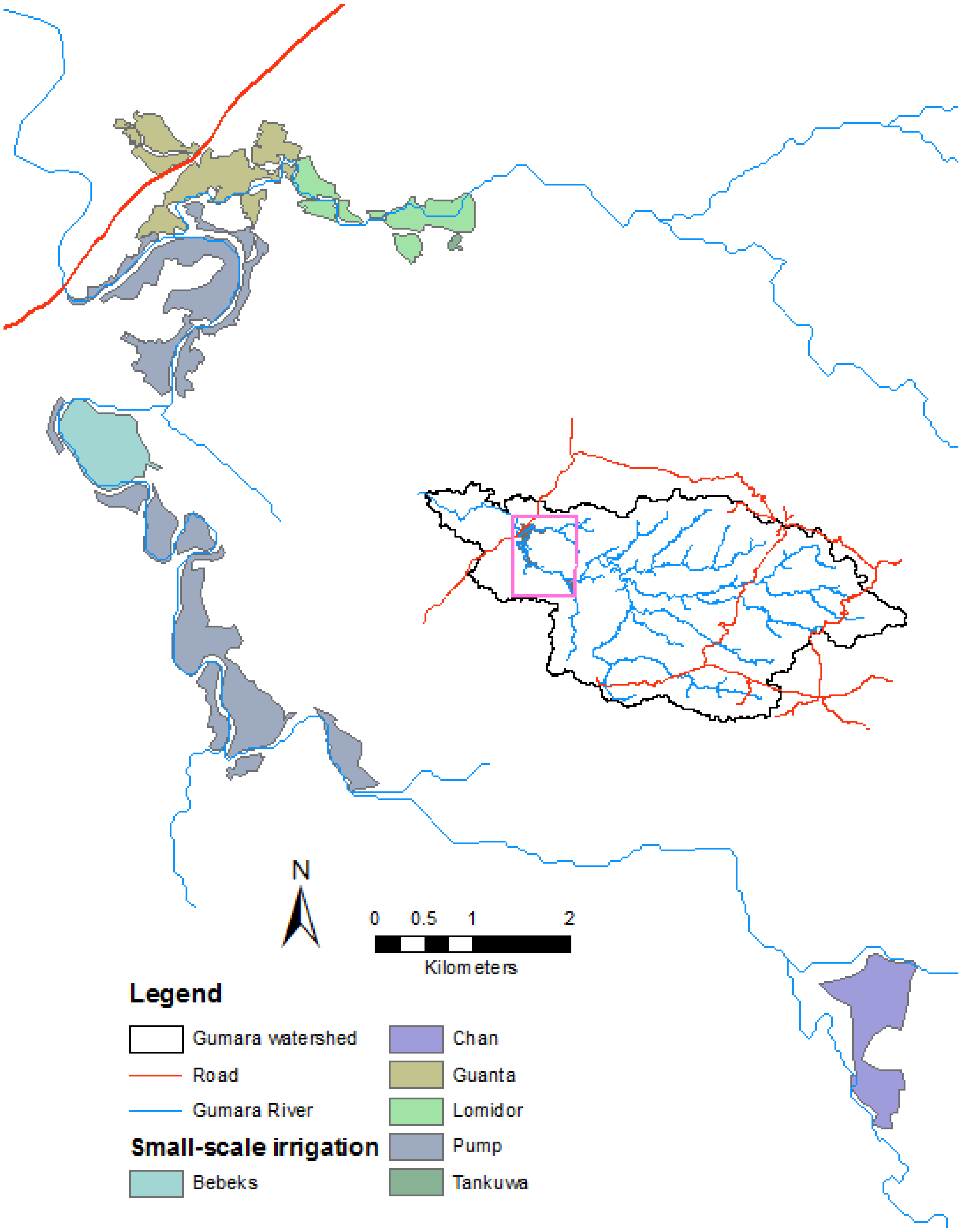


Figure 4-1 Location of *Guanta* and other small-scale irrigation schemes in *Gumara* watershed

A Water Use Association (WUA) was formed, and rules for water price, canal maintenance, and water allocation were established with the help of the government. However, no rules were functional. The canals were not maintained on time. Water allocation was done randomly mainly through agreements among some influential and wealthy farmers. In an in-depth analysis, Deneke et al. (2011) reported on the effect of group/village power on water allocation, lack of transparency in scheme boundaries and land redistribution, rule enforcement mechanisms, and theft and corruption with respect to water allocation.

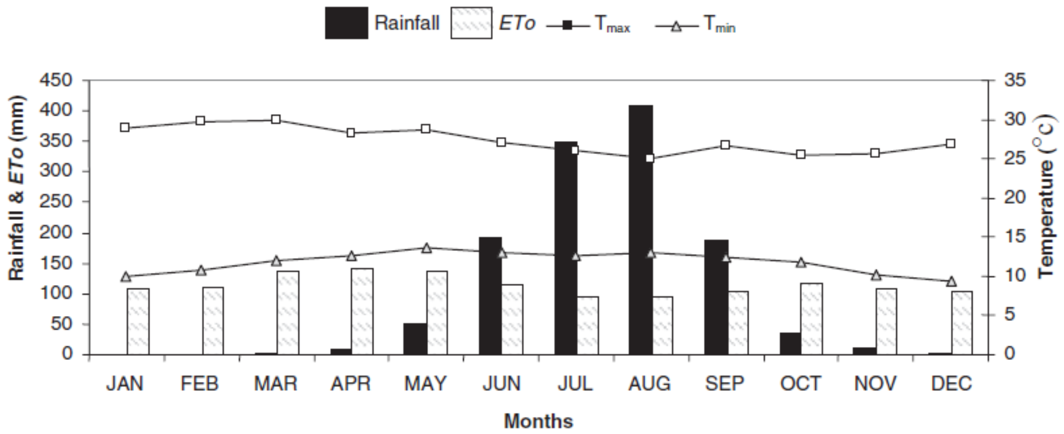


Figure 4-2 Average monthly rainfall (mm), monthly potential evapotranspiration (*PET*) (mm), daily maximum temperature ($T_{max}$) and minimum temperature ($T_{min}$) (◦C) for *Guanta* irrigation scheme (1991-2009).

***(weather data from nearby climatic station in Bahir Dar, (11°35´N, 37°23´E; 1798 m asl) and Woreta (14°40´N, 37°42´E; 1825 m asl).***

The main soil types in the scheme were Eutric Fluvisols and Eutric Vertisols (MoWR, 2008). Soil samples were taken at 0-50 cm and 50-100 cm depths for laboratory analysis and average soil characteristic values of each soil type were reported (MoWR 2008). The mean annual rainfall over the period 1991-2009 was 1248 mm, and mean maximum and minimum daily temperatures were 27 °C and 12 °C, respectively. Climate data were obtained from the nearby meteorological stations at *Bahir Dar* and *Woreta* (Figure 4.2).

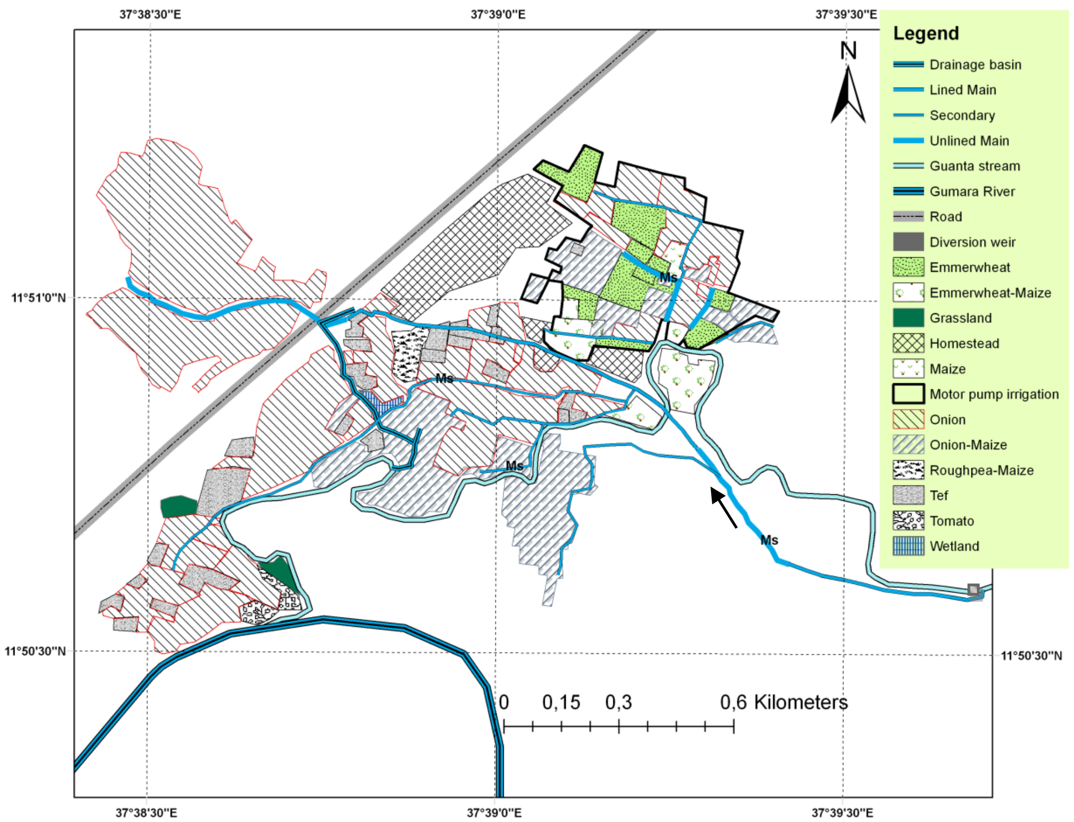


Figure 4-3 *Guanta* small-scale irrigation scheme, highlands of the Blue Nile Basin, Ethiopia.

***'Ms' shows the position of the canal discharge measurement stations.***

Farmers at the study site have mixed crop-livestock production systems. The average livestock holding was 3.2 TLU (tropical livestock unit, where 1 TLU is 250 kg live weight) per family, and the stocking rate was 2.3 TLU per ha (Descheemaeker, personal communication, 2010). There is a severe feed shortage in the flooded period of the main rainy season (Haileslassie et al. $2009_b$) when farmers commonly store crop residue to feed their livestock. Rice (*Oryza sativa*), finger millet (*Eleusine coracana*), Maize (*Zea mays*) and tef (*Eragrostis tef*) were the main crops cultivated during the rainy season (June to September). After harvesting rice, rough pea (*Lathyrus hirsutus*) and chick pea (*Cicer arietinum*) were grown between October and December using the residual soil moisture. Onion (*Allium cepa*) was the main irrigated crop in the dry season (from January to May). Other crops like emmer wheat (*Triticum dicoccum*), called wheat hereafter, tef, maize and tomato (*Lycopersicon esculentum*) were of secondary importance in the irrigation scheme (Figure 4-3 and Table 4-1). The cropping pattern in the irrigation scheme strongly depended on the availability of water and the market price. Thus, the farmers' decision on what crop type and when to grow was based on their evaluation of the market conditions at harvest time. For example, in 2009 farmers opted for wheat (low yielding and high market valued variety) due to the fear of market failure for onions as occurred in the previous year (data not given). Tef is a special crop in Ethiopia accounting for 25% of the cereal production and 66% of the protein in the national diet (NAS 1996). In addition, tef has soft, nutritious and palatable straw for use a livestock feed.

Table 4-1 Land-use in *Guanta* small-scale irrigation scheme in 2009 irrigation season (January to June).

| **Crop or land-use type** | **Area (ha)** | **%** |
|---|---|---|
| Emmer wheat | 9.92 | 11.0 |
| Maize | 0.41 | 0.5 |
| Onion | 71.31 | 79.2 |
| Rough pea-maize | 0.97 | 1.1 |
| Tef | 6.29 | 7.0 |
| Tomato | 0.87 | 1.0 |
| Wetland | 0.28 | 0.3 |
| Total | 90.03 | 100.0 |
| Maize* | 22.90 | 25.4 |

***Maize planted as a relay crop in onion fields before onion harvest***

A short-maturing tef variety (locally called *Bukri* and harvested within 47 days) was used by farmers during this study. About 79% of the scheme was covered by onion, 18% by wheat and tef, and 2% by grasslands around canals and wetlands during the 2009 irrigation season. About 25% of the scheme was covered by maize as a relay crop with onion. After the onion was harvested, the maize crop used the rain of the wet season until its maturity.

### 4.3.2 Sampling and data collection

The fields, wetlands and canals of the scheme were mapped before determining the number and position of the sampling points. A Garmin e-trax Geographical Positioning System (GPS) and Satellite Pour l'Observation de la Terre (SPOT) satellite imagery from Google Earth (www.googleearth.com) were used to locate the study plots and to formulate a land-use map of the scheme. Wetlands and drainage basins (Figure 4-4) were delineated and their dimensions were measured. Irrigation canals were characterized as main (Figure 4-5), secondary or field canals. All fields were characterized as fed either by pump or gravity irrigation. Unlined main and secondary canals had average grassland borders of 6.6 m width (range 2.5-10.2 m). Throughout the irrigation season (January to May), canal layout, canal maintenance, water distribution and water availability across the command area of the scheme were monitored and mapped. Informal surveys were conducted using participatory rural appraisal tools, particularly informal group and individual discussions, to understand the major causes of water shortage and water loss, and upstream-downstream complexities from the perspective of local farmers.

Figure 4-4 Drainage basin (left) and wetland (right)

To estimate biomass production, 11 irrigated fields (4 wheat fields, 3 onion fields and 4 tef fields) were selected to represent the major crops cultivated in the scheme and to represent spatial distribution. At each selected field, a plot of about 400 $m^2$ was delineated and pegged, and the amount of applied water was measured (as described later) for each irrigation event from planting to harvesting. Crop biomass samples were taken at harvest time from three 1-$m^2$ plots distributed along the central line of each plot of tef and wheat. One of the wheat fields was very large, and half of it missed one irrigation event. Therefore, six sample plots were taken from this field to address the farm size and irrigation variation within the field, i.e., a total of 15 sample plots for wheat. Onion biomass was taken from 5-m furrow segments at 24 positions in each field from two gravity-irrigated fields and at 12 positions from one pump-irrigated field with a total of 60 sample furrow segments. Four fields were selected for collection of data on maize relay cropping; however, the crop was destroyed by hail on 1 July 2009. Grass biomass, dominated by *Cyprus rotundus* and *Cynodon dactylon*, was sampled in ten 1-$m^2$ plots along canals and within wetlands. During the irrigation season (about 120 days), the grass was repeatedly mowed on the sample plots (32 samples from canal boundaries, 38 samples from drainage basins, and 14 samples from wetlands) when grass height reached about 0.2 m. Each sample was dried to constant weight, and grain, straw and grass biomass production determined using a 0.001-kg sensitive balance. Crop residue production from grass, wheat and tef (covering about 20% land of the scheme) was calculated. Based on an assessment study on TLU-dry matter (DM) need by FAO (1993), 8.5 kg DM per TLU per day was used to quantify the number of TLU that could be fed during 60 days, assuming a high feed shortage due to flooding for the whole main rainy season.

Figure 4-5 Grass production along main canal (left), Replogle-Bos-Clemmens flume (center) and cutthroat flume (right)

Canal flow measurements were taken at two points of a canal (100 m apart) to determine the amount of water lost through evaporation and seepage using inflow-outflow methods as described below. Continuous manual recordings of water levels were done twice monthly for four months, and every measurement took five hours. Replogle-Bos-Clemmens (RBC) flumes (Clemmens et al. 1984) were used to measure field canal loss and amount of water used to irrigate farm plots at every event throughout the irrigation season. Cutthroat flumes (Skogerboe et al. 1973) of 0.91 m length and 0.41 m width were used to measure the water flow in the main and secondary canals (Figure 4-5). Manual water levels measured with the cutthroat flumes were transformed to flow rates using theoretical rating equations according to the manufacturer's manual (Eijkelkamp, undated). Although field installation and construction errors are always present, the flumes used for this study were selected for their greater accuracy (Clemmens et al. 1984; Eijkelkamp, undated; Skogerboe et al. 1973) compared to other methods, such as Parshall flumes or the ponding method.

### 4.3.3 Data preparation and analysis

Potential evapotranspiration (*PET*) and crop water requirements were calculated using the Penman-Monteith and crop coefficient procedures described in Allen et al. (1998). The database was formulated to use this procedure in order to minimize the uncertainty of the *Bahir Dar* station data. Therefore, rainfall and temperature data from *Woreta* and relative humidity, wind speed and sunshine hours from *Bahir Dar* meteorological stations were used to calculate reference evapotranspiration.

The water balance of irrigated fields was calculated using the water balance equation (4-1) for the growing season at field level.

$$\Delta SM = \left(P_{eff} + I + Q_r\right) - (AET + D) \tag{4–1}$$

where $\Delta SM$ is the change in soil moisture content before the first irrigation and after harvest, $P_{eff}$ is effective rainfall, $I$ is total irrigation water applied, $AET$ is actual evapotranspiration, $D$ is drainage loss, and $Q_r$ is capillary rise.

All quantities were defined within the same time domain (growing period) and units (mm $H_2O$). Total irrigation need was computed using climate, crop and soil data with FAO CROPWAT version 8.0 (FAO, 2009). $\Delta SM$ was calculated as the difference between soil moisture content before the first irrigation and soil moisture content after harvest. Soil moisture data were determined using a gravimetric method with dry bulk density data adopted from MoWR (2008). $P_{eff}$ was calculated using the empirical formula of the United States Department of Agriculture's Soil Conservation Service. It was selected from the three options found in CROPWAT 8.0 software as it was developed for long-term climatic and soil moisture data (FAO 1978). Actual evapotranspiration (*AET)* was calculated by multiplying the crop coefficient, $K_c$, with the water stress factor, $K_s$. $K_s$ is a function of total available water, *TAW*, readily available water and root zone depletion. It was estimated from the daily water balance computation (Allen et al. 1998). The crop parameters crop growth stages, allowable depletion factor and rooting depth were adopted from Allen et al. (1998). Length of cropping season was taken from the field data. Since tef is a local crop where these important parameters are not given in the literature, grass values were adopted. Grass $K_c$ values are also almost similar to average values of cereal crops. The crop coefficient for the grasslands around canals, drainage basins and wetlands was formulated using the mean values of legumes and grasses previously reported (Haileslassie et al. $2009_{a;b}$). Drainage loss was calculated as the sum of irrigation water that was applied above field capacity at every irrigation event. It should be noted that drainage loss here is not the difference between irrigation water applied and irrigation water required. Capillary rise was not considered, as the groundwater table was more than 2 m deep (Allen et al. 1998; MoWR 2008). Soil physical characteristics, such as bulk density and *TAW* content, were adopted from MoWR (2008), as the data were generated from the same scheme. Field capacity was calculated from *TAW* and root depth.

Canal or conveyance loss (in l $s^{-1}$ 100 $m^{-1}$ canal length) was calculated as presented in equation 4-2 using the inflow-outflow method.

$$Conveyance\ loss = Q_{in} - Q_{out} \tag{4–2}$$

where $Q_{in}$ is water flow rate at the upper side of 100-m long canal segment (measured), and $Q_{out}$ is water flow rate at the lower end of 100-m long canal segment (measured).

Canal water loss was calculated as the percentage of conveyance loss to the average of $Q_{in}$ and $Q_{out}$ within 100-m canal segments. From field observations, data on total canal length and water loss per 100 m, an average of 30 l $s^{-1}$ water was reached at the end of the secondary canals and distributed to many field canals at the same time. Therefore, measured canal loss was calculated based on this 30 l s-1 for comparison.

Water productivity along canals and in irrigated fields was calculated using equations 4-3 and 4-4:

$$Irrigation\ water\ productivity = \frac{yield\ of\ the\ system}{Water\ diverted\ to\ the\ system} \tag{4–3}$$

$$AET\ water\ productivity = \frac{yield\ of\ the\ system}{Evapotranspired\ water\ from\ the\ system} \tag{4–4}$$

Irrigation and actual *ET* water productivity were calculated for both grain and dry straw biomass using two approaches. The traditional approach considered all the water supplied by irrigation and depleted by *AET* to compute grain or straw (but not for both) biomass water productivity. A new approach (Haileslassie et al. $2009_{a;b}$) used the water supplied by irrigation and depleted by *AET* for all biomass (both grain and straw) production. Therefore, yield of the system at the numerator side of the water productivity equations is larger than the traditional way of calculation. This can reflect the real situation in the farming system that both straw and grain were produced using the same *AET* water and that both were important for feed and food, respectively. Both approaches, hereafter termed as “traditional” and “new” water productivity, were used for comparison purposes.

Relative water supply (*RWS*), a performance indicator, was calculated using equation 4-5 taken from Levine (1982). It is the ratio of total water supplied by irrigation (*I*) and rainfall (*P*) to total water demanded by crop (i.e., actual crop evapotranspiration, *AET*).

$$RWS = \frac{I + P}{AET} \tag{4–5}$$

RWS was calculated for the growing season for selected crops for both gravity and pump irrigation.

After the field data had been processed using the above procedures, statistical analysis was conducted using descriptive statistics, one-way analysis of variance, which compares groups sample means with one factor at a time (SPSS Inc. 2007), for the 3 crop types, and t-test for gravity and pump irrigation types. Means were compared using the least significant difference test at significance level $p \leq 0.05$.

## 4.4 Results

### 4.4.1 Water loss and grass production around canals and wetlands

The highest water loss rate in l $s^{-1}$ 100 $m^{-1}$ was from the main canal while the lowest was from field canals (Table 4-2). The highest daily volume of water was lost from the field canals when a 30 l $s^{-1}$ flow rate was assumed for all canal types. Calculations of the loss for the total flowing rate (30 l $s^{-1}$) showed that about 26% of the water in the field canals was lost. This loss was much lower for the main and secondary canals at 4.49% and 4.00%, respectively (Table 4-2).

Grasslands and wetlands were part of the irrigation scheme and consumed irrigation water while producing biomass. The grasslands produced grass biomass using seepage water from the canals. Wetlands were formed under the influence of excess drainage water, and freely released water from the irrigated fields. Wetlands and drainage basins were not observed in the motor pump irrigation area. The *ET* water productivity of grassland varied with farm position from 0.4 to 1.2 kg $m^{-3}$, which was below the productivity of the rain-fed wetlands (Table 4-3). The grassland in the drainage basin was the most productive, while the wetland showed the lowest productivity. Land productivity was quite high, ranging from 3000 to 9000 kg $ha^{-1}$ (Table 4-3). Although grass production can be considered as a productive use of the water lost through canal seepage, only about 0.05% of the water lost from the canals was actually used for grass production. The other part was lost through canal storage, deep drainage, water surface evaporation and flow back to the river system.

Table 4-2 Canal water losses due to water surface evaporation and seepage from *Guanta* small-scale irrigation scheme

| Canal type | N† | Average flow rate (l/s) | Std. Error | Loss (l/s/100m) | Std. Error | % loss (100 $m^{-1}$)‡ | Std. Error | % loss/ 100m/30l/s |
|---|---|---|---|---|---|---|---|---|
| Main canal | 121 | $43.2^{a}$ | 0.4 | $2.4^{a}$ | 0.4 | $6.5^{a}$ | 1.0 | $4.5^{b}$ |
| Secondary canal | 57 | $33.0^{b}$ | 0.7 | $1.6^{b}$ | 0.6 | $4.4^{b}$ | 2.2 | $4.0^{b}$ |
| Field canal | 49 | $2.9^{c}$ | 0.3 | $0.4^{c}$ | 0.3 | $2.5^{c}$ | 12.9 | $25.9^{a}$ |

**†Number of observations**
**‡Percentage with respect to the seasonal average flow rate within each canal type**
**Values indicated by different superscript letter (a, b, and c) are significantly different at $p \leq 0.05$**

Table 4-3 Seasonal water productivity and land productivity of grasslands along earthen canals, in drainage basins, and in wetlands in *Guanta* irrigation scheme for the 2009 irrigation season

| | Seasonal water productivity (kg $m^{-3}$) | | | Seasonal land productivity (kg $ha^{-1}$) | | |
|---|---|---|---|---|---|---|
| | Canal boundaries† | Drainage basin‡ | Wetlands§ | Canal boundaries† | Drainage basin‡ | Wetlands§ |
| N† | 32 | 38 | 14 | 32 | 38 | 14 |
| Total area (ha) | 1.19 | 0.34 | 0.28 | 1.19 | 0.34 | 0.28 |
| Mean | $0.8^{b}$ | $1.2^{a}$ | $0.4^{b}$ | $6225.9^{b}$ | $9207.4^{a}$ | $3174.2^{b}$ |
| Std. Error | 0.1 | 0.1 | 0.1 | 641.9 | 1031.8 | 654.8 |
| Literature values (Haileslassie et al. $2009_{b}$) | 0.5-0.65 | 0.61-0.79 | | 1835-2386 | 3326-3866 | |

**†Grassland along canals; ‡wetland due to drainage water; §wetland due to overflow of irrigation water; †number of biomass samples. Values indicated by the different superscript letter (a, b, and c) are significantly different at $p \leq 0.05$.**

### 4.4.2 Comparative performance

Relative water supply, reflecting the availability of water in relation to crop demand, was 1.04 and 1.18 for wheat and onion, respectively (Table 4-4), indicating that the total water applied was similar to the crop needs. With a significantly different *RWS* value of 4.1, the average water applied for tef was four times (up to seven times in some plots) higher than the requirements. Tef had a much higher variation in *RWS* as compared to wheat and onion ($p \leq 0.05$.)

Relative water supply was significantly lower ($p \leq 0.05$) for motor pump than for gravity irrigation. Values were 0.5 and 1.35 under pump and gravity irrigation, respectively, for onion. Wheat and tef were not planted in either gravity or pump irrigation types, thus a comparison was not possible. This indicates that farmers under-irrigated their farms when using pumps and over-irrigated when using gravity irrigation.

Table 4-4 Relative water supply for different crops and irrigation types

| Parameter | Type | N† | Mean | Std. Error |
|---|---|---|---|---|
| Relative Water Supply (-) | Wheat | 4 | 1.0[b] | 0.1 |
| | Onion | 3 | 1.2[b] | 0.1 |
| | Tef | 4 | 4.1[a] | 0.6 |
| Relative Water Supply (-) | Pump | 5 | 0.8[b] | 0.1 |
| | Gravity | 6 | 1.9[a] | 0.2 |

**†Number of observations.**
**Values indicated by different superscript letter (a and b) are significantly different at $p \leq 0.05$**

### 4.4.3 Crop production and productivity

The productivity analysis revealed that grain biomass yield for tef and wheat was very similar at 770 and 759 kg $ha^{-1}$, respectively, whereas straw yield was slightly higher for tef at 2048 kg $ha^{-1}$ compared to 1864 kg $ha^{-1}$ for wheat (Table 4-5). The onion yield was 5903 kg $ha^{-1}$. Water productivity was higher for onion than for the cereals. On the other hand, irrigation water productivity (*IWP*) of crops was lower than evapotranspired water productivity (*EWP*) due to irrigation water application losses for both water productivity approaches for all crops, and for grain/bulb and crop residues. Due to high application losses, onion and tef had statistically similar *EWP* but statistically different *IWP*. Conventional *IWP* ranged from 0.18 to 1.39 kg $m^{-3}$, while improved *IWP* ranged from 0.68 to 1.78 kg $m^{-1}$ (Table 4-5).

In addition to *RWS*, a comparison of the amount of irrigation water applied to the amount of crop water needed showed that the total amount of irrigated water did not match that needed by the crops, especially for tef. The water input was much higher than the evapotranspiration water requirement. The irrigation water requirement and water application varied greatly among the selected crops. The irrigation water requirements of the crops were significantly different ($p \leq 0.05$), but farmers applied almost equal amounts of water for wheat and onion. As a result, a strong variation ($p \leq 0.05$) in irrigation water losses (ranging from 0 to 78% of the required water) due to over-irrigation was observed between the crop types (Table 4-6). Wheat was not irrigated beyond field capacity, and no irrigation loss was observed. Farmers irrigated wheat and tef two to three times in the growing season, while onion was irrigated seven to eight times. The short-maturing tef variety can produce grain and straw within 47 days, requiring the lowest irrigation water amount. However, farmers applied most water to tef fields resulting in the highest water loss (78% of the required water or 30% of the applied water was lost through drainage). Thus, the lowest irrigation water productivity was observed here (table 4-6). The high water application for tef was due to the flood irrigation method and crack formation at each irrigation event.

Table 4-5 Yield and water productivity of main crops in *Guanta* irrigation scheme

| | **Crop type** | **N†** | **Mean** | **Std. Error** |
|---|---|---|---|---|
| Grain/bulb yield ($kg\ ha^{-1}$) | Wheat | 15 | 758.7$^{b}$ | 60.9 |
| | Onion | 60 | 5903.0$^{a}$ | 352.1 |
| | Tef | 12 | 770.8$^{b}$ | 56.7 |
| Straw biomass yield ($kg\ ha^{-1}$) | Wheat | 15 | 1864.0$^{a}$ | 210.4 |
| | Tef | 12 | 2048.3$^{a}$ | 170.0 |
| Conventional straw *EWP* ($kg\ m^{-3}$)‡ | Wheat | 15 | 0.8$^{b}$ | 0.1 |
| | Tef | 12 | 1.1$^{a}$ | 0.1 |
| Conventional grain/bulb *EWP* ($kg\ m^{-3}$) | Wheat | 15 | 0.3$^{b}$ | 0.04 |
| | Onion | 60 | 1.5$^{a}$ | 0.09 |
| | Tef | 12 | 0.4$^{b}$ | 0.03 |
| Conventional straw *IWP* ($kg\ m^{-3}$)§ | Wheat | 15 | 0.5$^{a}$ | 0.05 |
| | Tef | 12 | 0.5$^{a}$ | 0.10 |
| Conventional grain/bulb IWP ($kg\ m^{-3}$) | Wheat | 15 | 0.2$^{b}$ | 0.02 |
| | Onion | 60 | 1.4$^{a}$ | 0.09 |
| | Tef | 12 | 0.2$^{b}$ | 0.03 |
| Improved rain/bulb/straw *EWP* ($kg\ m^{-3}$) | Wheat | 15 | 1.2$^{b}$ | 0.13 |
| | Onion | 60 | 1.8$^{a}$ | 0.10 |
| | Tef | 12 | 1.5$^{a}$ | 0.10 |
| Improved grain/bulb/straw *IWP* ($kg\ m^{-3}$) | Wheat | 15 | 0.7$^{b}$ | 0.07 |
| | Onion | 60 | 1.6$^{a}$ | 0.11 |
| | Tef | 12 | 0.7$^{b}$ | 0.12 |

**†N: number of observations; ‡EWP: evapotranspired water productivity; §IWP: irrigation water productivity**
**Values indicated by different superscript letter (a and b) are significantly different at $p \le 0.05$**

Table 4-6 Irrigation water application and requirement for different crops in *Guanta* irrigation scheme

| | Irrigation water applied (mm) | | | Irrigation requirement (mm) | | | Drainage loss (% of requirement) | | |
|---|---|---|---|---|---|---|---|---|---|
| | Wheat | Onion | Tef | Wheat | Onion | Tef | Wheat | Onion | Tef |
| No. of cases | 4 | 3 | 4 | 4 | 3 | 4 | 4 | 3 | 4 |
| Mean | $388.9^{b}$ | $484.3^{b}$ | $541.2^{a}$ | $370.6^{b}$ | $452.0^{a}$ | $143.3^{c}$ | $0.0^{c}$ | $17.1^{b}$ | $77.8^{a}$ |
| Std. Error | 19.1 | 21.4 | 82.5 | 2.0 | 4.2 | 4.0 | 0.0 | 0.8 | 11.4 |

***Values indicated by different superscript letter (a, b, and c) are significantly different at p ≤ 0.05***

Farmers at the upstream side of the gravity-fed scheme invested in motor pumps, fuel and technicians to pump water to their fields. Farmers with land but without pumps shared half of their produce with those providing pumped water. However, water from gravity irrigation was free. As a result, strong differences in amounts of applied water were observed for pump and gravity irrigation (Table 4-7). Even though crops needed similar amounts of water independent of whether they were irrigated by pump or gravity (a small difference was observed due to difference in crop type and plantation and harvest time), farmers applied more water to gravity-irrigated crops than to pump-irrigated. Consequently, pump-irrigated crops were under-irrigated while gravity-irrigated crops were over-irrigated (Table 4-7). Even though there was overall under-irrigation during pump irrigation, in some cases excess water was applied above soil field capacity. As such, about 3.4% of the applied water or 2.5% of the required water was lost due to drainage.

Table 4-7 Irrigation water application and requirement for pump and gravity irrigation

| | Irrigation water applied (mm) | | Irrigation water requirement (mm) | | Drainage loss (% of requirement) | |
|---|---|---|---|---|---|---|
| | Pump | Gravity | Pump | Gravity | Pump | Gravity |
| No. of cases | 5 | 6 | 5 | 6 | 5 | 6 |
| Mean | $309.2^{b}$ | $550.6^{a}$ | $429.1^{a}$ | $380.2^{a}$ | $2.5^{b}$ | $31.6^{a}$ |
| Std. Error | 20.4 | 19.8 | 12.9 | 15.7 | 0.6 | 3.8 |

***Values indicated by different superscript letter (a and b) are significantly different at p ≤ 0.05***

Discussions with farmers revealed that there was an increasing irrigation water demand (data not presented). The diversion and main canal capacity was designed for 46 ha. However, about 20 ha of additional farmland were included by the farmers at the tail end of the scheme. In addition, farmers in the upstream irrigated 21 ha of land using motor pipes, which was not originally part of the scheme. Increasing water demand by both upstream and downstream communities aggravated the water shortage leading to prolonged irrigation intervals. As a result, the soil was deeply cracked in many locations, leading to high losses of irrigation water due to water percolation through the cracks.

## 4.5 Discussion

The results of this study indicate that irrigation cost had implications for water management decisions and variations in water productivity. Production costs associated with pump irrigation forced farmers to save water and to maintain canals frequently, which were evidenced by the absence of water draining away from the fields. Farmers minimized water losses by using deficit irrigation and by transferring water immediately to the next plot. On the other hand, over-irrigation and high water losses were observed on fields irrigated by gravity-fed water. In this part of the irrigation scheme, farmers were reluctant to maintain canals appropriately, and water was released to the drainage basin in spite of the high water need at the tail. The difference in water requirement for the same crop came from differences in planting and maturity time in different fields.

### 4.5.1 Irrigation water losses and shortage

Higher small-scale irrigation canal water losses were observed in this study when compared to the findings of Akkuzu et al. (2007), who reported an average loss from lined field canals of about 9.3% and 1.1% loss from lined secondary canals in Turkey at a similar flow capacity (30 l $s^{-1}$). Bakry and Awad (1997) reported 0.17 to 0.70% losses per 100 m canal in Egypt for a canal capacity of 2000 to 12 100 l $s^{-1}$, which was also lower than the findings in this study. Here the canal water loss was highest from the main canal due to its higher capacity (43.21 l $s^{-1}$) and proximity to the riverbank as compared to the other canal types. Expressed as percentage of the water flow capacity of the canals, the canal loss was highest for the field canals, since these were destroyed during tillage, so that the canal banks were not stabilized like the main and secondary canals. The negative impact of seepage on production was more pronounced in the case of field canals, as it led to more water logging than the seepage from other canals.

In addition, the field canal network covered the largest area in the scheme. Farmers preferred field canals because they allowed them to keep their plot sizes. Apart from high seepage losses, field canals dried and cracked before the next irrigation event. Field canals overtopping during night irrigation was common and increased water logging and unmeasured canal water loss. These factors resulted in high irrigation water loss, water logging and production losses. Therefore, large farmlands within 8-15 m from the field canals were out of production. Although farmers thought secondary canals occupied more land than field canals, in practice field canals rendered more land unproductive and resulted in higher water losses than secondary canals. The total volume of water lost from the 3077-m long canal system (comprising all canal types) could have irrigated 9 ha of land at 50 mm irrigation depth per day for the irrigation season.

The increasing water demand due to the extension of tail and pump irrigation have made management of the irrigation water more complicated. The duration of the irrigation intervals increased, which resulted in crop water stress and cracks in the vertic soils. In addition, due to decreased canal flow capacity, the time needed for sufficient irrigation increased, and farmers were forced to conduct nighttime irrigation, resulting in large losses due to inefficiency and unpredicted canal flow rate during the night.

Water was a more constraining factor than land around the scheme during the irrigation season. Ample downstream plain land was out of production six months a year (December to June). On the other hand, water from night stream flow, springs and shallow groundwater was still not used properly. Night water storage will increase water use efficiency. It is possible to use the stream bank for this temporary storage. A simple profile leveling survey of the *Guanta* stream bank showed great potential for night water storage (up to 20 000 to 45 000 $m^3$), which could be used during the day. Farmers invested about 50% of their produce in kind for pump irrigation, with an increasing trend of pumping activities.

However, because of higher production costs, pump irrigation typically resulted in lower financial water productivity than downstream gravity irrigation. This means that there is a greater possibility to improve water productivity in downstream gravity irrigation than in upstream pump irrigation.

The variation in *RWS* indicates that more water was lost for tef and under gravity irrigation. Values ranged from 0.8 to 4.0, where 0.8 indicates deficit irrigation to maximize water productivity (Molden et al. 1998). In a public surface irrigation scheme in Mexico, *RWS* was higher than 2.0 and showed differences with respect to water access and water cost (Kloezen and Garcés-Restrepo 1998). Compared to the above study that used *RWS* at scheme level, *RWS* for tef was extremely high.

### 4.5.2 Production and productivity

Area and water productivity of selected crops was comparable with findings of other studies around the study area. Haileslassie et al. ($2009_b$) reported yields of 892-972 kg $ha^{-1}$ for wheat and 981-1312 kg $ha^{-1}$ for tef produced in rain-fed conditions in the same watershed. The *EWP* values were 0.21-0.23 kg $m^{-3}$ for wheat and 0.24- 0.33 kg $m^{-3}$ for tef in the study of Haileslassie et al. ($2009_b$), which used the improved approach of water productivity calculation. In this study, land productivity was relatively lower while the water productivity was three times higher as compared to values in the study of Haileslassie et al. ($2009_b$). The difference observed between these rain-fed and irrigation values arose from differences in crop varieties and water management practices. On the one hand, short-maturing tef and wheat varieties with lower *ETc* values than for rain-fed production were used for irrigation. On the other hand, irrigation intervals were too long to create acceptable soil water stress conditions whereby the water stress coefficient was reduced to 0.3 during some irrigation intervals. Bekele and Tilahun (2007), using experimental deficit irrigation at *Sekota*, Ethiopia obtained onion yields of 5500-25000 kg $ha^{-1}$ with 9-10 kg $m^{-3}$ water, which is about eight times higher than the observations in this study. This shows that opportunities exist to increase onion production and productivity in the area. Flood irrigation using a very low flow rate (less than 1 l $s^{-1}$ during the night or day) and irrigating deep cracks after prolonged irrigation intervals decreased the water productivity of tef and wheat as compared to the field observations on water application. For example, tef irrigation water was almost half as productive as *ET* water compared to wheat and onion productivity due to higher drainage water losses.

The conventional way of quantifying water productivity underestimated water productivity values, since the total water transpired was used to produce total biomass while the estimation considered either grain or straw. This approach has more a practical application in mixed crop-livestock systems where the straw biomass is a very important livestock feed.

### 4.5.3 Implications for livestock production

As the importance of crop production for livestock is worth considering, it is also important to stress the importance of crop residue as livestock feed during the irrigation season. About 11428 kg grass, 18490 kg wheat straw and 12884 kg tef straw (42884 kg DM in total) were produced from 18 ha (20%) land of the scheme during the irrigation season. Based on 8.5 kg DM per day maintenance need for one TLU, 84 TLU can be fed for 60 days. This can cover TLU from 26 households or TLUs on 37 ha according to the livestock holding and stocking rate of the area studied determined by Descheemaeker (personal communication, 2010). Dry matter production from the relay maize cropping and other minor crops in the scheme was not considered in this calculation, and the potential of the scheme to support livestock feed is expected to exceed the above indicated figures. Therefore, increasing the biomass productivity of each drop of irrigation water and on each plot of land within the scheme has strong implications for livestock water productivity of the mixed crop-livestock systems.

## 4.6 Recommendations

1. Based on the above findings, recommendations for improving water use efficiency and productivity in the irrigation scheme include careful design and construction of secondary canals and decreasing the use of field canals to minimize canal water loss. Careful planning of the cropping pattern and irrigation scheduling could result in more efficient water distribution. Given the fact that over-irrigation is less common with pumped irrigation, allocating a water price to gravity-fed water could positively influence water management. However, water pricing has to be based on accurate water flow data as well as on equitable, adequate and reliable water distribution rules governed by the water user associations. Water flow measurements can be conducted using cement, wooden or iron sheet cutthroat flumes by trained farmers.

2. Production of high-value crops (e.g., fruits) and/or high quality feeds along canals and drained water could maximize water productivity for livestock, and there is an opportunity to increase irrigation water productivity.

3. In order to improve water productivity of these system, farmers, water users associations and development agents should receive training on canal water management, crop water requirement, and equitable and efficient water distribution.

4. Different alternatives for improved water management, such as water pricing and facilities for night water storage need to be considered in policy development.

5. Considering the trade-offs between downstream gravity irrigation and upstream pump irrigation needs further research for supporting policy articulations.

6. Shallow and frequent irrigation of tef using sprinkler or border irrigation could minimize water loss and increase irrigation water productivity, but needs further research on the applicability in the local context.

# 5 HANDLING MISSING METEOROLOGICAL DATA

## 5.1 Summary

The Penman-Monteith equation is a commonly used method to estimate potential evapotranspiration in most of the hydrological models and for water management design. The equation is more input demanding compared to other approaches. Spatial distribution of rainfall and temperature data is very important for hydrological modeling. However, missing data is common in the measurements of meteorological stations, e.g., solar radiation and relative humidity are not measured by most meteorological stations in the study area. These problems are common in the Blue Nile Basin in Ethiopia. Methods to fill rainfall and temperature data were developed and compared in this study. Solar radiation and relative humidity data were derived from temperature data. The estimation performance was done using statistical values. The results of the estimation are promising for exploiting the existing database of the area for better understanding and decision making.

## 5.2 Introduction

Meteorological variables, especially rainfall and temperature, are important for hydrological modeling and for the design of water resources developments. Lack of long-term and continuous data has been a challenge for water resources development in Ethiopia. These data gaps have an impact on the value of environmental time series (Presti et al. 2010) and hydrological modeling. Inconsistent and biased hydrologic analysis and conclusions can affect water development planning (Kim and Ahn 2009). Missing values have to be considered and filled before using the data for further investigations. Temporal and spatial regression and interpolation methods were used to fill the missing data of a selected station through values from the neighboring stations.

Rainfall is an important factor in climate and agriculture studies (Ayoade 1983) that are conducted on problems related to floods, drought, and landslides, etc.. It has a strong influence on relative humidity, temperature and solar radiation (Neitsch et al. 2011). An incomplete rainfall record (missing data) influences the consistency and continuity of the data (De Silva et al. 2007). Computational methods starting from the simplest sample mean method to the complex multiple imputation method have been used to fill missing data (Presti et al. 2010). Presti et al. (2010) used the strengths of both simple and complex methodologies in Italy to achieve better estimations using rainfall data of neighboring stations.

Different methods have been used to fill missing temperature data. Allen and DeGaetano (2001) grouped these methods into within-station, between-station and regression types. Average measured values prior to and following a missing date were used to fill the missing values in the within-station method. This method is temporal and depends only on data from one station, but is not suitable for stations with consecutive days of missing data as observed in the study area. The between-station method uses measured values of neighboring stations to fill the missing temperature values of a given station. Regression models can be developed using one or more neighboring stations to fill missing temperature data. Regression techniques such as multiple regression and weighted regression (Eischeid et al. 1995) and optimized regression (Allen and DeGaetano, 2001; Kotsiantis et al. 2006) have given more accurate estimates of missing data as compared to the within-station and between-station methods.

Relative humidity and solar radiation data are further inputs for Penman-Monteith potential evapotranspiration calculation, but such values are scarce for the study area. Data on sunshine hours have only been collected at sparsely distributed class-one meteorological stations. In addition, the data are full of gaps due to failure of the Campbell-Stokes recorder or/and lack of the treated card or/and lack of personnel. Most of the stations in the area are of class-three or -four. For such stations, no instruments are installed to measure relative humidity and sunshine hours. Allen (1998) suggested that the missing data could be adopted from the nearby stations or generated from daily temperature data.

Rainfall, maximum and minimum temperature, relative humidity, wind speed and sunshine hour data are recorded in class-one stations. These stations have been monitored more seriously and have better data availability than others. However, they only cover a limited area and show a considerable amount of missing data due to lack of personnel for fixing the measuring instruments and due to political unrest in the country. Most stations have only been equipped with rainfall and temperature recording instruments (class-three stations) and some only for rainfall (class-four stations).

The objective of this study is to identify and to evaluate methods to fill missing rainfall, temperature, solar radiation and relative humidity data of meteorological stations around *Gumara* watershed in the Blue Nile Basin of Ethiopia.

## 5.3 Materials and methods

### 5.3.1 Study area

The study area, the *Gumara* watershed, is located in the Lake *Tana* Basin of the Blue Nile in Ethiopia. Lake *Tana,* covering about 3000 km$^2$, is considered as the source of the Blue Nile River. The lake basin contributes 7% of the Blue Nile water at the Sudan boarder (Kebede et al. 2006). It has four main rivers that contribute 93% of the inflow of the lake (Kebede et al. 2006). The climate of the area is tropical highland monsoon. Seasonal rainfall distribution is controlled by the movement of the inter-tropical convergence zone and moist air from the Atlantic and Indian Ocean in summer (June-September) (Kebede et al. 2006). The four seasons in the country are winter (January-March with some rain; called "*bulg*" in some parts of Ethiopia), spring (April–June, dry), summer (July-September, main rainy season) and autumn (October–December, dry air) (Latron et al. 2008). The rainfall in the study area is uni-modal with the main rainfall occurring during June to September. There are nine meteorological stations within and around the *Gumara* watershed: *Debre Tabor* (class-one), *Wanzaye* (class-three), *Arb Gebeya* (class-four) and *Luwaye* (class-four) stations in the watershed, and *Gassay* (class-three), *Mekane Eyesus* (class-three), *Bahir Dar* (class-one), *Woreta* (class-three) and *Amed Ber* (class-three) around the watershed.

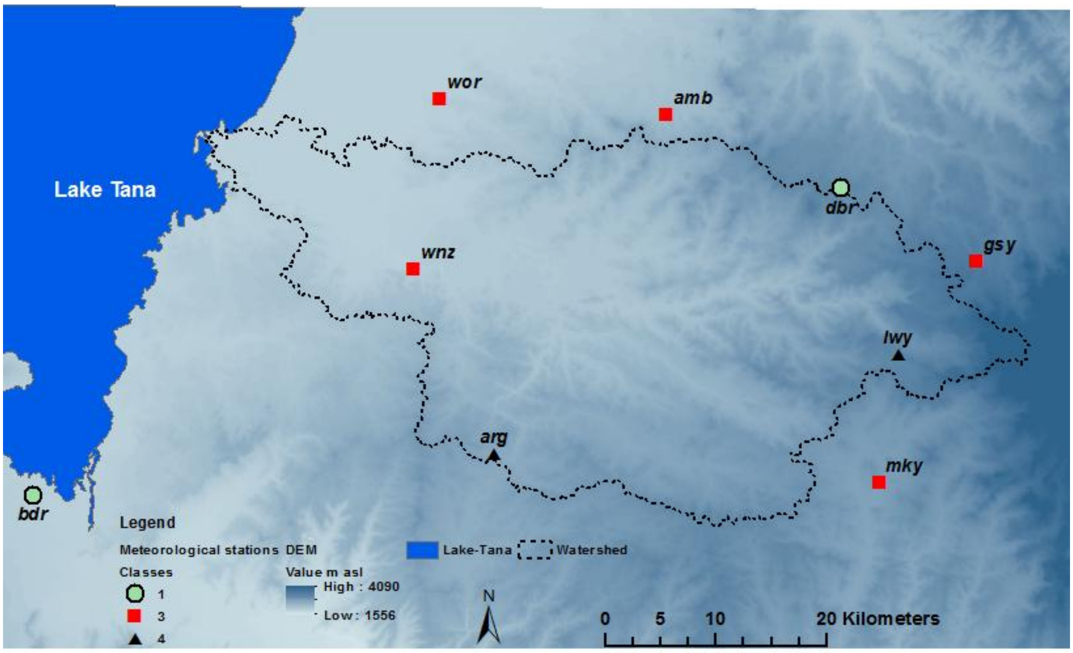


Figure 5-1 Distribution, classes and altitudinal categories of meteorological stations around and inside the *Gumara* watershed.
***(For details see Table 5-1)***

### 5.3.1 Database

Meteorological stations are distributed along the boundaries of the watershed since they are located along the road. Daily data over 22 years (1987-2008) from nine meteorological stations were taken from the National Meteorological Services Agency (NMSA) of Ethiopia. However, data availability is different from station to station (Table 5-1). The stations are distributed along different elevations. Data from *Bahir Dar* and *Debre Tabor* have been frequently used for water development studies (MoWR 2008; Setegn et al. 2008). Data from the other stations have not been used for study and water resource planning due to missing data. However, *Bahir Dar* is located relatively far from the watershed as compared to the other stations (Figure 5-1).

Table 5-1 Location of meteorological stations and their database status

| No. | Name | ID | Latitude (UTM) | Longitude (UTM) | Elevation (m) | Database | Class |
|---|---|---|---|---|---|---|---|
| 1 | *Amed Ber* | *amb* | 1340550.3 | 367213.4 | 1940 | 2004-2008 | 3 |
| 2 | *Arb Gebeya* | *arg* | 1286558.9 | 362767.0 | 2247 | 2003-2008 | 4 |
| 3 | *Bahir Dar* | *bdr* | 1282807.4 | 321159.1 | 1798 | 1987-2008 | 1 |
| 4 | *Debre Tabor* | *dbr* | 1310581.5 | 394163.9 | 2684 | 1987-2008 | 1 |
| 5 | *Gassay* | *gsy* | 1303967.2 | 406458.9 | 2794 | 2004-2008 | 3 |
| 6 | *Luwaye* | *lwy* | 1295542.0 | 399349.2 | 2733 | 2004-2008 | 4 |
| 7 | *Mekane Eyesus* | *mky* | 1283935.6 | 397645.7 | 2403 | 1994-2008 | 3 |
| 8 | *Wanzaye* | *wnz* | 1303243.7 | 355606.8 | 1824 | 1987-2008 | 3 |
| 9 | *Woreta* | *wor* | 1318594.6 | 357948.9 | 1825 | 1987-2008 | 3 |

***UTM = Universal Transverse Mercator***

Some meteorological stations have data for less than five years. Days with missing data were excluded before evaluating to estimate daily rainfall data. Scrutiny of the data was conducted, and systematic errors were adjusted using graphical and statistical checks. Predictor stations for a given predictand station were selected based on long-term data availability, correlation between stations, and spatial proximity criteria. Best stations combination was finally selected using trial and error and least error of estimation. Monthly and annual totals were also compared with the statistical criteria to evaluate the methods for these time scales.

### 5.3.2 Spatial interpolation methods for rainfall data

Spatial interpolation methods are classified as global or local, exact or inexact, deterministic or stochastic and gradual or abrupt depending on the range of variation, measured value, assessment of error factor and spatial smoothness, respectively. Li and Heap (2008) present details of these classifications. Inverse distance weight (IDW) and spline are among the deterministic methods, and kriging is a stochastic method. Interpolation methods like kriging and cokriging are also called geostatistical interpolation methods. The basic interpolation principles of geostatistical methods is to optimize weights assigned to neighboring data points to give interpolation results at different un-sampled points in space (Phillips et al. 1992). These geostatistical methods were found superior to the deterministic models for precipitation (Phillips et al. 1992). They are best when correlation between precipitation and other topographic auxiliary variables like elevation, relief and leeward direction are used to model the interpolation at uniform grid levels of the area. Therefore, geostatistical methods of interpolation of meteorological variables are very important for hydrological methods that use uniform grids of the given watershed. Since SWAT uses hydrologic response units (HRU) rather than uniform grid cells, the following four deterministic interpolation methods were compared to fill the missing rainfall data of the *Gumara* watershed for this study.

**1) Arithmetic (local) mean (*AM*) method**

The arithmetic mean can be used when the annual normal rainfall of the neighboring stations varies within 10% of the rainfall of station to be modeled (Chow et al. 1988; Tabios & Salas 1985). The method was used in this study for filling the missing rainfall values of the selected station

**2) Normal ratio (*NR*) method**-

The normal ratio method is used when the variation of the normal annual rainfall of the surrounding stations exceeds 10% of the values of the station under consideration (De Silva et al. 2007). This method assigns weights of each surrounding station (Sing 1994). The missing data of station *n*, $\phi_n$ , was calculated using equation 5-1:

$$\phi_n = \frac{\phi_n^a}{r}\sum_{i=1}^{r}\left[\frac{\phi_i}{\phi_{ni}^a}\right] \qquad (5\text{–}1)$$

where $\phi_n$ is estimate of missing data for gauged station *n*, $\phi_{ni}$ *is* measured rainfall values of surrounding station *i*, $\phi_n^a$ is normal annual rainfall of station $n$ , $\phi_{ni}^a$ is normal annual rainfall of surrounding stations *i*, $\phi_i$ is the observed value at station *i*, and *r* is number of surrounding stations.

**3) Inverse distance weighting (*IDW*) method**

Inverse distance weighting is derived based on the assumption that sample or station measurement values are inversely proportional to the distance from the point being estimated (Lam 1983). It is also known as a reciprocal-distance method. It is the most commonly used method to estimate missing data at place *n* using the neighboring measured data. It is mathematically expressed as equation 5-2:

$$\phi_n = \frac{\sum_{i=1}^{r} \phi_i d_{ni}^{-k}}{\sum_{i=1}^{r} d_{ni}^{-k}} \quad (5\text{-}2)$$

where, $\phi_n$ is the value of missing data at station *n*, *r* is the number of stations with measured data at a given time, $\phi_i$ is the observed value at station $i$, $d_{ni}$ is the distance between station *i* and station *n*, $d_{ni}^{-k}$ is the weighting factor. The equation is sometimes known as the distance ratio method. The exponent *k* is mostly used as 2 but varies from 1.0 to 6.0 (Teegavarapu and Chandramouli 2005). However, in this study, the *k* value was optimized using the solver program in Microsoft Excel.

**4. Coefficient of correlation weighting (*CCW*) method**

The weighting factor is derived from correlation of the historical data between stations rather than the distance between them as explained above for the IDW method. CCW is mathematically expressed using equation 5-3.

$$\phi_n = \frac{\sum_{i=1}^{m} \phi_i R_{ni}^{-k}}{\sum_{i=1}^{m} R_{ni}^{-k}} \quad (5\text{–}3)$$

where $R_{ni}$ is the coefficient of correlation between stations *n* and *i*. According to Teegavarapu and Chandramouli (2005), testing the existence of correlation of data between any two stations is very important. This method has given better results in studies (e.g., Teegavarapu and Chandramouli 2005) than the IDW method, since distance is not the only case to detect correlation of measurements.

### 5.3.3 Regression models for temperature

**Data selection and handling regression models**

Class-one and class-three meteorological stations (Table 5-6) with daily minimum and maximum temperatures were selected in the Upper Blue Nile Basin of Ethiopia. The data were checked for problems like spurious zeros and digital point places before regression equation development. Neighboring stations are selected considering geographic distance, correlation coefficient between stations and elevation with respect to station with missing data. The correlation coefficient (*R*) was also used as a criterion to choose regressor stations.

Multiple linear regression models of equation 5-4 were used for each station:

$$\phi_n = \sum_{i=1}^{r} \beta_i \phi_i + \beta_o + \varepsilon \tag{5–2}$$

where $\phi_n$ is the value of missing data at station *n, r* is the number of stations with measured data at a given time, $\beta_i$ is the coefficient of the repressor $\phi_i$, $\beta_o$ is the constant term of the regression model, and $\varepsilon$ is the error term associated with the model. Although regression models are considered the best to model temperature values of a given station using measured values of the neighboring stations, collinearity (linear dependency) between regressors is a problem causing inflation of the variance. Variance inflation changes the sign of regression coefficients during linear multiple regression. Marquardt's variance inflation factor (VIF) (Marquardt 1970) was used to identify collinear explanatory stations. Studies suggest that a VIF greater than 10 has multicollinearity problems (e.g., Neter et al. 1996; Weisberg 2005). Miles and Shevlin (2001) suggest VIFs equal to 4 as a cutting point. Regression models with explanatory variables that create VIFs less than 4 are selected as regressors in this study.

After regressor station selection and data screening, multiple regression was done using SPSS software. Standard error of coefficients and coefficient of determination ($R^2$) statistics were used as statistical measures for error and accuracy.

### 5.3.4 Estimation of relative humidity using temperature data

Relative humidity expresses the relative degree of saturation of the air. It is the ratio of vapor pressure at actual and saturated water levels of the air at a given temperature *T* (equation 5-5 and 5-6).

$$RH = \frac{e_a}{e^o(T)} \tag{5-5}$$

where $$e^o(T) = 0.6108 \exp\left[\frac{17.27T}{T + 273.3}\right] \tag{5–3}$$

where $e_a$ is the actual vapor pressure of the air in kilo Pascal (kPa), $e^o(T)$ is the saturated vapor pressure (kPa) of the air at a temperature *T* in °C, and Exp […] is base of natural logarithm (2.7183) raised to […].

Relative humidity indicates what proportion of the air holds water at a given temperature relative to the maximum amount it can hold at this temperature. Values vary over time of the day due to variations of $e^o(T)$ that can vary with *T* from sunrise to sunset. The daily average $e^o(T)$ value can be calculated using minimum ($T_{\min}$) and maximum daily temperature ($T_{\max}$) using equation 5-7:

$$e^o(T) = e_s = \frac{e^o(T_{\max}) + e^o(T_{\min})}{2} \tag{5–4}$$

The actual vapor pressure of the air can be calculated using the dew point temperature $T_{dew}$(Equation 5-8). Dew point is the temperature at which air needs to be cooled to reach saturation with the existing amount of water content. Allen (1998) recommends using $T_{\min}$ in place of $T_{dew}$ when data for dew point temperature is not available (equations 5-8 and 5-9):

$$e_a = e^o(T_{dew}) = 0.6108\exp\left[\frac{17.27T_{dew}}{T_{dew}+273.3}\right] \tag{5-8}$$

$$e_a = e^o(T_{\min}) = 0.6108\exp\left[\frac{17.27T_{\min}}{T_{\min}+273.3}\right] \tag{5–9}$$

The substitution of $T_{dew}$ by $T_{\min}$ is used for the condition when the cover crop is well watered. $T_{\min}$ is greater than $T_{dew}$ for arid climates and the minimum temperature used needs to be adjusted by subtracting 2-3 °C Therefore, $T_{\min}$-*a* was used in this study where the value of *a* (°C) was optimized using the solver program for the best fit of estimated and measured *RH* time series data of the area that varies from season to season. *RH* in terms of $T_{min}$ and $T_{max}$ is given in equation 5-10:

$$RH = \frac{e_a}{e^o(T)} = \frac{0.6108\exp\left[\frac{17.27(T_{\min}-a)}{T_{\min}-a+273.3}\right]}{\frac{0.6108\exp\left[\frac{17.27T_{\max}}{T_{\max}+273.3}\right]+0.6108\exp\left[\frac{17.27T_{\min}}{T_{\min}+273.3}\right]}{2}}$$

$$RH = 2\frac{\exp\left[\frac{17.27(T_{\min}-a)}{T_{\min}-a+273.3}\right]}{\exp\left[\frac{17.27T_{\max}}{T_{\max}+273.3}\right]+\exp\left[\frac{17.27T_{\min}}{T_{\min}+273.3}\right]} \tag{5–5}$$

### 5.3.5 Derivation of solar radiation

Solar radiation can be calculated from measured weather parameters like sunshine hours, air temperature and vapor pressure. Radiation derived from sunshine hours of the day is well formulated in Allen (1998). However, if no sunshine hour data are available, values can be derived from nearby stations, from air temperature differences and from empirical formulas related to the universal solar radiation constant, extraterrestrial radiation ($R_a$). $R_a$ is the amount of solar radiation reaching a horizontal surface on the earth atmosphere in KJ m$^{-2}$ day$^{-1}$. Its value changes with latitude, with day of the year and with time of the day. Part of this radiation is scattered, emitted or absorbed by the atmosphere (gases, clouds or dust), and the rest reaches the earth surface. The part reaching the earth surface is called solar radiation, global radiation or shortwave radiation ($R_s$). From this radiation, part ($\alpha R_s$) is reflected back to the atmosphere, and only 1-$\alpha$ is retained on the surface. Some of the long-wave radiation is emitted and retained within the atmosphere, where $\alpha$ is known as the albedo.

$$\alpha = \begin{cases} 0.95 & for\ freshly\ fallen\ snow \\ 0.05 & for\ wet\ bare\ soil \\ 0.02 - 0.25 & for\ green\ vegetation\ cover \\ 0.23 & for\ reference\ grass\ crop\ cover \end{cases} \tag{5-11}$$

Pyranometers, radiometers or solarimeter sensors can measure solar radiation directly. However, solar radiation can be estimated using the duration of daily bright hours in the absence of these sensors as observed in the area of this study where Campbell-Stokes sunshine hour recorders burned holes in a specially treated card.

The daily $R_a$ values in the study area were calculated from solar constant, solar declination, and day number in the given year (equation 5-12):

$$R_a = \frac{24(60)}{\pi} G_{sc} d_r \left[\omega_s \sin(\varphi)\sin(\delta) + \cos(\varphi)\cos(\delta)\sin(\omega_s)\right] \tag{5-12}$$

where $R_a$ is extraterrestrial radiation [MJ m$^{-2}$ day$^{-1}$], $G_{sc}$ is solar constant = 0.0820 MJ m$^{-2}$ min$^{-1}$, $d_r$ inverse relative distance Earth-Sun (equation 5-13), $\omega_s$ sunset hour angle (equation 5-15) [rad], $\varphi$ is latitude [rad] given by $\pi/180(latitude\ in\ decimal\ \deg ree)$, and $\delta$ is solar declination (equation 5-14) [rad].

$$d_r = 1 + 0.033\cos\left(\frac{2\pi}{365}J\right) \quad (5\text{-}13)$$

$$\delta = 0.409\sin\left(\frac{2\pi}{365J} - 1.39\right) \quad (5\text{-}14)$$

$$\omega_s = \arccos[-\tan(\varphi)\tan(\delta)] \quad (5\text{-}15)$$

where *J* is the day number in the year (e.g., 1 for January 1st). Solar constant is the solar radiation reaching the earth surface perpendicular to the solar rays at the top of the earth's atmosphere, and $R_a$ is the radiation on a horizontal surface at the upper layer of the earth's atmosphere. The solar radiation, $R_s$, is estimated using equation 5-16.

$$R_s = (a_s + a_b \frac{n}{N})R_a \quad (5\text{-}16)$$

where $a_s$=0.25 and $b_s$=0.50 for areas without any $R_a$ and $R_s$ data. On clear-sky days, $R_s = R_{so}$ (clear-sky radiation). The daylight hour for day of the year is calculated using equation 5-17:

$$N = \frac{24}{\pi}\omega_s \quad (5\text{-}17)$$

$R_{so} = (a_s + b_s)R_a$ for areas with calibrated $a_s$ and $b_s$ where $a_s + b_s$ is the fraction of $R_a$ reaching the earth's surface on a clear-sky day, and

$R_{so} = (0.75 + \frac{2z}{10^5})R_a$ for not available calibrated values of $a_s$ and $b_s$, and $z$ is the elevation of the station above sea level in meters.

Allen (1998) suggested transferring solar radiation data from the nearby stations or deriving radiation from temperature differences. According to the author, three basic things need to be considered before transferring radiation data from nearby stations. First, the region under study has to be small. Second, there has to be identical air mass movement and cloudiness. Third, relative solar radiation ($R_s / R_{so}$) and relative sunshine duration ($n/N$) have to be identical for the given stations. The author also suggested checking the physiographic homogeneity of stations like similar side of a mountain and north-south distances. If north-south distance between stations exceeds 50 km, the equation 5-18 is better to use than transferring other station data.

$$R_s = \frac{R_{s,i}}{R_{a,i}} R_a \tag{5-18}$$

where $R_{s,i}$ is solar radiation at station $i$ [MJ m$^{-2}$ day$^{-1}$], and $R_{a,i}$ is extraterrestrial radiation at station $i$ [MJ m$^{-2}$ day$^{-1}$].

The second option to fill gaps in measured solar radiation data is deriving solar radiation from temperature differences. The maximum and minimum daily temperature difference is directly related to cloudiness of the day, i.e., maximum temperature is low during a cloudy day, as solar radiation is reflected by the cloud during the day on the one hand. On the other hand, the daily minimum temperature is relatively higher on a cloudy day, since outgoing long-wave radiation is retained in the air by the cloud cover at nighttime. This principle is formulated for solar radiation by Hargreaves and Samani (1982) as given by equation 5-19:

$$R_s = K_{RS} \sqrt{(T_{\max} - T_{\min})} R_a \tag{5-19}$$

where, $K_{RS}$ is the adjustment coefficient ($K_{RS}$ =0.16 for interior locations where land mass predominates, and 0.19 for coastal locations where air mass movement from water bodies influences weather conditions). This method is used when imported radiation data are not good due to lack of climate similarity between stations like the rugged topography of the study area.

### 5.3.6 Comparison methods for estimates

Estimated and actual values can be compared by measuring how close the estimated values are to the actual values by descriptive statistics of error criteria. These are error mean ($\mu$), standard deviation (*S*), correlation coefficient (*R*), root mean square error (*RMSE*) and mean absolute error (*MAE*). Error mean indicates the deviation of mean of estimated value from mean of measured value. *RMSE, MAE* and *R* are used to measure the performances of the methods to estimate missing values in this study (equations 5-20, 5-21 and 5-22). *RMSE* measures the average magnitude of daily estimation error using the quadratic square score, while *MA*E indicates the deviation of estimated values from measured values using the linear square score. *RMSE* uses higher weights for days with greater estimation errors, since the error of every single value is squared before the average is analyzed; *MAE* gives equal weights for individual errors. Therefore, *RMSE* can indicate the occurrence of large errors in the time series together with *MAE*. If the time series of error is composed of the same magnitude, both *RMSE* and *MAE* will have almost equal values.

$$RMSE = \sqrt{\frac{1}{r}\sum_{i=1}^{r}(\phi_{nmi} - \phi_{nei})^2} \tag{5-20}$$

$$MAE = \frac{1}{r}\sum_{i=1}^{r}\left|\phi_{nmi} - \phi_{nei}\right| \tag{5-21}$$

$$R = \frac{\sum_{i=1}^{r}\left(\phi_{nmi} - \overline{\phi_{nm}}\right)\left(\phi_{nei} - \overline{\phi_{ne}}\right)}{\sqrt{\sum_{i=1}^{r}\left(\phi_{nmi} - \overline{\phi_{nr}}\right)^2}\sqrt{\sum_{i=1}^{r}\left(\phi_{nei} - \overline{\phi_{ne}}\right)^2}} \tag{5-22}$$

where $\phi_{nmi}$ is the $i^{th}$ day value measured at station *n*, $\phi_{nei}$ is the $i^{th}$ day estimated value, $\overline{\phi_{nm}}$ is the mean of measured rainfall values of station *n*, $\overline{\phi_{ne}}$ is the mean of estimated values of station *n, r* is the number of days with measured and estimated rainfall values of a given station. Correlation statistics, *R*, is a dimensionless index that indicates the relationship of measured and estimated values. *RMSE* and *MAE* measure model errors that have similar units of the variable they measured (Morid et al. 2002). *MAE* is a robust measure, since it is less sensitive to outliers (Allen and DeGaetano 2001).

## 5.4 Results

### 5.4.1 Rainfall

The results of the comparison of four methods to model daily rainfall data are discussed below. Monthly and annual sum of rainfall for each method are compared across stations. Error values are discussed with respect to results of similar studies.

**Daily rainfall**

There was no clear relation between distance between stations and the correlation coefficient of their daily rainfall values. For example, meteorological stations more far apart like the stations *Bahir Dar* (*bdr*) and *Debre Tabor* (*dbr)* or *Arb Gebeya* (*arg)* and *Bahir Dar* (*bdr)* had more correlated daily rainfall data than those closer like *Bahir Dar* and *Woreta* or *Arb Gebeya* and *Wanzaye*. This indicates that other factors like orographic factors are more influential than distance between stations. The *CCW* method gave the best performance for most stations for estimating daily rainfall data as compared to the other three methods with the exception of three stations where *IDW* and *AM* performed best (Table 5-2). The *NR* method gave the poorest estimation, because this method is based on annual rainfall value as a weighing factor. As there is occurrence of successive missing values for as much as a year, *NR* is not suitable for this case.

Table 5-2 Combination and error results for meteorological stations

| Predictand (N) | Predictor | Distance from predictand (km) | Correlation | Statistical model performance | | | | |
|---|---|---|---|---|---|---|---|---|
| | | | | Stat. measures | AM | NR | IDW | CCW |
| *bdr* (6258) | *wnz* | 40.0 | 0.468 | *R* | **0.538** | 0.385 | 0.527 | 0.532 |
| | *wor* | 51.5 | 0.388 | *MAE* | **3.696** | 10.170 | 3.720 | 3.720 |
| | *dbr* | 78.4 | 0.420 | *RMSE* | **8.359** | 29.986 | 8.582 | 8.415 |
| *dbr* (6307) | *bdr* | 78.4 | 0.420 | *R* | 0.557 | 0.463 | 0.558 | **0.558** |
| | *wnz* | 38.9 | 0.448 | *MAE* | 3.533 | 9.844 | 2.599 | **2.598** |
| | *wor* | 37.3 | 0.440 | *RMSE* | 7.626 | 25.767 | 6.437 | **6.294** |
| *wnz* (6258) | *dbr* | 38.9 | 0.448 | *R* | **0.569** | 0.391 | 0.512 | 0.570 |
| | *bdr* | 40.0 | 0.468 | *MAE* | **3.725** | 10.020 | 3.957 | 3.725 |
| | *wor* | 15.4 | 0.429 | *RMSE* | **8.131** | 29.987 | 8.745 | 8.123 |
| *wor* (6259) | *dbr* | 37.3 | 0.440 | *R* | 0.538 | 0.481 | 0.480 | **0.541** |
| | *bdr* | 37.3 | 0.388 | *MAE* | 3.752 | 9.384 | 4.066 | **3.488** |
| | *wnz* | 15.4 | 0.429 | *RMSE* | 8.376 | 23.350 | 9.314 | **8.120** |
| *mky* (5089) | *dbr* | 26.8 | 0.449 | *R* | 0.505 | 0.505 | 0.499 | **0.508** |
| | *wnz* | 46.3 | 0.404 | *MAE* | 3.468 | 6.330 | 3.508 | **2.832** |
| | | | | *RMSE* | 7.560 | 13.941 | 7.710 | **6.562** |
| *gsy* (1523) | *dbr* | 13.9 | 0.630 | *R* | 0.653 | 0.657 | 0.617 | **0.692** |
| | *mky* | 21.8 | 0.535 | *MAE* | 3.189 | 8.533 | 3.315 | **2.868** |
| | *wnz* | 50.4 | 0.418 | *RMSE* | 6.441 | 17.947 | 7.522 | **6.004** |
| | *wor* | 50.5 | 0.432 | | | | | |
| *amb* (990) | *dbr* | 17.2 | 0.641 | *R* | 0.720 | 0.716 | **0.729** | 0.706 |
| | *mky* | 38.3 | 0.510 | *MAE* | 2.619 | 8.514 | **2.630** | 2.654 |
| | *wor* | 20.6 | 0.529 | *RMSE* | 5.894 | 18.058 | **5.938** | 6.022 |
| *lwy* (1400) | *dbr* | 15.7 | 0.470 | *R* | 0.593 | 0.600 | 0.597 | **0.623** |
| | *gsy* | 10.9 | 0.536 | *MAE* | 3.202 | 9.684 | 3.165 | **2.161** |
| | *mky* | 11.6 | 0.501 | *RMSE* | 7.370 | 19.562 | 7.329 | **4.794** |
| *arg* (1497) | *dbr* | 39.5 | 0.379 | *R* | 0.471 | 0.557 | 0.411 | **0.468** |
| | *bdr* | 41.9 | 0.470 | *MAE* | 3.405 | 5.440 | 3.421 | **3.385** |
| | *wnz* | 18.3 | 0.360 | *RMSE* | 6.765 | 12.133 | 7.369 | **6.709** |

***AM is arithmetic mean, NR is normal ratio, IDW is inverse distance weighting, CCW is coefficient of correlation weight. Stations: Bahir Dar (bdr), Debre Tabor (dbr), Wanzaye (wnz), Woreta (wor), Mekane Eyesus (mky), Gassay (gsy), Amed Ber (amb), Luwaye (lwy) and Arb Gebeya (arg). Bold figures are the results of the best models.***

Values of upstream stations like *Debre Tabor, Gassay, Mekane Eyesus* and *Luwaye* were estimated better than those of the downstream stations with relatively low error values. *RMSE* values are about three times higher than *MAE* values, indicating occurrence of low estimation performance for some daily rainfall events. The time series curves show that these events occurred sometimes when there was no or very low rainfall at a given station while high rainfall was recorded by the neighboring station(s).

Meteorological stations with class-one standard have better daily rainfall data availability (Table 5-2). They are also situated at different topographical locations surrounded by class-three and class-four stations (Figure 5-1).

Table 5-3 Descriptive statistics of daily rainfall values before and after filling missing data

| | Station | N | Missed data (%) | Min | Max | Mean | Std. error | Std. Dev. | Skewness Statistic | Skewness Std. error |
|---|---|---|---|---|---|---|---|---|---|---|
| Before filling missing data | *amb* | 1762 | 78.1 | 0.00 | 82.60 | 3.73 | 0.197 | 8.283 | 3.283 | 0.058 |
| | *arg* | 1579 | 80.4 | 0.00 | 56.70 | 2.48 | 0.130 | 5.146 | 3.696 | 0.062 |
| | *dbr* | 7309 | 9.0 | 0.00 | 104.30 | 4.06 | 0.098 | 8.420 | 3.357 | 0.029 |
| | *bdr* | 7869 | 2.1 | 0.00 | 124.70 | 3.95 | 0.108 | 9.597 | 4.044 | 0.028 |
| | *gsy* | 1623 | 79.8 | 0.00 | 62.10 | 4.00 | 0.202 | 8.125 | 2.861 | 0.061 |
| | *lwy* | 2007 | 75.0 | 0.00 | 90.00 | 3.99 | 0.187 | 8.360 | 3.767 | 0.055 |
| | *mky* | 5288 | 34.2 | 0.00 | 84.80 | 3.59 | 0.103 | 7.470 | 3.280 | 0.034 |
| | *wnz* | 7531 | 6.3 | 0.00 | 134.20 | 3.96 | 0.109 | 9.438 | 3.738 | 0.028 |
| | *wor* | 7176 | 10.7 | 0.00 | 115.00 | 3.93 | 0.112 | 9.492 | 3.937 | 0.029 |
| After filling missing data | *amb* | 7769 | 3.3 | 0.00 | 82.60 | 3.59 | 0.077 | 6.788 | 2.926 | 0.028 |
| | *arg* | 7740 | 3.7 | 0.00 | 84.80 | 3.12 | 0.075 | 6.601 | 3.581 | 0.028 |
| | *dbr* | 7837 | 2.5 | 0.00 | 104.30 | 4.00 | 0.094 | 8.331 | 3.365 | 0.028 |
| | *bdr* | 7918 | 1.5 | 0.00 | 124.70 | 3.95 | 0.108 | 9.575 | 4.050 | 0.028 |
| | *gsy* | 7769 | 3.3 | 0.00 | 69.88 | 3.90 | 0.083 | 7.360 | 2.787 | 0.028 |
| | *lwy* | 7738 | 3.7 | 0.00 | 90.00 | 3.71 | 0.079 | 6.929 | 3.148 | 0.028 |
| | *mky* | 7740 | 3.7 | 0.00 | 84.80 | 3.12 | 0.075 | 6.601 | 3.581 | 0.028 |
| | *wnz* | 7744 | 3.6 | 0.00 | 134.20 | 3.96 | 0.107 | 9.378 | 3.733 | 0.028 |
| | *wor* | 7858 | 2.2 | 0.00 | 115.00 | 3.82 | 0.104 | 9.189 | 4.021 | 0.028 |

***where N is number of days included in the analysis, Min (minimum), Max (maximum), std. (standard), Dev. (deviation), Bahir Dar (bdr), Debre Tabor (dbr), Wanzaye (wnz), Woreta (wor), Mekane Eyesus (mky), Gassay (gsy), Amed Ber (amb), Luwaye (lwy) and Arb Gebeya (arg).***

From the database of 1987 to 2008 (8036 days), 2% to 80% data were missing. Four stations (*bdr*, *wnz, dbr* and *wor*) had lost less than 11% of daily rainfall data. *Mekane Eyesus (mky)* had about 34% missing data and the remaining four stations had 75% to 80% missing data (Table 5-3). Optimization of the exponent *k* for equations 4-2 and 4-3 resulted in around 2.0 for this study.

Table 5-4 Statistical performance of monthly rainfall estimation

| **Stations** | **Stat. measures** | **AM** | **NR** | **IDW** | **CCW** |
|---|---|---|---|---|---|
| | *R* | **0.92** | 0.91 | 0.92 | 0.92 |
| *bdr* | *MAE* | **34.37** | 257.80 | 33.51 | 34.85 |
| | *RMSE* | **59.54** | 420.93 | 61.20 | 60.35 |
| | *R* | 0.93 | 0.90 | 0.92 | **0.93** |
| *dbr* | *MAE* | 35.70 | 252.44 | 38.50 | **35.42** |
| | *RMSE* | 58.70 | 416.98 | 62.11 | **58.30** |
| | *R* | **0.94** | 0.88 | 0.93 | 0.94 |
| *wnz* | *MAE* | **30.81** | 253.80 | 47.31 | 36.51 |
| | *RMSE* | **56.44** | 415.87 | 81.66 | 67.15 |
| | *R* | 0.90 | 0.93 | **0.90** | 0.90 |
| *wor* | *MAE* | 39.21 | 234.51 | **39.02** | 39.56 |
| | *RMSE* | 72.27 | 374.75 | **72.22** | 72.46 |
| | *R* | 0.93 | 0.92 | 0.93 | **0.93** |
| *mky* | *MAE* | 36.37 | 138.03 | 38.21 | **36.30** |
| | *RMSE* | 58.80 | 235.46 | 61.28 | **58.77** |
| | *R* | 0.97 | 0.97 | 0.98 | **0.97** |
| *gsy* | *MAE* | 24.91 | 225.23 | 34.95 | **23.19** |
| | *RMSE* | 37.30 | 355.65 | 53.23 | **35.00** |
| | *R* | **0.98** | 0.92 | 0.98 | 0.98 |
| *amb* | *MAE* | **16.59** | 242.74 | 20.32 | 18.82 |
| | *RMSE* | **24.50** | 379.79 | 34.03 | 30.22 |
| | *R* | 0.95 | 0.96 | 0.96 | **0.83** |
| *lwy* | *MAE* | 25.63 | 254.08 | 25.06 | **17.56** |
| | *RMSE* | 42.32 | 388.72 | 41.02 | **32.28** |
| *arg* | *R* | 0.83 | 0.97 | **0.81** | 0.83 |
| | *MAE* | 57.23 | 131.84 | **57.02** | 57.44 |
| | *RMSE* | 93.49 | 220.65 | **91.06** | 93.63 |

***where , figures shown in bold are results of the best models. Bahir Dar (bdr), Debre Tabor (dbr), Wanzaye (wnz), Woreta (wor), Mekane Eyesus (mky), Gassay (gsy), Amed Ber (amb), Luwaye (lwy) and Arb Gebeya (arg).***

After filling the missing data with the best method for each station, the percent of missing data decreased to less than 4%. Descriptive statistics before and after filling missing daily rainfall values show that the structure of the database is not altered, especially the mean and maximum daily rainfall values.

**Monthly rainfall**

Better correlation coefficients for monthly than daily rainfall data can be observed for all meteorological stations. The *AM* and *CCW* methods showed comparable performance with values of monthly estimated rainfall close to corresponding measured values (Table 5-4). Monthly comparison of model performance reveals the weakness of *R* to identify the best model. The value of *R* is the same for most methods while *RMSE* and *MAE* values are different. For example, *CCW* and *AM* provided comparable and better estimates for daily rainfall at *wnz*. However, *AM* was the best for monthly rainfall estimation for *wnz* even if the value of *R* (*R*=0.94) for both *AM* and *CCW* is the same. The higher *R* value was not the best as seen in the case of *gsy* where IDW gave the best *R* value on a monthly time scale, while *CCW* performed best for both *RMSE* and *MAE* values (Table 5-4). *AM* showed the best estimation at both daily and monthly time scales at the downstream meteorological stations and *CCW* the best at the upstream stations.

The time series of average monthly measured and estimated rainfall shows how close the estimation is to the measures data (Figure 5-2). It makes clear the effect of small statistical differences in *MAE* and *RMSE* as shown, for example, for *wnz*. *NR* values are not included in Figure 5-2, since they are much more overestimated as compared to the other methods.

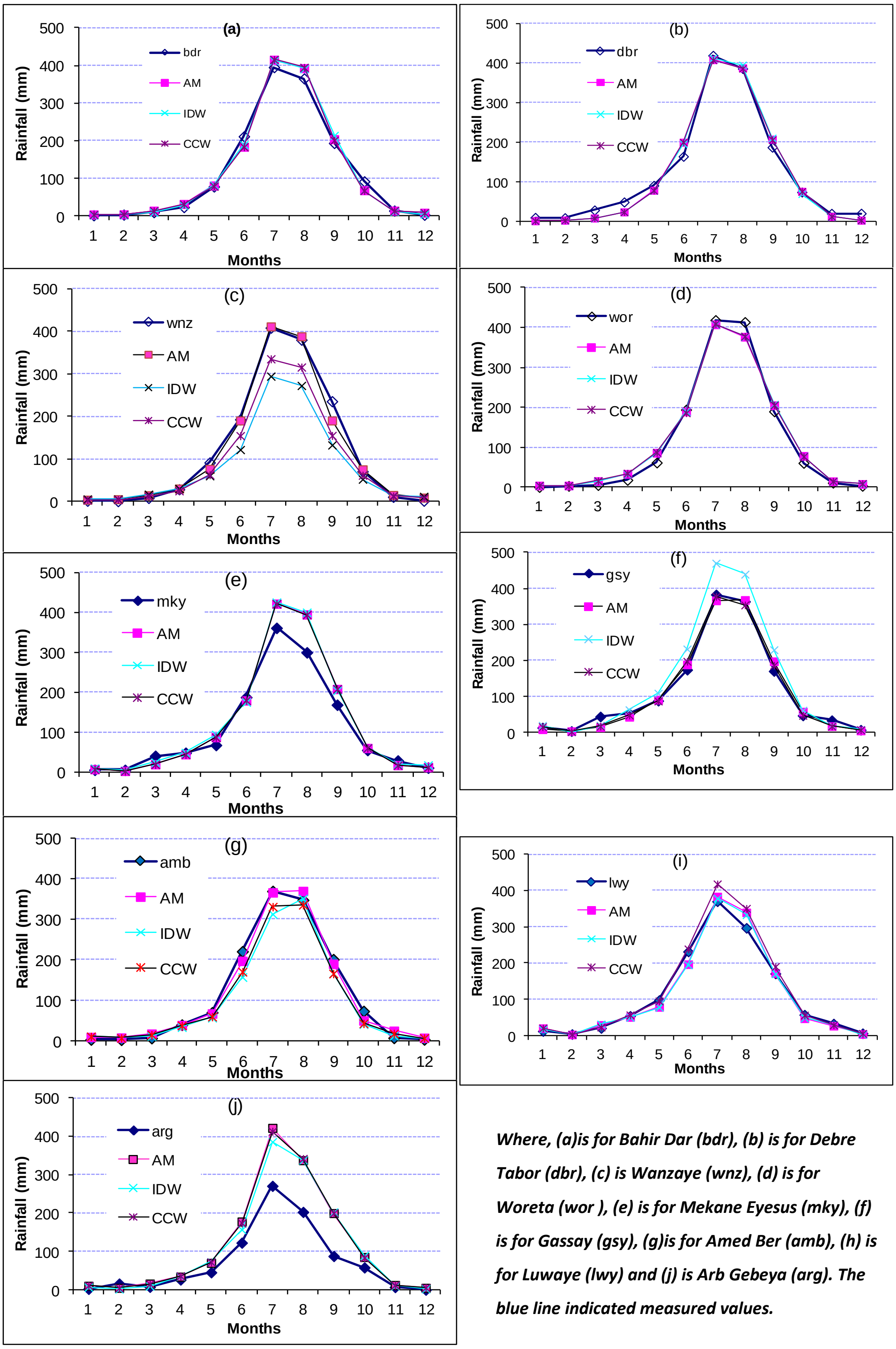


***Where, (a)is for Bahir Dar (bdr), (b) is for Debre Tabor (dbr), (c) is Wanzaye (wnz), (d) is for Woreta (wor ), (e) is for Mekane Eyesus (mky), (f) is for Gassay (gsy), (g)is for Amed Ber (amb), (h) is for Luwaye (lwy) and (j) is Arb Gebeya (arg). The blue line indicated measured values.***

Figure 5-2 Time series of estimation methods as compared to measured (thick blue line) averaged monthly rainfall (mm).

***AM is arithmetic mean, IDW is inverse distance weighting and CCW is coefficient of correlation weighting.***

**Annual rainfall**

The mean annual rainfall value was estimated well except at one station (*arg*) as shown in Table 5-5 and Figure 5-3. The statistical performance is also improved. *AM* is the best method for downstream stations and CCW is best for upstream stations (data not presented) as observed on daily and monthly time scales. However, the CCW method is identified as best for *mky* and *gsy* where CCW and AM were almost equally good for monthly time scales.

Table 5-5 Statistical performance of annual rainfall estimation

| | | *AM* | *NR* | *IDW* | *CCW* |
|---|---|---|---|---|---|
| *bdr* | *R* | **0.92** | 0.97 | 0.92 | 0.92 |
| | *MAE* | **147.41** | 2484.05 | 153.45 | 149.36 |
| | *RMSE* | **194.44** | 2583.89 | 191.56 | 198.29 |
| *dbr* | *R* | 0.89 | 0.84 | 0.88 | **0.89** |
| | *MAE* | 157.63 | 2367.91 | 156.14 | **156.98** |
| | *RMSE* | 245.61 | 2576.75 | 255.64 | **243.63** |
| *wnz* | *R* | **0.93** | 0.80 | 0.91 | 0.93 |
| | *MAE* | **134.51** | 2449.15 | 355.59 | 242.15 |
| | *RMSE* | **188.76** | 2608.79 | 412.20 | 306.77 |
| *wor* | *R* | **0.86** | 0.98 | 0.86 | 0.85 |
| | *MAE* | **187.28** | 2268.81 | 187.04 | 187.13 |
| | *RMSE* | **274.99** | 2505.50 | 275.27 | 278.80 |
| *mky* | *R* | 0.93 | 0.80 | 0.92 | **0.93** |
| | *MAE* | 171.87 | 1395.31 | 199.02 | **169.72** |
| | *RMSE* | 208.59 | 1326.26 | 235.25 | **207.11** |
| *gsy* | *R* | 0.90 | 0.95 | 0.94 | **0.91** |
| | *MAE* | 96.77 | 2291.74 | 259.14 | **90.14** |
| | *RMSE* | 114.70 | 2435.56 | 275.50 | **112.50** |
| *amb* | *R* | **1.00** | 1.00 | 1.00 | 1.00 |
| | *MAE* | **28.71** | 2330.28 | 147.54 | 120.21 |
| | *RMSE* | **34.55** | 2395.45 | 164.94 | 131.15 |
| *lwy* | *R* | 0.88 | 0.86 | **0.89** | 0.96 |
| | *MAE* | 76.24 | 2388.38 | **73.27** | 118.66 |
| | *RMSE* | 97.03 | 2439.46 | **92.89** | 133.29 |
| *arg* | *R* | **0.60** | 0.99 | 0.54 | 0.58 |
| | *MAE* | **455.08** | 1081.20 | 434.75 | 456.41 |
| | *RMSE* | **549.29** | 1232.24 | 541.02 | 553.55 |

***Correlation coefficient( R), root mean square error (RMSE), mean absolute error (MAE), Bahir Dar (bdr), Debre Tabor (dbr), Wanzaye (wnz), Woreta (wor), Mekane Eyesus (mky), Gassay (gsy), Amed Ber (amb), Luwaye (lwy) and Arb Gebeya (arg). Measured data from 1987 to 2008 was used. Figures shown in bold are results of the best models.***

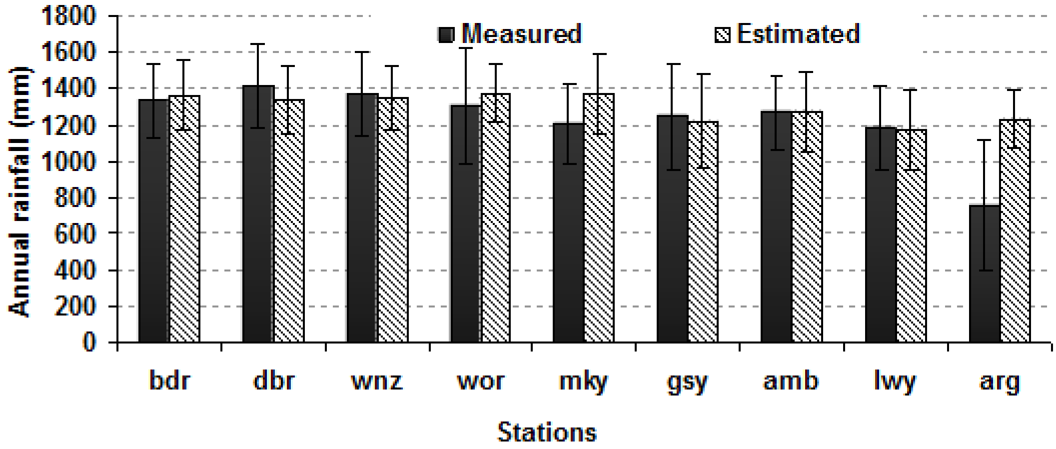


Figure 5-3 Annual rain fall (mm) at meteorological stations indicating measured and estimated values

***Bahir Dar (bdr), Debre Tabor (dbr), Wanzaye (wnz), Woreta (wor), Mekane Eyesus (mky), Gassay (gsy), Amed Ber (amb), Luwaye (lwy) and Arb Gebeya (arg) Error bar indicates standard deviation. Measured data from 1987 to 2008was used.***

The time series of the annual total rainfall shows that there is less variation estimated as compared to variation of individual cases from their mean (Figure 5-3). Data before 1991 were still not improved after filling missing data. This is because at this particular time, the country was under political unrest hence data at most stations were not recorded. The class-four station (*Arb Gebeya*) showed overestimated values (Figure 5-2). The results for *Arb Gebeya* were not good, as less data were available and also a lack of measured rainfall values as compared to the neighboring stations.

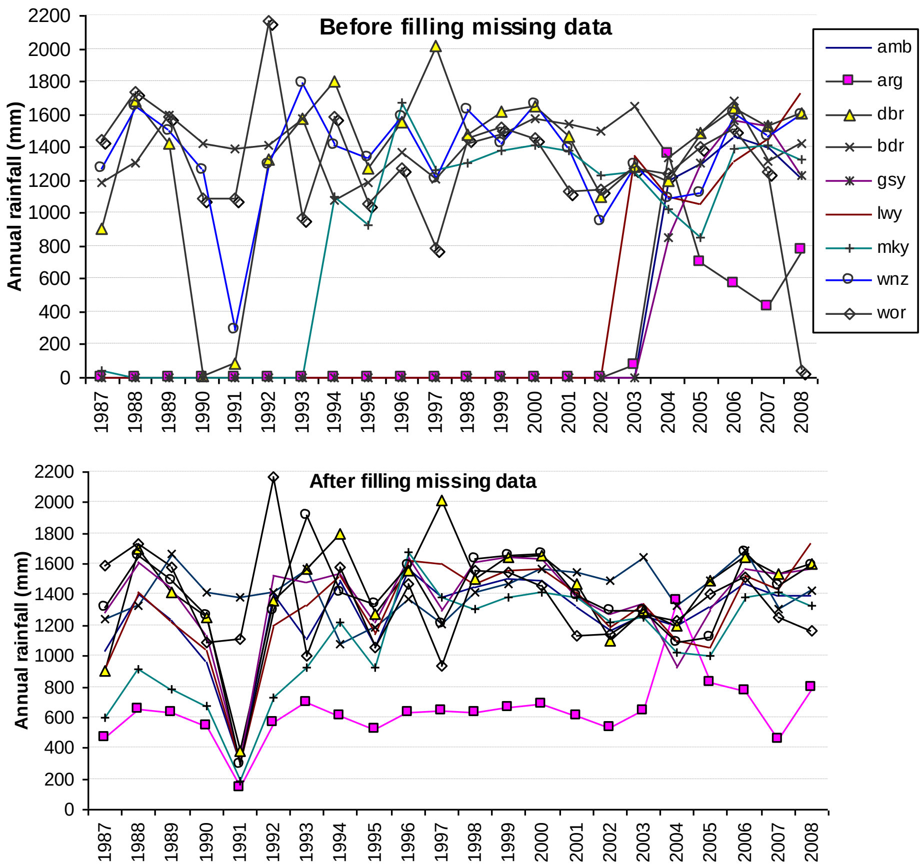


Figure 5-4 Annual rainfall time series after and before filling missing data.

***Bahir Dar (bdr), Debre Tabor (dbr), Wanzaye (wnz), Woreta (wor), Mekane Eyesus (mky), Gassay (gsy), Amed Ber (amb), Luwaye (lwy) and Arb Gebeya (arg). The data in 1991 is not good since most stations were not functional due to political unrest.***

### 5.4.2 Maximum and minimum temperature

The maximum temperatures of the study stations show higher positive correlation to each other than minimum temperature values (Figure 5-5). Minimum temperature values have low positive correlation with each other. The correlation between minimum and maximum temperature is low and negative for most of the times. This correlation behavior indicates that regression models based on within minimum temperature and within maximum temperature provide better estimation results than regression models based on minimum and maximum temperature. Furthermore, multicollinearity problems are expected with regression models between maximum temperature values, since multiple regressions between regressors with high correlation coefficients within themselves are liable for collinearity and erogeneity.

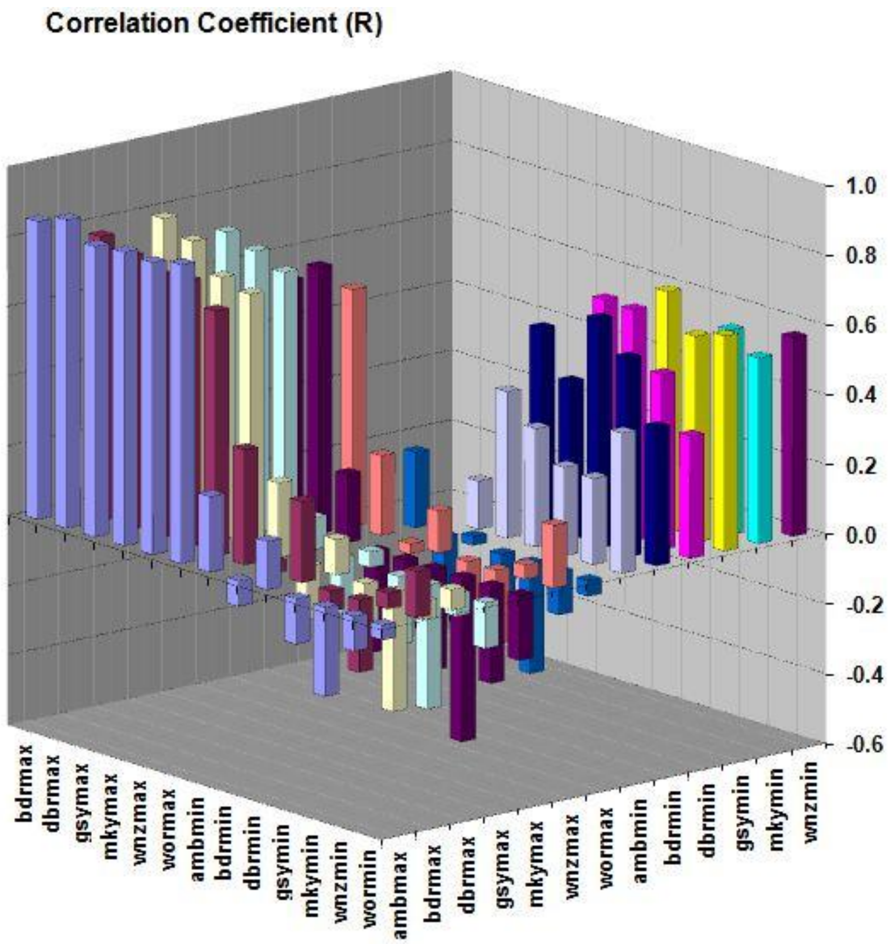


Figure 5-5 Correlation coefficients of maximum (max) and minimum (min) temperature data between stations

***bdr is Bahir Dar, dbr is Debre Tabor, wnz is Wanzaye, wor is Woreta, mky is Mekane Eyesus, gsy is Gassay, amb is Amed Ber, lwy is Luwaye, and arg is Arb Gebey)***

Table 5-6 shows maximum and minimum temperature data availability of seven climate stations used for developing the regression model. Four stations have better data availability and spatial distribution along the watershed to fill the other stations that have relatively short-term databases. The standard deviation of each station indicates that minimum temperature is more variable than maximum temperature.

Table 5-6 Descriptive statistics of daily maximum and minimum temperature used to develop regression models

| | **Station** | **N** | **Missed (%)** | **Min** | **Max** | **Mean** | **Std. deviation** | **Skewness** |
|---|---|---|---|---|---|---|---|---|
| Maximum temperature | *amb* | 2125 | 73.6 | 18.0 | 38.0 | 27.7 | 2.8 | -0.1 |
| | *bdr* | 7842 | 2.4 | 2.6 | 35.0 | 27.1 | 2.5 | 0.0 |
| | *dbr* | 7227 | 10.1 | 1.0 | 30.0 | 21.9 | 2.6 | -0.4 |
| | *gsy* | 1623 | 79.8 | 13.5 | 28.0 | 21.5 | 2.3 | -0.2 |
| | *mky* | 5098 | 36.6 | 15.5 | 36.9 | 26.3 | 3.2 | -0.4 |
| | *wnz* | 6266 | 22.0 | 18.0 | 40.0 | 28.6 | 2.9 | 0.0 |
| | *wor* | 6441 | 19.8 | 13.4 | 37.8 | 28.0 | 2.9 | -0.2 |
| Minimum temperature | *amb* | 1761 | 78.1 | 1.0 | 18.0 | 11.3 | 2.6 | 0.0 |
| | *bdr* | 7835 | 2.5 | 1.0 | 23.3 | 12.7 | 3.0 | -0.6 |
| | *dbr* | 7266 | 9.6 | -9.0 | 19.0 | 9.6 | 1.8 | -0.3 |
| | *gsy* | 1622 | 79.8 | -1.0 | 16.0 | 7.2 | 2.4 | -0.3 |
| | *mky* | 4982 | 38.0 | -6.3 | 19.9 | 8.4 | 3.3 | -0.5 |
| | *wnz* | 5537 | 31.1 | 1.0 | 23.0 | 12.1 | 3.1 | -0.2 |
| | *wor* | 6399 | 20.4 | 1.0 | 20.5 | 11.1 | 3.4 | -0.3 |

***N= number of days with available data (total N=8036) from 1987-2008, Min=minimum and Max=maximum.***

Multiple linear regression models performed well for maximum temperature for most of the stations (Table 5-7). The standard errors of the estimates are less than two and the coefficient of regression ($R^2$) is more than 0.7 for most of the stations. The model performed relatively less good for *Wanzaye* station, which is located in a pocket area and near to *Gumara* riverbed.

Table 5-7 Regression models for daily maximum temperature

| Predictand | Predictors (constant) | $\beta_i$* & $\beta_{oi}$ | Std. errors | $R^2$ |
|---|---|---|---|---|
| *bdr* (n=1075) | Constant | 7.447 | 0.32 | 0.78 |
| | *wor* | 0.388 | 0.02 | |
| | *dbr* | 0.394 | 0.02 | |
| *dbr* (n=2698) | Constant | -2.217 | 0.26 | 0.80 |
| | *mky* | 0.35 | 0.01 | |
| | *bdr* | 0.423 | 0.02 | |
| | *wor* | 0.131 | 0.01 | |
| *wor* (n=1027) | Constant | 0.183 | 0.50 | 0.79 |
| | *bdr* | 0.477 | 0.03 | |
| | *wnz* | 0.316 | 0.03 | |
| | *mky* | 0.216 | 0.02 | |
| *wnz* (n=2696) | Constant | 4.027 | 0.43 | 0.59 |
| | *bdr* | 0.435 | 0.03 | |
| | *wor* | 0.301 | 0.03 | |
| | *mky* | 0.186 | 0.02 | |
| *mky* (n=2698) | Constant | -0.134 | 0.33 | 0.74 |
| | *dbr* | 0.727 | 0.02 | |
| | *wor* | 0.229 | 0.02 | |
| | *wnz* | 0.133 | 0.02 | |
| *amb* (n=1534) | Constant | 0.927 | 0.34 | 0.83 |
| | *dbr* | 0.647 | 0.02 | |
| | *bdr* | 0.451 | 0.02 | |
| *gsy* (n=1081) | Constant | 2.872 | 0.28 | 0.81 |
| | *dbr* | 0.587 | 0.02 | |
| | *mky* | 0.21 | 0.02 | |

***Significant at p<0.05, n is number of daily data used and for description of codes of the stations see Table** 5-1

However, the model developed for minimum temperature showed poor performance (Table 5-8). The $R^2$ is less than 0.7 and the standard error is around 2. The *Amed Ber* station, which is located in the transition from low-plain land to high elevation in the watershed showed poor performance for minimum temperature.

Table 5-8 Regression models for daily minimum temperature

| Predictand | Predictor(s) /constant | $\beta_i$* & $\beta_{oi}$ | Std. error | $R^2$ |
|---|---|---|---|---|
| *bdr* (n=3886) | Constant | 3.753 | 0.25 | 0.63 |
| | *mky* | 0.375 | 0.02 | |
| | *wor* | 0.303 | 0.02 | |
| | *wnz* | 0.150 | 0.02 | |
| *mky* (n=2451) | Constant | -6.251 | 0.24 | 0.61 |
| | *bdr* | 0.306 | 0.02 | |
| | *dbr* | 0.447 | 0.03 | |
| | *wnz* | 0.247 | 0.02 | |
| | *wor* | 0.275 | 0.02 | |
| *dbr* (n=2451) | Constant | 4.703 | 0.16 | 0.51 |
| | *mky* | 0.239 | 0.01 | |
| | *wor* | 0.147 | 0.01 | |
| | *wnz* | 0.074 | 0.01 | |
| *wor* (n=2451) | Constant | 3.815 | 0.24 | 0.50 |
| | *mky* | 0.299 | 0.02 | |
| | *bdr* | 0.269 | 0.02 | |
| | *dbr* | 0.298 | 0.03 | |
| *wnz* (n=2451) | Constant | 2.100 | 0.22 | 0.56 |
| | *bdr* | 0.333 | 0.02 | |
| | *wor* | 0.302 | 0.01 | |
| | *dbr* | 0.236 | 0.03 | |
| *amb* (n=1136) | Constant | 5.512 | 0.40 | 0.34 |
| | *wor* | 0.389 | 0.04 | |
| | *dbr* | 0.351 | 0.04 | |
| | *bdr* | -0.165 | 0.03 | |
| *gsy* (n=991) | Constant | 0.280 | 0.31 | 0.57 |
| | *mky* | 0.332 | 0.03 | |
| | *dbr* | 0.246 | 0.03 | |
| | *wor* | 0.148 | 0.03 | |

****Significant at p<0.05, n is number of daily data used and for description of code of the station see Table 5-1***

Multiple regression models developed for daily temperature data were used to fill missing data of each meteorological station. Time series of daily maximum temperature before and after filling the missing data are shown in Figure 5-6. Since data availability of *gsy* and *amb* stations are from 2003 to 2008, the relation of these stations with their regressor meteorological stations is assumed the same for 1992 to 2002. Missing values are assigned -20 as shown on the top time series curve in Figure 5-6 to indicate how much missing data occurred in each station and was treated after filling. All missing data from 1992 to 2008 is filled using the regression models. The relative structure of the time series curves are maintained after filling missing data.

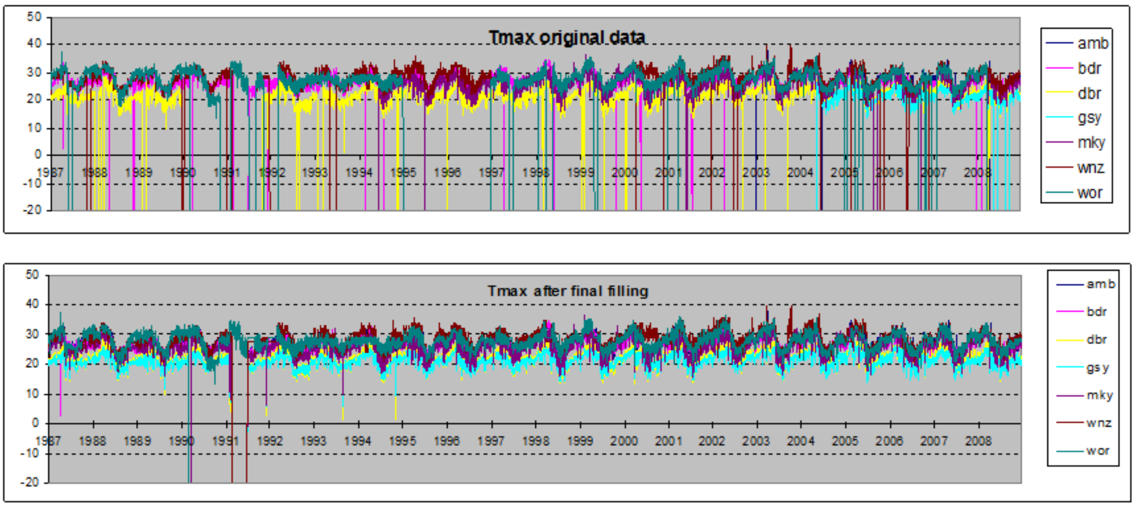


Figure 5-6 Maximum temperature before (top) and after (bottom) filling missing data

Data before 1991 was still not improved after filling missing data. This is because at this particular time the country suffered from political unrest and civil war, and hence at most stations data were not recorded.

### 5.4.3 Relative humidity

Three seasonal relative humidity categories were found using a trial and error method of optimization on a spreadsheet (Table 5-9). The first category was the season with low relative humidity values in the dry winter season of the area. It covers January to May. The second category was with highest relative humidity values in the rainy season from June to September. The relative humidity category is for a short time in June during the transition from the low humidity to high humidity period.

Table 5-9 Seasonal categorization of relative humidity (RH) values

| Category value | Description |
|---|---|
| **1** | Low RH values from February to May |
| **2** | Medium RH values in June and October to January |
| **3** | High RH values from July to September |

The dew point temperature adjustment factor, *a*, was optimized both with and without seasonal categories. The statistical parameters Nash-Sutcliffe coefficient *(NSE), R* and root mean square error (*RMSE*) were used to measure modeling performance. Both *Bahir Dar* and *Debre Tabor* stations have the same adjustment factor when without seasonal category. However, they have different factors for each seasonal category (Table 5-10). Error is minimized and *NS* and *R* are improved during seasonal categorization. The model performs better for the *Bahir Dar* station than for the *Debre Tabor*.

Table 5-10 Optimized dew point adjustment temperature, *a*, and optimized statistical values

| | **Without seasonal categorization** | | **With seasonal categorization** | | |
|---|---|---|---|---|---|
| | ***bdr*** | ***dbr*** | **Category** | ***bdr*** | ***Dbr*** |
| Dew point adjustment factor, *a* | 1.12 | 1.1 | 1 | 4.0687 | 3.4386 |
| | | | 2 | 0.6067 | 1.2894 |
| | | | 3 | -0.6986 | -1.1956 |
| | | Calibration (N=2803) | | | |
| *NSE* | 0.45 | 0.43 | | 0.71 | 0.61 |
| *R* | 0.72 | 0.79 | | 0.84 | 0.80 |
| *RMSE* | 0.10 | 0.14 | | 0.08 | 0.12 |
| | | Validation (N=2811) | | | |
| *NSE* | 0.46 | 0.40 | | 0.67 | 0.59 |
| *R* | 0.64 | 0.75 | | 0.78 | 0.83 |
| *RMSE* | 0.19 | 0.26 | | 0.15 | 0.22 |

***Nash-Sutcliffe coefficient (NSE), correlation coefficient ( R) and root mean squared error (RMSE)***

The time series of measured and simulated relative humidity for the *Bahir Dar* and *Debre Tabor* stations are shown in Figure 5-7 and Figure 5-8, respectively. The difference in seasonal categorization can be clearly observed. Seasonal categorization estimates minimum and maximum relative humidity values better than without categorization.

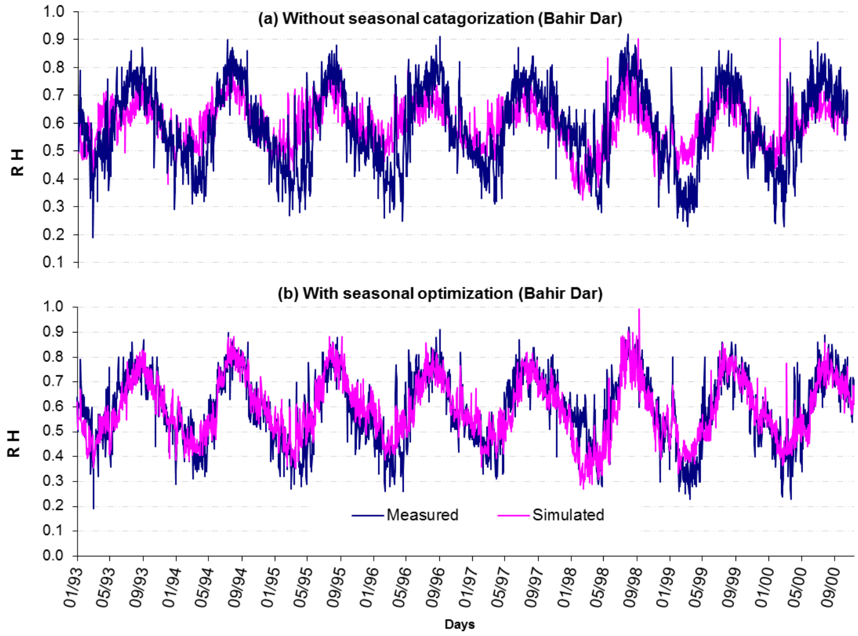


Figure 5-7 **Time series of relative humidity for *Bahir Dar* meteorological station with (b) and without (a) seasonal categorization**

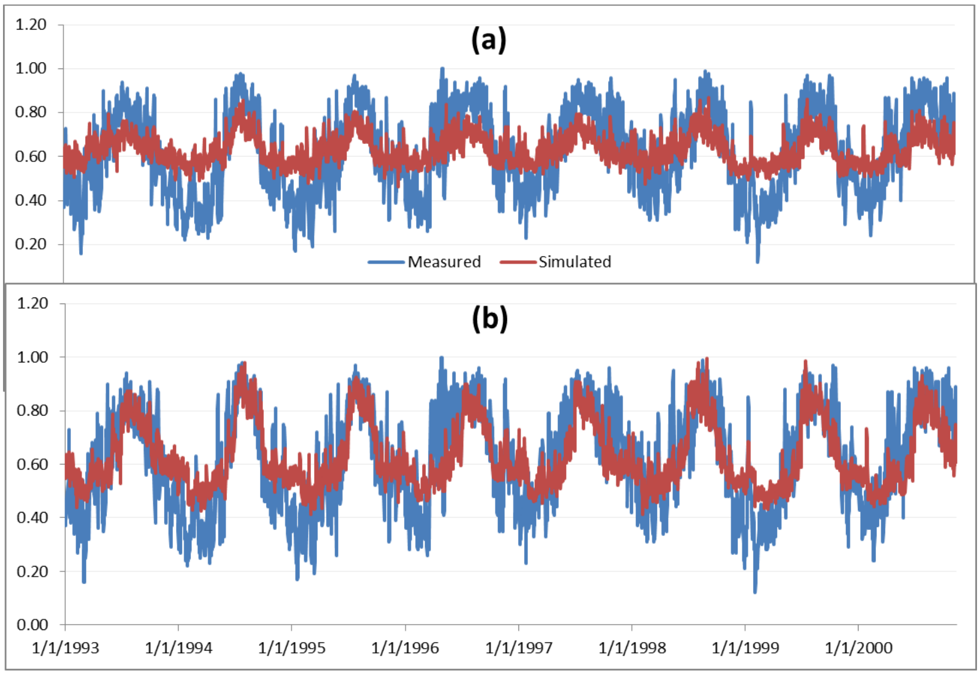


Figure 5-8 Time series of relative humidity for *Debre Tabor* meteorological station with (b) and without (a) seasonal categorization

### 5.4.4 Solar radiation

The correlation coefficient, *R*, is used to identify the relation between different derivative temperature parameters with $R_s/R_a$ as shown in Figure 5-9. Parameters like $T_m$-$T_d$, $\delta$, $\omega_s$, *N* and $T_{mn}$ have low and negative correlation, while those derived forms like $T_m$, $T_{mx}$ and $T_d$ have high and positive correlation. Variables with high correlation coefficients are selected and used in equation 5-17 to optimize the solar radiation *($R_s$)* of the given station.

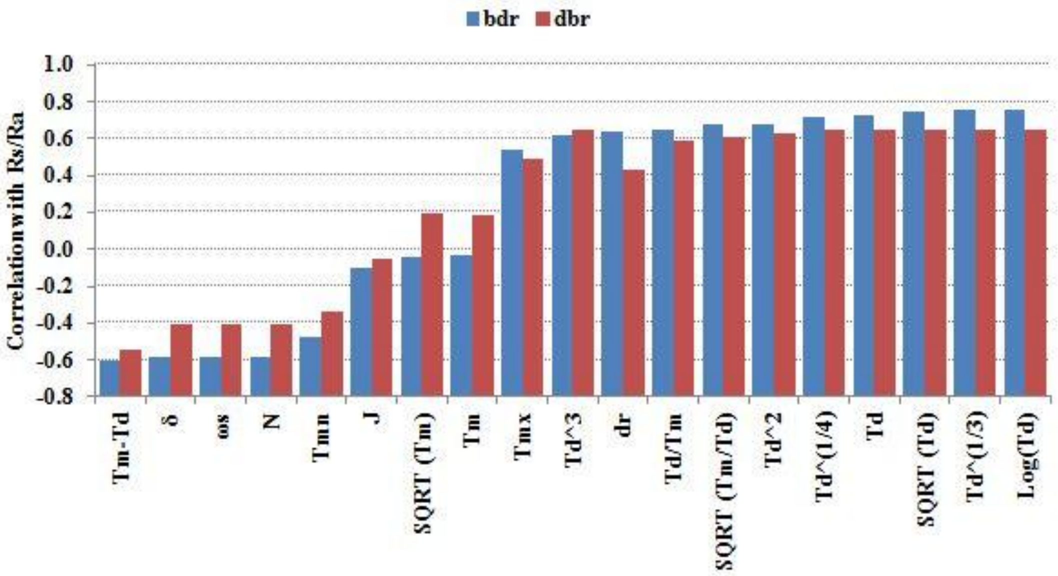


Figure 5-9 Correlation of different parameters with relative solar radiation, $R_s/R_a$.

***$T_m$, is mean temperature, $T_d$ is difference of maximum and minimum temperature, $\delta$ is solar declination, $\omega_s$ is sunset hour angle, N is daylight hour, J is day number in the year, $T_{mx}$ is maximum temperature, $T_{mn}$ is minimum temperature, SQRT is square root, ^ is power of, $d_r$ is inverse relative distance earth-sun and log is logarithm. $R_s/R_a$ is the ratio of extraterrestrial radiation ( $R_a$ ) and shortwave radiation ( $R_s$ ).***

Four seasonal categories arose during optimization of equation 5-17 (Table 5-11). Many trial and error categorization efforts showed low performance of optimization during the process (results not shown here). Seasonality for solar radiation is different from that of relative humidity as shown by two peaks (Figure 5-10). This is also the case for different months for lowland and highland areas.

Table 5-11 Seasonal categories with best solar radiation estimation

| Season | *Bahir Dar* | *Debre Tabor* |
|---|---|---|
| 1 | March and April | April, May |
| 2 | July and August | June, July and August |
| 3 | October, November, and | September, October and November |
| 4 | January, February, May, June | December, January, and February |

Table 5-12 Performance of estimation without seasonal categorization at *Bahir Dar* station

| | Calibration | Validation |
|---|---|---|
| *NSE* | 0.40 | 0.35 |
| *R* | 0.65 | 0.63 |
| *RMSE* | 2.85 | 3.08 |

***Nash-Sutcliffe coefficient (NSE), correlation coefficient ( R) and root mean squared error (RMSE)***

Results of the statistical performance when estimating solar radiation from other meteorological parameters are shown in Table 5-12, 5-13, and 5-14. Estimation performance without seasonal categorization is lower as compared to seasonal categorization. The square root function of $T_d$ leads the estimation of solar radiation at both meteorological stations (Table 5-12 and Table 3-13). The estimation performance of the station located in the cold and highland part of the area is lower as compared to that of the station in the hot and lowland part of the area.

Table 5-13 Performance of modeling solar radiation using seasonal categories and different functions of $T_d$ for *Bahir Dar* station

| | | $(T_d)^{1/2}$ | $(T_d)^{1/3}$ | $Log(T_d)$ |
|---|---|---|---|---|
| *NSE* | Val | 0.50 | 0.47 | 0.47 |
| | Cal | 0.51 | 0.45 | 0.45 |
| *R* | Val | 0.71 | 0.68 | 0.69 |
| | Cal | 0.72 | 0.67 | 0.69 |
| *RMSE* | Val | 7.43 | 7.93 | 7.82 |
| | Cal | 6.55 | 7.38 | 7.28 |

$T_d = T_{max} - T_{min}$

***Nash-Sutcliffe coefficient (NSE), correlation coefficient ( R) and root mean squared error (RMSE)***

Table 5-14 Performance of modeling solar radiation using seasonal categories and different functions of $T_d$ for *Debre Tabor* station

| | | $(T_d)^{1/2}$ | $(T_d)^{1/3}$ | Log($T_d$) |
|---|---|---|---|---|
| *NSE* | Val | 0.30 | 0.24 | 0.27 |
| | Cal | 0.40 | 0.33 | 0.34 |
| *R* | Val | 0.57 | 0.50 | 0.53 |
| | Cal | 0.63 | 0.59 | 0.59 |
| *RMSE* | Val | 10.39 | 11.37 | 10.86 |
| | Cal | 8.72 | 9.76 | 9.58 |

$T_d = T_{max} - T_{min}$

***Nash-Sutcliffe coefficient (NSE), correlation coefficient ( R) and root mean squared error (RMSE)***

Table 5-15 Seasonal optimized adjustment coefficient ($K_{RS}$)

| Season | *Bahir Dar* | *Debre Tabor* |
|---|---|---|
| 1 | 0.156090 | 0.161129 |
| 2 | 0.139151 | 0.153889 |
| 3 | 0.167163 | 0.165440 |
| 4 | 0.155991 | 0.161093 |

The solar radiation adjustment coefficient ($K_{RS}$) for each season at each station varies from 0.14 to 0.16 (Table 5-15). Although the variation seems small, the effect of the optimized adjustment coefficient is relatively high on performance of estimation (Table 5-12 and Table 5-14). Therefore, the $K_{RS}$ values are given with six significant digits in Table 5-15.

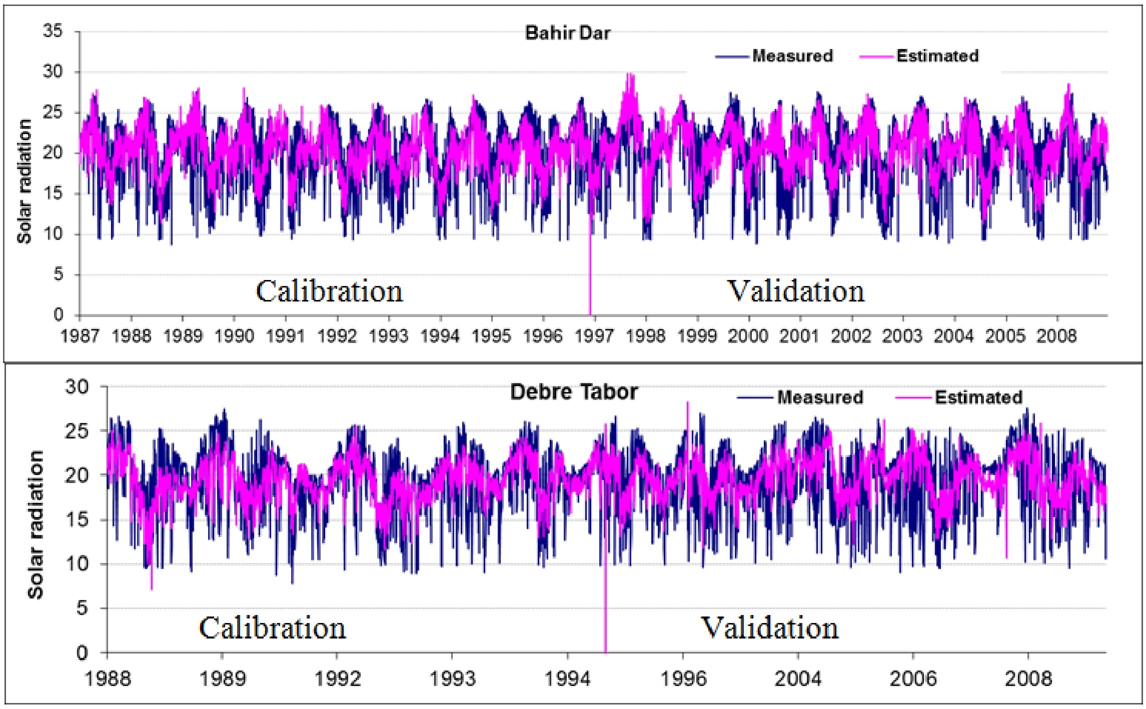


Figure 5-10 Time series showing measured and estimated daily solar radiation (MJ/m$^2$/day) in calibration and validation period

The weakness of the developed solar radiation model can be clearly observed in the time series graph (Figure 5-10) and scatter plots (Figure 5-11). Upper and lower peak radiation values are not properly addressed as compared to relative humidity. The lower peaks of the coldest highland station, *Debre Tabor*, are not addressed very well as compared to those of the hot lowland station *Bahir Dar*.

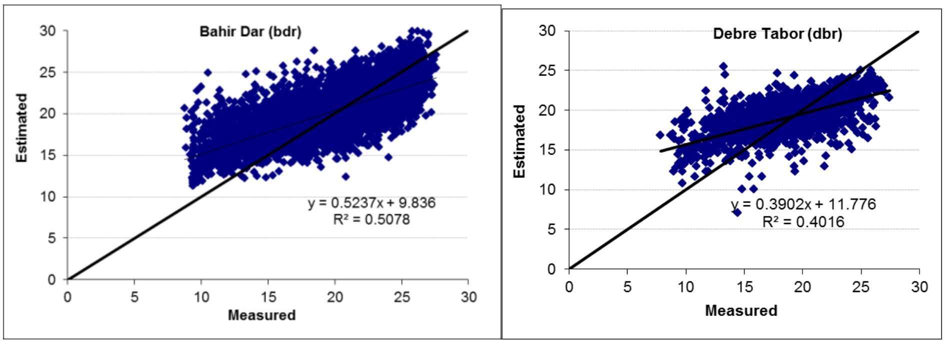


Figure 5-11 **Scatter plots of measured and estimated daily solar radiation (MJ/m$^2$/day) of Bahir Dar and Debre Tabor stations**

## 5.5 Discussion

Two rainfall estimation methods, *AM* and *IDW*, have comparable performance with respect to filling missing daily rainfall values for the area. The results match studies in other parts of the world. For example, Tang et al. (1996) obtained similar results in Malaysia, where *NR* and *IDW* performed best as compared to ten other methods for estimating monthly and annual rainfall. De Silva et al. (2007) also identified *IDW* as being the best compared to *AM*, *NR* and two other methods to estimate monthly rainfall values. However, *CCW* was not included in the studies by Tang et al. (1996) and De Silva et al. (2007). Teegavarapu and Chandramouli (2005) found *CCW* and artificial neural networks (*ANN*) the best. *CCW*, however, was recommended due to its practicality, spatial implication, and simplicity. Different rainfall estimation methods showed different performances at different elevation positions of the study watershed. Similar findings also exist for a study in Sri Lanka. De Silva et al. (1997) compared *AM*, *NR*, *IDW* and aerial precipitation ratio methods using monthly rainfall where *AM* was found to be the best for upstream locations. They also reported about *RMSE* values of 90 to 100, which are higher than those in this study. The statistical estimation performance in this study is comparable with that in a study by Teegavarapu and Chandramouli (2005) in Kentucky, USA, with 7801 data days that resulted in an average value of 1.93 mm *MAE* and 5.78 mm *RMSE* values. Although the methods in this study generally showed poorer performance, they are still promising, especially when compared to findings for the technically superior meteorological stations in the USA.

However, after filling missing data all descriptive statistics (Table 5-3) showed lower values, thus indicating the problem of underestimation and minimizing the real variability from the mean. Data for the class-four station (*Arb Gebeya*) were overestimated. The reason may be the inaccuracy of measurements, since the station was not managed with skilled manpower, and there were no frequent observation and data quality checks as at other stations (personal observation during fieldwork).

The relationship between maximum and minimum temperature shows negative and low correlation. That means that very hot days have very cold nights. This extreme fluctuation has impacts on agricultural productivity, since plants need a smooth shift from hot to cold temperature events (Zinn et al. 2010). The performance when estimating daily minimum temperatures is poorer than that for daily maximum temperatures. This is due to the fact that minimum temperatures are highly locally variable, which resulted in low correlation with respect to neighboring station. Kotsiantis et al. (2006) used temperature data of previous years of a given station to fill missing data of a given year of the same station using the regression equation. The correlation coefficient of 0.9 between estimated and measured air temperature is comparable with the estimation of maximum daily air temperature in this study.

Maximum and minimum temperatures are used to estimate relative humidity and solar radiation. Seasonal categorization improves estimation performance for relative humidity better than for solar radiation. The dew-point temperature adjustment coefficient varies greatly when compared to the adjustment coefficient for solar radiation.

Measured solar radiation values vary for successive days especially at the lower peak value days as compared to relative humidity. Therefore, the performance of the temperature-based solar radiation estimation method is poorer than for relative humidity. Low peak values occurred during the main rainy season where there is a high cloud cover. This indicates that other variables like occurrence of cloud may be important together with daily temperature values to estimate solar radiation. On the other hand, higher peaks during the clear-sky dry seasons are underestimated. Calibration using hourly time-scale measured data may improve addressing the peaks. $\sqrt{T_{max} - T_{min}}$ of a given day is better for the estimation of daily solar radiation than other temperature derivatives as equated by Hargreaves and Samani (1982) for the study area. However, these authors produce the same adjustment coefficient throughout the year in the relationship between $\sqrt{T_{max} - T_{min}}$ and $R_a / R_s$. Morid et al. (2002) derived the adjustment coefficient using maximum and minimum temperature at an alpine catchment in Iran, and the resulting 0.16 is within the range of the value in this study.

## 5.6 Conclusions

Different approaches and methods were used to estimate missing daily meteorological variables, i.e., rainfall, maximum temperature, minimum temperature, relative humidity and solar radiation. Data from nine stations that ranged from 5 to 22 years coverage were used to compare spatial daily rainfall estimation methods at the headwater of the Blue Nile basin in Ethiopia. The statistical performance of the estimation methods showed results comparable with other similar studies done elsewhere. The methods arithmetic mean (*AM*) and coefficient of correlation weighting (*CCW*) provided better daily rainfall estimation than normal ratio (*NR*) and inverse distance weighting (*IDW*) in most of the stations. Different estimation methods performed best for different locations of the meteorological stations with respect to elevation. *AM* performed best for stations at downstream locations, while *CCW* was best at upstream locations.

It is very important to establish additional representative meteorological stations so that interpolation and extrapolation of measured relative humidity and solar radiation values are possible using the methods discussed above. The estimation of relative humidity and solar radiation values using air temperature data from several stations as in this study is promising when compared to estimations using data from only two meteorological stations for local water management planning.

Further research is recommended that includes more stations and a larger area cover for better water resources management. Altitude can be included as one factor if more meteorological stations at different elevation are considered for better performance with respect to filling missing data. This methodology will help to make stations with low quality and quantity databases suitable for water resources management of the area, as these stations have been excluded under the existing water development. The importance of using every database in the area can be evaluated further regarding efficiency of hydrological models.

# 6 EFFECT OF CLIMATE STATION DENSITY AND POTENTIAL EVAPOTRANSPIRATION CALCULATION METHODS ON WATER BALANCE MODELING

## 6.1 Summary

Water balance modeling increases our understanding to make decisions on using water resources effectively and sustainably. However, hydrological modeling needs a meteorological database with reliable time series. Obtaining reliable data for these meteorological variables is difficult at spatial and temporal scales in developing countries. Therefore, it is of utmost importance to study the effect of data availability on hydrological modeling to be able to quantify uncertainty caused by boundary conditions. Different modeling setups were used for the Soil and Water Assessment Tool (SWAT) to quantify the performance of the water balance simulation. They considered meteorological station density, different methods for calculating potential evapotranspiration (*PET*) (Penman-Monteith and Hargreaves) and different approaches for handling missing data. Penman-Monteith and Hargreaves *PET* calculation methods gave comparable river flow modeling performance. Modeling using six and four stations gave better performance concerning the water balance patterns as compared to using two stations. It is important to have a minimum density of meteorological stations in the mountainous highland parts of the Blue Nile to manage the water resources at micro- and meso-watershed scales.

## 6.2 Introduction

Spatially distributed meteorological variables are highly important for hydrological modeling and design of water resources projects. Rainfall is the major driving force for runoff and solute transport as compared to the other meteorological variables (Cho et al. 2009; Bormann et al. 1999). Gassman et al. (2007) reviewed previous SWAT applications and identified inadequate representation of meteorological input variables, especially rainfall. The representation can be inadequate due to lack of rain gauges in the watershed or due to a sub-watershed configuration that is too coarse to capture all spatially distributed stations. This inadequacy caused weak or incorrect hydrological simulation results.

Some studies investigated the effects of spatial resolutions of input data on the accuracy of hydrological modeling (Chaplot et al*.* 2005; Chaubey et al. 2005; Wang and Melesse, 2006; Cho et al. 2009). Cho et al. (2009) performed a study on the effect of spatially variable rainfall data on the uncertainty of SWAT output. SWAT takes climate input data that is nearest to each sub-watershed centroid (Neitsch et al. 2002). Therefore, the SWAT algorithm causes a sharp difference in rainfall and other water balance components at the boundary of each sub-watershed.

River master plans, irrigation and hydropower projects have been developed and implemented throughout Ethiopia to reduce poverty and to mitigate climatic change effects. These water development projects need accurate hydrometeorological analysis methodology and tools. In many countries, not only is the station density too low and the period of measurements too short but data is also missing due to the effect of device failure during the collection of climate data. The missing values affect environmental time series (Presti et al. 2010) and hydrological modeling. Inconsistent and biased hydrologic analysis and conclusions in water resources development planning are the result of missing data (Kim and Ahn 2009). Missing values have to be filled before using the data for further investigations.

Hydrological modeling is crucial for planning water development activities as well as for controlling and implementing water use during and after implementation of the projects. Previous studies in the study area used coarse databases, so that evaluation of the results at the local scale, e.g., the *Gumara* watershed, is very difficult. For example, Setegn et al. (2008) used only five stations for the 15,000 km$^2$ Lake *Tana* Basin; *Gumara* watershed is one of its sub-basins. This means that station density is one station for an area of 3,000 km$^2$. For planning irrigation water requirement and for flood frequency analysis for the *Gumara* irrigation project (*GIP*), the MoWR (Ministry of Water Resources of Ethiopia, 2008) use data from a station located 50 km away (*Bahir Dar*). This may create discrepancies, since the physical status of the area of interest (dam catchment of *GIP*) is different from that of the total catchment.

In this chapter, the effects of different setups in water balance modeling using SWAT hydrological models are compared for the following objectives.

## 6.3 Objectives

The general objective is to calibrate the SWAT model for the *Gumara* watershed in the Blue Nile Basin. This is guided by the following specific objectives:

1. To identify the effect of the meteorological station density on the water balance modeling of the watershed.
2. To evaluate the effect of Penman-Monteith and Hargreaves potential evapotranspiration methods on model performance.
3. To identify the effect of methods for filling missing spatial and temporal data on SWAT modeling results.

## 6.4 Materials and methods

### 6.4.1 Description of the study area

The study was performed in the *Gumara* watershed in the Blue Nile Basin of Ethiopia. It covers 1,360 km$^2$, and is located between 37˚38' to 38˚ 11' E and 11˚ 35' to 11˚ 54' N (Figure 2-1). *Gumara* River is one of the rivers draining to Lake *Tana* (Kebede, 2006), which is one of the largest water bodies in Africa. The lake receives 93% of drained water from four main rivers: *Gilgel-Abbay*, *Reb*, *Gumara* and *Megetch* (Kebede 2006; Vijverberg et al*.* 2009). The climate is tropical highland monsoon where the seasonal rain distribution is dominated by the movement of the inter-tropical convergence zone (ITCZ) and by moist air from the Atlantic and Indian Ocean in the summer (June-September) (Kebede 2006). The mean annual rainfall and mean temperature is 1400 mm and 20°C, respectively. The study area is characterized by a mixed crop-livestock farming system with rice-based cash crops, maize, small cereals and cereal-pulse (Haileslassie et al. 2009$_a$).

### 6.4.2 Database development

SWAT needs spatially distributed data, i.e., digital elevation model (DEM), land-use, soil and meteorological data (rainfall, temperature, relative humidity, solar radiation and wind speed). These data were collected and checked for consistency before SWAT modeling was applied.

The 30-m resolution Global Digital Elevation Model (GDEM) was downloaded free from http://asterweb.jpl.nasa.gov/gdem.asp (Advanced Spaceborne Thermal Emission and Reflection Radiometer (ASTER)). This DEM was used for watershed and sub-watershed delineation, reach identification and slope-class categorization. The land-use map and stream network data of the watershed were taken from the MoWR database that was organized for the feasibility study of the *Gumara* irrigation project (*GIP*). The data were checked using ground control points data that had been collected during field observations in different seasons in 2009 and 2010.

Soil physical and chemical data at each soil unit and soil depth layer are important spatial data for modeling hydrological balance components in SWAT. It was difficult to obtain all soil data in Ethiopia, and different soil databases were used in this study. The MoWR did a detailed soil survey study for the downstream side of *Gumara* watershed (MoWR 2008) for the *GIP* feasibility study. This recent soil database was used to fill most of soil physical and chemical properties in the watershed. Soil texture and soil layer data were taken from the *Abbay* River Basin Integrated Development Master Plan Project (ARBIDMPP) database of the MoWR, who had performed a semi-detailed soil survey in the Blue Nile Basin (BCOM 1998). Figure 6-1 shows the DEM, soil and land-use database maps.

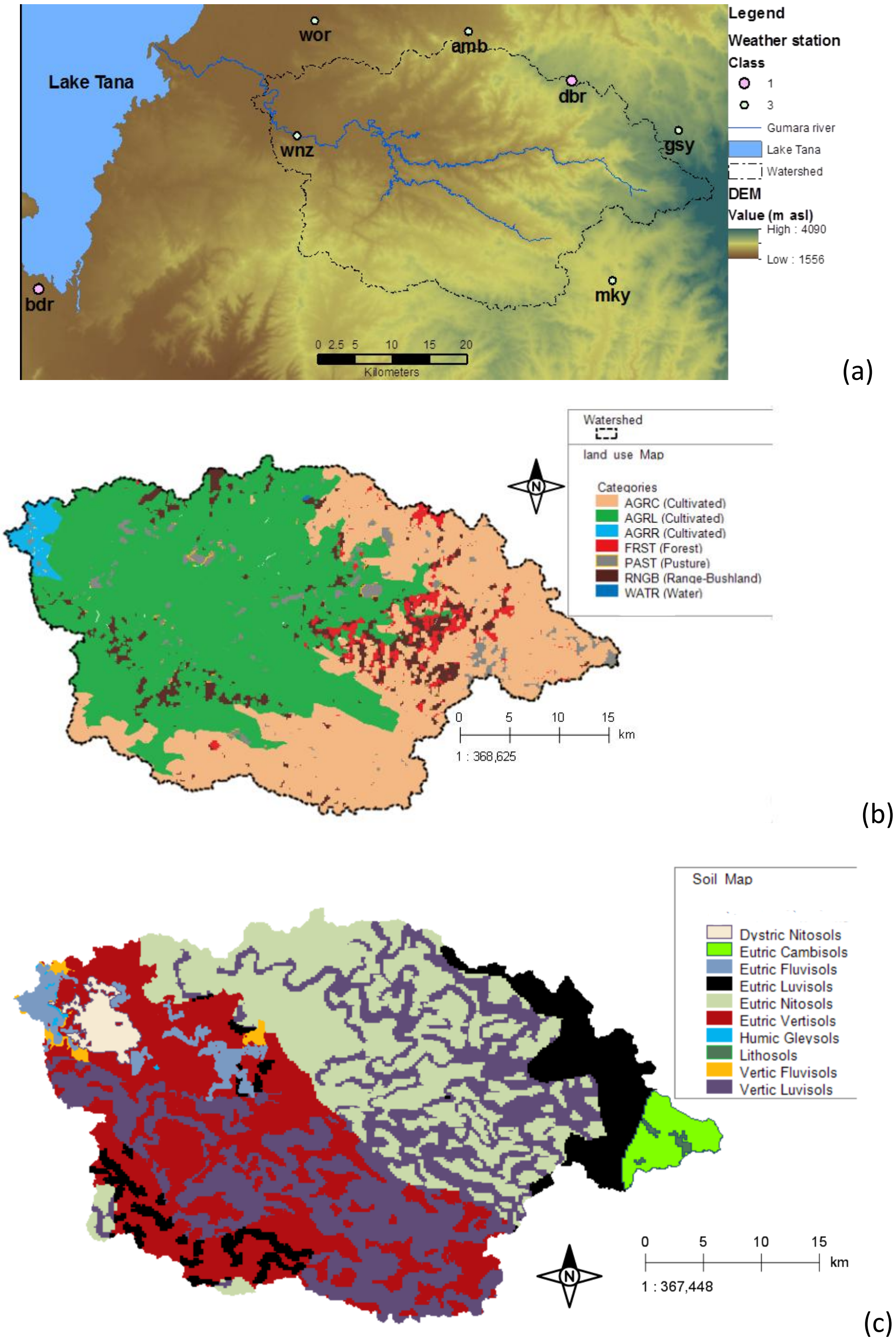


Figure 6-1 DEM and map of meteorological station distribution (a), soil map (b) and land-use map (c) of *Gumara* watershed.

***(Source: Soil data from MoWR (2008) and BCOM (1998), land-use from MoWR (2008), field investigation by the author and farming system data from Haileslassie et al. (2009$_a$); DEM downloaded from http://asterweb.jpl.nasa.gov/gdem.asp)***

***Meteorological station category: Class 1 (Bahir Dar-bdr and Debre Tabor-dbr), Class 3(Wanzaye-wnz, Werota-wor, Amed Ber-amb Gasay-gsy and Mekane Eyesus-mky) and Class (Arb Gebeya-arg and Luwaye-lwy)***

***SWAT land-use units: Agricultural Land –Close-Grown (AGRC), Agricultural Land – Generic (AGRL), Agricultural Land – Row Crops (AGRR), Forest-Mixed (FRST), Pasture (PAST), Range –Bush (RNGB), and WATeR body (WATR).***

Meteorological data were provided by the Ethiopian National Meteorological Agency (ENMA). Four classes of meteorological stations are installed in Ethiopia at different geographical locations. First class (synoptic) stations are stations where the meteorological observation data are used for synoptic meteorology. Second class (principal or indicative) stations are stations providing observation data for the purpose of climatology. At third class (ordinary) stations, only maximum temperature, minimum temperature and rainfall data are recorded. Forth class stations are used to record only rainfall. About 22 and 150 synoptic and principal meteorological stations, respectively, are located in Ethiopia (http://www.ethiomet.gov.et/stations/regional_information/1#Synoptic (Cited on 24/04/2012)).

Of the annual rainfall, 21% and 70% occurred in the second (April-May-June) and the third (July-August-September) seasons (Figure 6-2), respectively. Almost 50% of the year is dry. The first season is the land preparation season, and the second is the main rainy season. Not only rainfall amount, but also its variability and temporal occurrence are very important for the crop and livestock productivity of the area. The rainfall amount was highly variable in the main rainy season.

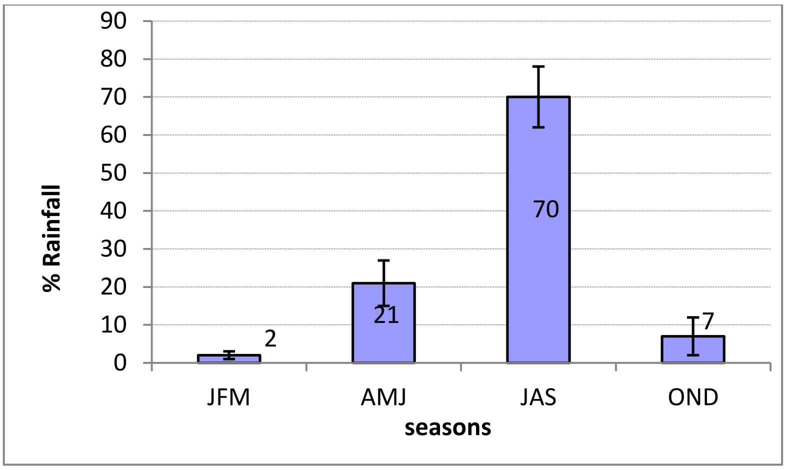


Figure 6-2 Seasonal rainfall contribution from 1992 to 2001.

***JFM = January-February-March, AMJ =April-May-June, JAS = July-August-September, OND = October-November-December. Basin rainfall data were calculated using the Thiessen polygon method from four stations.***

### 6.4.3 Modeling setup

Meteorological stations within and around the watershed were categorized into groups depending on data availability and on meteorological stations that had been used frequently in other studies. Missing data of all meteorological variables of the stations were filled using the weather generator routine of SWAT (*WXGEN*), which is well discussed in the theoretical documentation by Neitsch et al. (2011). The best missing meteorological data handling methods (see section 5) were used to compare their effect on water balance modeling. Meteorological variables that are not measured in Class 3 stations were substituted with measured values from the nearby Class 1 stations. The substitution is based on the topographical similarities like relief and elevation (i.e., *Bahir Dar* for *Woreta, Amed Ber* and *Wanzaye* and *Debre Tabor* for *Mekane-Eyesus* and *Gassay*). The following three groups of meteorological stations were formed to observe the effect of station density on modeling performance:

1. Class 1 stations (*Bahir Dar* and *Debre Tabor*): These stations have long-term databases of rainfall, temperature, sunshine hours, relative humidity and wind speed. *Bahir Dar* was used for most of the studies done for the watershed as it is located far away from *Gumara* watershed as compared to the other stations (Figure 6-1). The Class 1 group is called "two stations" hereafter.
2. The best four stations (*Woreta*, *Wanzaye*, *Debre Tabor* and *Mekane Eyesus*): These stations are called best since they are located at relatively representative positions in the watershed. The stations had relatively better long-term databases as compared to the others during both the calibration and validation period. These stations are grouped together and named "four stations". The data were used during calibration and validation.
3. Class 1 and Class 3 stations (*Debre Tabor, Woreta, Amedber, Gassay, Mekane-Eyesus* and *Wanzaye*): - Class 3 stations record rainfall and temperature data. This setup is named "six stations" hereafter. SWAT excluded *Bahir Dar* automatically as an input since the additional Class 3 stations covered every sub-watershed, which was covered by *Bahir Dar*.

Discharge data were grouped into two periods: 1992 to 1995 for calibration and 1998 to 2001 for validation (Figure 6-3). Data within 1990-1991 and 1996-1997 were used for model warm-up for calibration and validation, respectively. This grouping for calibration and validation was formed after checking the validity of the meteorological and hydrometric time series data.

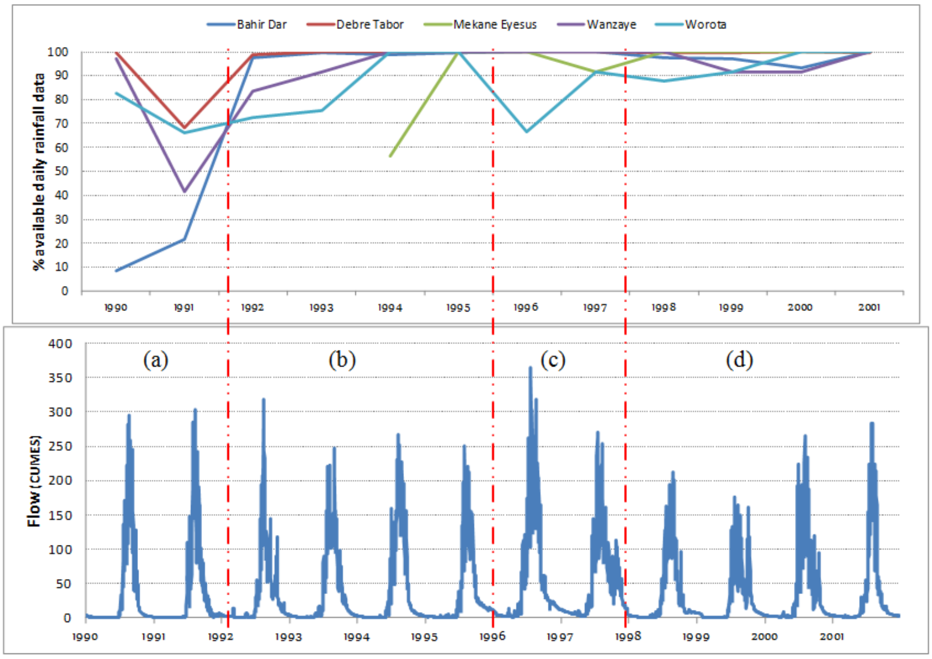


Figure 6-3 Time series data for calibration and validation

***Note: Data in region (a) and (c) were used for model warm-up, (b) for calibration and (d) for validation.***

Two approaches were tested to evaluate the effect of filling missing data on SWAT modeling performance, i.e., the SWAT weather generator routine (*WXGEN*) and the regression method (*REG*) discussed (see section 5). *WXGEN* uses the Markov chain-skewed (Nicks 1974) or the Markov chain-exponential (Williams 1995) models to generate daily rainfall data for a given station. The first-order Markov chain is used to define the day as wet or dry. A skewed distribution or exponential distribution is used to generate the precipitation amount. A wet day is defined as a day with 0.1 mm of rain or more. The *WXGEN* needs monthly average meteorological values over many years as parameters. These parameters can be easily prepared for SWAT based on independent procedures like pcpSTAT for rainfall and dew.exe for dew point temperature (Liersch 2003$_{a,b}$). The *WXGEN* weather generator model (Sharpley and Williams 1990) was developed to generate climatic data or to fill in gaps in measured records. The SWAT routine for weather generation of each meteorological variable is explained in the SWAT theoretical documentation (Neitsch et al. 2011). Three station densities, two missing data filling methods, and two evapotranspiration procedures give 12 combinations. However, *Gumara* was not the experimental watershed so that historical data were not measured in a condition to compare all these combinations. Only four stations had relatively better historical data for calibration and validation than the other two stations (see section 5). Therefore, only five of the combinations were selected for calibration and validation of the SWAT model for the watershed due to lack of data from some stations during the calibration and validation periods.

As the number of climate stations for the watershed increases, the number of sub-watersheds and Hydrological Response Unit (*HRU*) has to be increased to incorporate each additional station. Finally, sub-watershed and *HRU* discretization was carried out in order to accommodate all the data layers for the model setups. Thus, 37 sub-watersheds and 113 HRU were formed for calibration and validation.

#### 6.4.4 Model performance and uncertainty evaluation

The calibration was performed using the Sequential Uncertainty Fitting _version 2 (SUFI-2) interface of SWAT-CUP. SWAT-CUP is a separate calibration and uncertainty program developed by Abbaspour et al. (2004). SUFI-2 is a frequently used procedure for calibration and uncertainty analysis (Setegn et al. 2008). Yang et al. (2008) compared different procedures and found SUFI-2 better, as it gives good results even with the smallest number of runs as compared to other procedures.

Graphical and statistical techniques were applied to evaluate model performance. Moriasi et al. (2007) recommend one dimensionless and two error indices from several statistical model evaluation techniques. These measures were used for this study. The dimensionless Nash-Sutcliffe efficiency (*NSE*) (Nash and Sutcliffe 1970) measures normalized magnitude of the residual variance relative to measured flow variance. The value of *NSE* ranges from $-\infty$ to 1, while the value 1 for *NSE* indicates the perfect fit from the 1:1 line. *NSE* values less than zero indicate unsatisfactory performance. One of the error indices used for this study was percent bias (*PBIAS*) (Gupta et al. 1999). It indicates the average difference between simulated and measured discharge. A zero value of *PBIAS* indicates perfect fit; a negative value indicates overestimation while a positive value indicates underestimation of the model

(Moriasi et al. 2007). The ratio of root mean square error (*RMSE*) to observation standard deviation (*RSR*) was recommended by Singh et al. (2004), which benefits the additional scaling or normalization factor to the error index given by *RMSE. RSR* varies from 0 to $+\infty$ where 0 indicates perfect simulation. Table 6-1 shows the mathematical representations of these techniques and recommended range of performance for the SWAT model.

Table 6-1 Model performance rating for stream flow at monthly time scale

| Performance rate | Equations | | |
|---|---|---|---|
| | $NSE = 1 - \left[\frac{\sum_{i=1}^{n}(Q_o - Q_s)^2}{\sum_{i=1}^{n}(Q_o - \overline{Q_o})^2}\right]$ | $PBIAS = \left[\frac{\sum_{i=1}^{n}(Q_o - Q_s)}{\sum_{i=1}^{n}(Q_o)}\right]*100$ | $RSR = \frac{\sqrt{\sum_{i=1}^{n}(Q_o - Q_s)^2}}{\sqrt{\sum_{i=1}^{n}(Q_o - \overline{Q_o})^2}}$ |
| Very good | 0.75 < NSE $\leq$ 1.00 | \|PBIAS\| < 10 | 0.00 $\leq$ RSR $\leq$ 0.50 |
| Good | 0.65 < NSE $\leq$ 0.75 | 10 $\leq$ \|PBIAS\| < 15 | 0.50 < RSR $\leq$ 0.60 |
| Satisfactory | 0.50 < NSE $\leq$ 0.65 | 15 $\leq$ \|PBIAS\| < 25 | 0.60 < RSR $\leq$ 0.70 |
| Unsatisfactory | NSE $\leq$ 0.50 | \|PBIAS\| $\geq$ 25 | RSR > 0.70 |

***Source: (Moriasi et al. 2007)where, NSE is Nash-Sutcliffe efficiency, PBIAS is percent bias, RSR is the ratio of root mean square error to observation standard deviation, and $Q_o$, $Q_s$ and $\overline{Q_o}$ are measured simulated and mean of measured discharge values, respectively.***

Coefficient of determination ($R^2$) and mean separation statistical techniques were used to measure the level of correlation among model variables, and to measure mean differences of water balance components using different station densities. Coefficient of determination is the square of the correlation between observed and simulated values that measures how much measured values variation is explained the in simulation (Krause et al. 2005). It ranges between 0 and 1. The value 1 indicates that the variation of the simulation is equal to the variation of the observed time series.

Hydrological modeling produces uncertain predictions due to model structure (structural uncertainty), input data (input uncertainty), and parameters (parameter uncertainty) (Brown and Heuvelink 2005; Abbaspour 2011). Model uncertainty includes uncertainties due to simplifications of hydrological processes, to processes occurring in the watershed but not included in the model, to processes that are included in the model where their occurrences in the watershed are unknown to the modeler, and to processes unknown to the modeler and not included in the model. Input uncertainty is uncertainty due to errors in input data such as rainfall, like extension of point data to large areas in distributed models. Parameter uncertainty is uncertainty caused by inherent non-uniqueness of parameters in inverse modeling. Due to the uncertainty that reflects in hydrological processes, parameters can compensate each other giving many sets of parameters that produce the same output signal. The occurrence of such sets of parameter non-uniqueness is known as equifinality (Beven and Freer 2001). More details of these prediction uncertainty sources are given by Abbaspour (2011).

SUFI-2 accounts for all the three sources of prediction uncertainties. Two uncertainty measures, i.e., p-factor and r-factor, are used in SUFI-2 (Abbaspour 2011). The p-factor measures the percentage of observations within 2.5% and 97.5% percentiles, or 95% of prediction uncertainty (95PPU). The percentage of observation captured (bracketed) by 95PPU measures the strength of the calibration. The higher the percent of observations bracketed by 95PPU the more perfect is the model. The r-factor measures the distance or the thickness of the 95PPU band divided by the standard deviation of the measured data. The p-factor ranges from 0-100%, while the r-factor ranges from 0 to $\infty$. A p-factor of 1 or 100% and r-factor of 0 indicate a perfect fit of simulation with the measured value. The objective of the uncertainty analysis is to get a p-factor > 0.5 and r-factor <1.0 (Abbaspour, 2011).

### 6.5 Results

Data from four stations were used to calibrate SWAT for the *PET* calculation methods and missing data filling methods. This is because these stations had better historical data than the additional two stations in the calibration period. Penman-Monteith and regression methods gave better discharge simulation than Hargreaves and *WXGEN*. Finally, calibration of SWAT for two and six stations was done only using Penman-Monteith and regression methods to minimize time cost and computer memory.

### 6.5.1 Time series and statistics

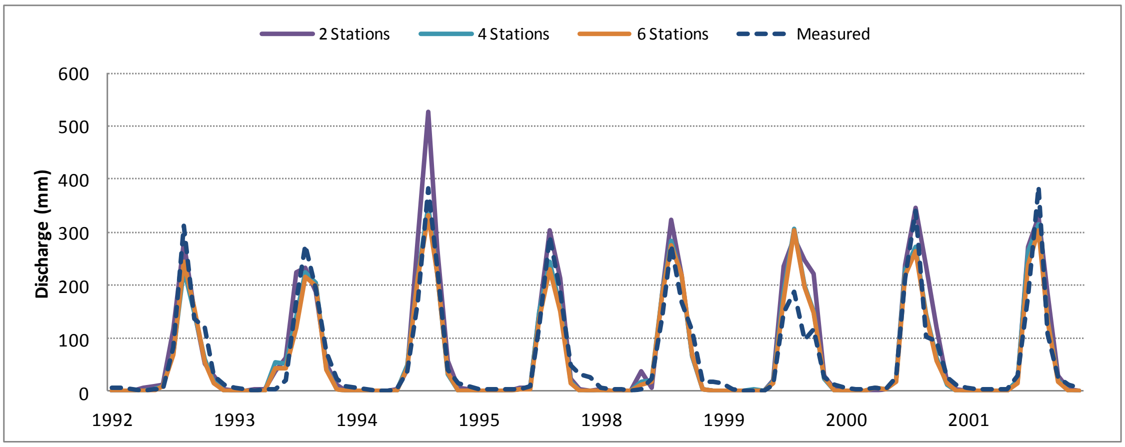


Figure 6-4 Monthly mean measured and simulated river discharge using different meteorological densities.

***(All stations groups were treated using Penman-Monteith PET procedure and regression missing data filling method)***

Monthly time series of measured and simulated streamflow (*YLD*) at the outlet of the watershed is shown for the calibration and validation years in Figure 6-4. Simulated discharge curves using four and six stations lie one over the other. They represent the measured discharge better than the simulation curve using two meteorological stations. The rising and recession parts of the hydrograph curve were better simulated than the peak. The time to peak was well captured. The simulation based on two meteorological stations does not fit measured values for some years e.g., the peak of 1995 as compared to simulation results using four and six stations. Generally, SWAT could not simulate daily peaks resulting from high local rainfall events at the daily level (data not shown) in 1992 and 1995, which resulted in underestimation. However, two well identified seasonal peaks at the monthly level in 1999 were simulated as a single overestimated peak.

The statistical performance is shown in Table 6-2 using the three statistical measures (*NSE, PBIAS* and *RSR*) at daily, weekly and monthly scales. The modeling performance was very good at every time scale except when using two meteorological stations during validation where an overestimation was observed. *NSE* improved from 63% to 75% and 87% to 92% at daily and weekly scales, respectively, when station density increased from two to six. *PBIAS* gave negative values showing overestimation during flow simulation using two stations. Statistical performance measures were neither good nor stable using two stations. Higher flow modeling performance was observed when six meteorological stations were used instead of two and four.

Table 6-2 Statistical performances of modeling monthly river discharge using different station density during calibration (cal) and validation (val).

| Time scale | Statics | Two stations | | Four station | | Six stations | |
|---|---|---|---|---|---|---|---|
| | | ***Cal*** | ***Val*** | ***Cal*** | ***Val*** | ***Cal*** | ***Val*** |
| Daily | *NSE* | 0.63 | 0.43 | 0.70 | 0.66 | 0.75 | 0.71 |
| | *PBIAS* | -1.86 | -29.90 | 12.63 | 8.33 | -6.21 | 10.45 |
| | *RSR* | 0.37 | 0.57 | 0.30 | 0.34 | 0.25 | 0.29 |
| Weekly | *NSE* | 0.87 | 0.64 | 0.91 | 0.82 | 0.92 | 0.83 |
| | *PBIAS* | -1.75 | -29.83 | 12.85 | 8.46 | -6.32 | 10.57 |
| | *RSR* | 0.13 | 0.36 | 0.09 | 0.18 | 0.08 | 0.17 |
| Monthly | *NSE* | 0.95 | 0.80 | 0.96 | 0.91 | 0.97 | 0.92 |
| | *PBIAS* | -2.81 | -30.26 | 11.67 | 8.88 | -4.83 | 10.79 |
| | *RSR* | 0.05 | 0.20 | 0.04 | 0.09 | 0.03 | 0.08 |

***(All station groups were treated using Penman-Monteith PET procedure and regression missing data filling method)***

Table 6-3 Uncertainty of modeling river discharge at daily level using different station density

| **Uncertainty measures** | Two stations | | Four stations | | Six stations | |
|---|---|---|---|---|---|---|
| | *WXGEN* | *REG* | *WXGEN* | *REG* | *WXGEN* | *REG* |
| *p_factor* | 0.79 | 0.78 | 0.79 | 0.76 | 0.79 | 0.80 |
| *r_factor* | 0.47 | 0.47 | 0.48 | 0.35 | 0.47 | 0.49 |

***Note: WXGEN: missing meteorological data was filled using SWAT weather generation; REG: missing data of stations were filled using regression models from the neighboring stations.***

The uncertainty analysis (Table 6-3) led to acceptable results. About 80% of the measured flow values were captured within 95PPU. However, a higher width of the 95PPU band was observed to capture more observations in 95PPU. The same level of prediction uncertainty strength was observed for every model setup.

Table 6-4 Parameters fitted values under different model setups

| No. | Parameter ID | Modelng setup[1] | | | | |
|---|---|---|---|---|---|---|
| | | 2_REG_PM | 4_WXGEN_PM | 4_REG_PM | 4_REG_HG | 6_REG_PM |
| 1 | *CN* | -9.24 (-13,-6) | -2.74(-6,1) | -8.52(-11,-6) | -7.72(-12,-3) | -11.03(-13.18,-8.88) |
| 2 | *ALPHA_BF* | 0.05(0,0.1) | 0.18(0.1,0.26) | 0.1(0.05,0.2) | 0.2(0.1,0.3) | 0.15(0.05,0.24) |
| 3 | *SOL_AWC* | 0.16(-0.02,0.34) | -0.19(-0.3,-0.09) | -0.13(-0.25,-0.01) | 0.12(-0.06,0.3) | -0.12(-0.29,-0.09) |
| 4 | *SOL_K* | -0.78(-0.88,-0.68) | -0.72(-1.5,0.06) | -0.81(-0.97,-0.65) | -0.86(-0.9,-0.8) | -0.78(-0.93,-0.63) |
| 5 | *RCHRG_DP* | 0.06(0.05,0.06) | 0.06(0.05,0.07) | 0.06(0.06,0.07) | 0.04(0.04,0.05) | 0.05(0.04,0.06) |
| 6 | *GWQMN* | 53.35(35,72) | 47.33(26,69) | 35.37(29,42) | 41.75(31,53) | 27.83(20.32,35.32) |
| 7 | *GW_REVAP* | 0.09(0.02,0.1) | 0.03(0.01,0.06) | 0.05(0.02,0.05) | 0.03(0.01,0.03) | 0.06(0.04,0.07) |
| 8 | *REVAPMN* | 30.56(21,40) | 25.78(13,38) | 29.27(20,39) | 47.53(29,66) | 26.29(18.29,34.29) |
| 9 | *ESCO* | 0.81(0.41,1.21) | 0.26(-0.05,0.58) | 0.71(0.57,0.84) | 0.28(0.15,0.42) | 0.63(0.42,0.828) |
| 10 | *GW_DELAY* | 3.79(1,7) | 14.81(7,23) | 11.17(5,14) | 18.79(11,27) | 15.68(5.17,26.17) |
| 11 | *SURLAG* | 0.46(0,0.89) | 0.87(0.3,1.4) | 0.51(0,1) | 0.42(0,0.84) | 0.81(-0.98,2.61) |

***[1]Numbers indicate number of stations used for calibration, WXGEN-weather generator, REG-regression, PM-Penma-Monteith and HG-Hargreaves. The maximum and minimum fitted values are given in brackets. Descriptions of the parameters and their initial values are given in Table 3-1.***

Table 6-4 shows the values of fitted model parameters for the different station densities and missing data fitting. It is difficult to obtain a meaningful trend of parameter variation. However, *CN2* and *SOL_K* show decreasing values compared to the initial values given at the beginning of modeling. *CN2* decreased more when six and four stations were used. This leads to higher *SUR_Q* at the expense of actual evapotranspiration (*AET)* when data from two stations were used. Higher *ESCO* for two stations led to low *AET* simulation due to the low temperature recorded at *Debre Tabor*.

### 6.5.2 Potential evapotranspiration calculation methods

The effect of the Penman-Monteith and Hargreaves potential evapotranspiration methods on river discharge modeling is presented in scatter plots (Figure 6-5). Both methods have comparable performances for modeling river discharge. However, the Penmann-Monteith method shows advanced performance compared to the Hargreaves method. This is a good opportunity to use Class 3 stations data without solar radiation, relative humidity and wind speed measurements. On the other hand, six stations show better performance than four stations.

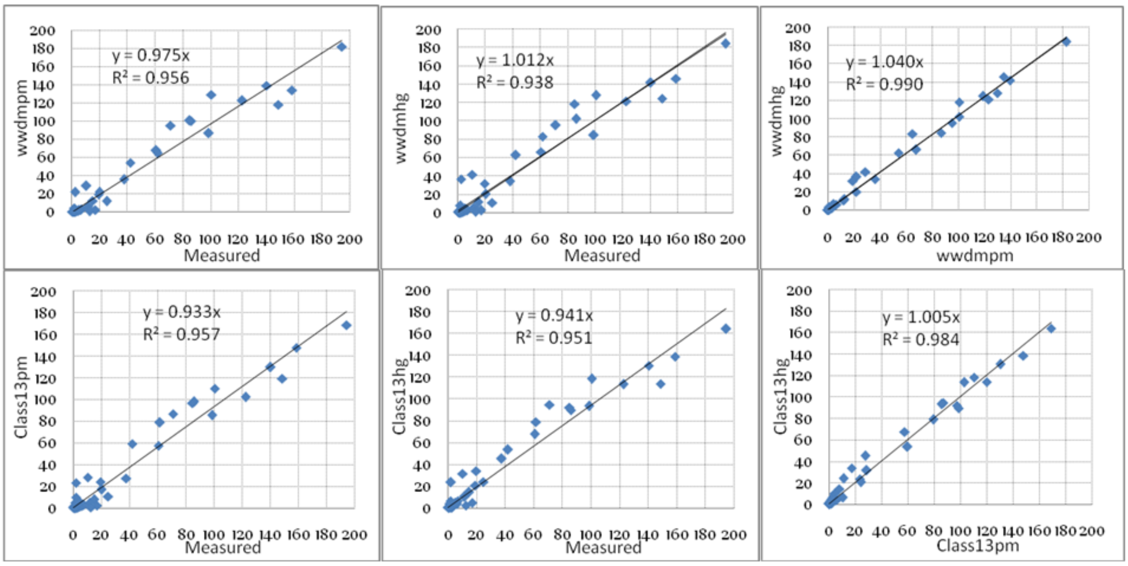


Figure 6-5 Effect of *PET* calculation methods on modeling river discharge ($m^3/s$) at monthly level

***(wwdmpm = 4 stations with Penman-Monteith, wwdmhg = 4 stations with Hargreaves; class13 = 6 stations).***

### 6.5.3 Meteorological station density

Figure 6-6 shows scatter plots of measured and simulated water yield (*YLD*) considering different station density. Four and six meteorological stations gave comparable simulation results. The simulation using two, four and six meteorological stations represented about 90% of the measured water yield. Cluster groups can be observed on measured and simulated scatter plots. Simulation was weak for water yield measurements of less than 100 mm per month, which indicates that low flows were not addressed well by any station density experiment. Monthly water yields between 100 mm and 300 mm were underestimated and yields more than 300 mm overestimated. This indicates underestimation at the rising and recession limb of the hydrograph, while the peak was overestimated when using two meteorological stations. Modeling using four and six meteorological stations showed close agreement with measured data, while modeling using two stations overestimated the measured flow at the monthly level.

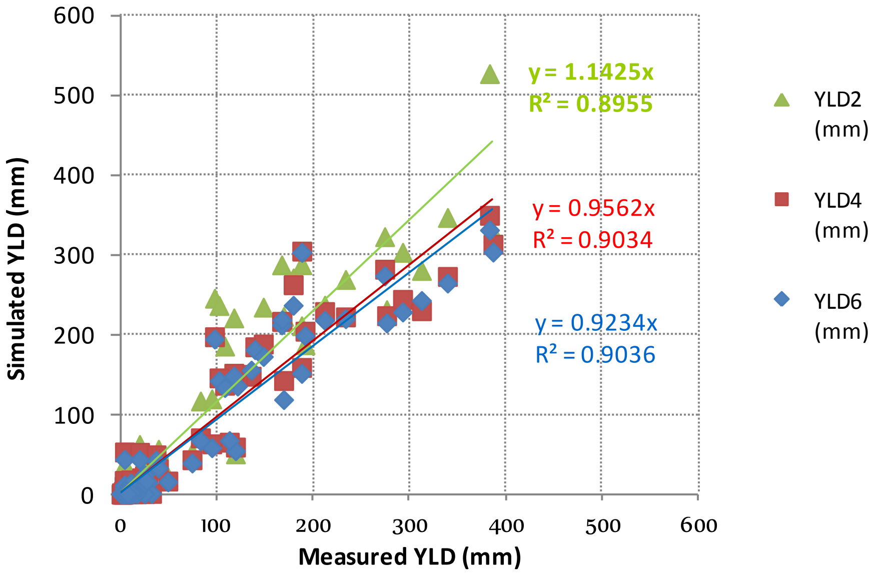


Figure 6-6 Scatter plot of measured and simulated river discharge (in mm/month).

*(YLD = water yield at the outlet of the watershed; numbers are number of stations)*

The relationship between simulated discharge using different station densities and watershed rainfall at the monthly level is shown in Figure 6-7. All *YLD* values have similar correlation with rainfall observations especially for simulated *YLD* using four and six meteorological stations. Weaker correlation was observed for *YLD* values less than 100 mm. Monthly rainfall less than 100 mm gave almost no *YLD*. The rainfall-*YLD* relation showed a hysteresis effect. Rainfall at the onset of the rainy season resulted in lower *YLD* than rainfall at the middle and end of the season. The slope of the line indicates the average runoff coefficient at the monthly level. This runoff coefficient differed for each model setup and for measured flow. Increasing meteorological stations decreased the runoff coefficient value. Almost the same runoff coefficient (0.53) was achieved during the modeling experiment using six stations and with measured river flow as shown by the slope of the trend line. The coefficient of determination, $R^2$, shows the proportion of variability of the dependent variable, *YLD* or measured flow ($Q_{meas}$), which can be controlled by the independent variable, i.e., monthly rainfall. More simulated *YLD* variability (75% to 80%) was controlled by rainfall than measured *YLD* variation determined by rainfall (68%).

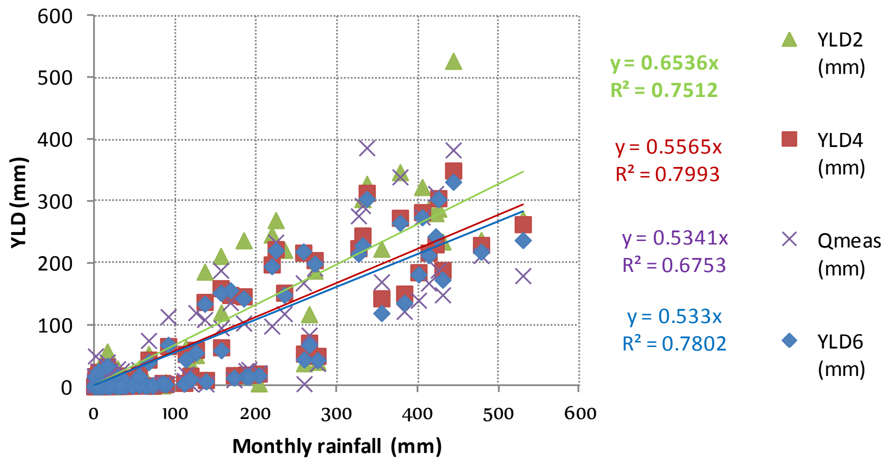


Figure 6-7 Scatter plot of river discharge (YLD in mm/month) with rainfall

***(YLD2, YLD4 and YLD6 are simulated discharge using two, four and six meteorological stations, respectively, and $Q_{meas}$ is measured river discharge. All station groups were treated using Penman-Monteith PET procedure and regression missing data filling method).***

### 6.5.4 Spatial patterns

Figure 6-8 shows the spatial pattern of modeled annual water balance components using two, four and six meteorological stations. Sharp boundaries were formed along the sub-watershed boundaries that were grouped within a Thiessen polygon of each meteorological station. There was more spatial variation in water balance components due to *HRU* when two meteorological stations were used as compared to four and six stations. This is because the variation due to rainfall was controlled, since most of the watershed gets rainfall from one station (*Debre Tabor*) located at the upstream position when two meteorological stations were used. This heterogeneity was found for water yield (*YLD*). Different spatial patterns were observed for each water balance component due to densly distributed meteorological stations.

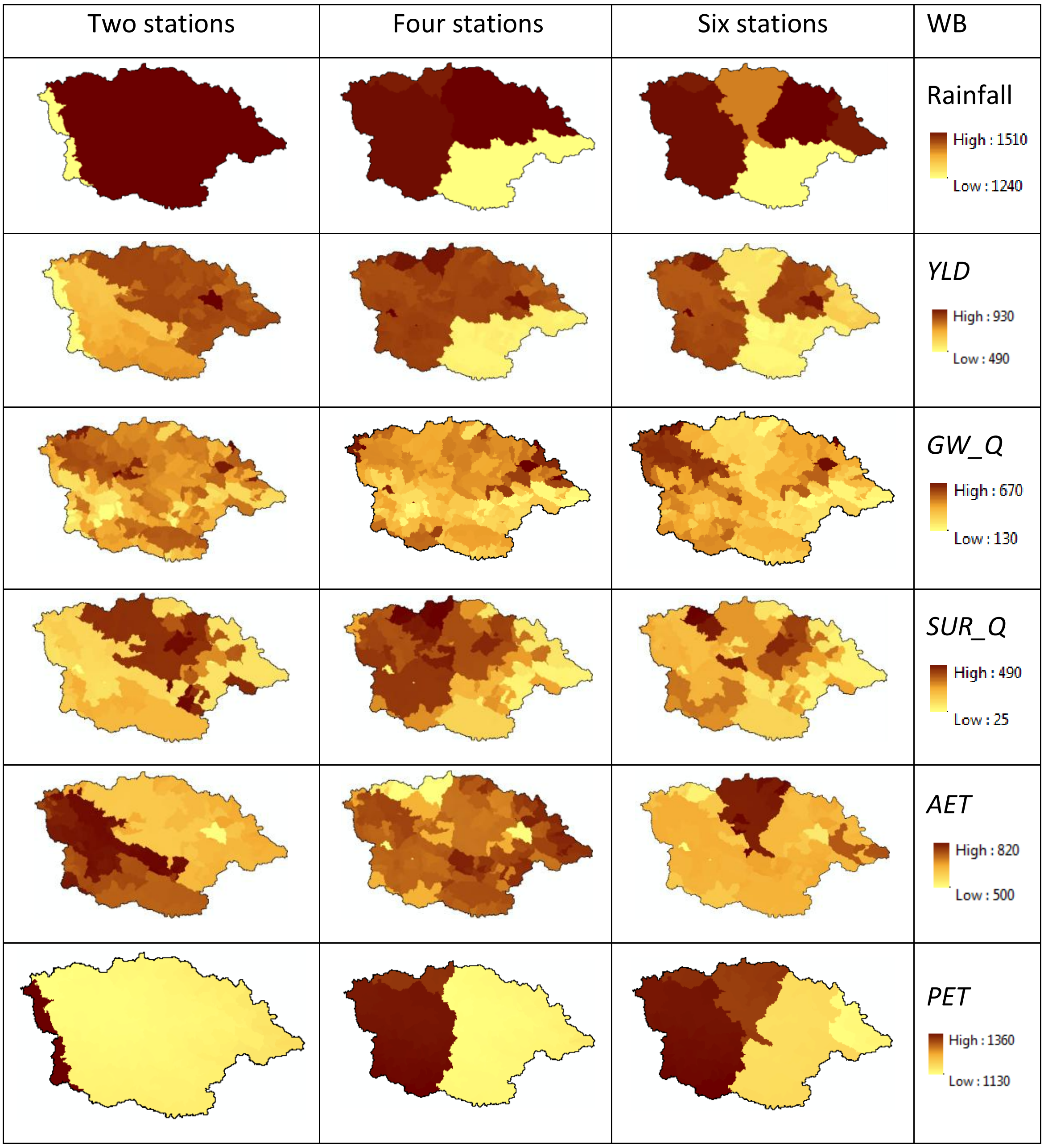


Figure 6-8 Spatial patterns of modeled annual discharge using different station densities.

***Abbreviations for SWAT water balance (WB) components are: YLD (water yield or river discharge), GW_Q-(ground water flow), SUR_Q (surface runoff), AET (actual evapotranspiration), and PET (potential evapotranspiration). All stations groups were treated using Penman-Monteith PET procedure and regression missing data filling method.***

### 6.5.5 Water balance

The effect of methods for filling missing climatic data, i.e., SWAT weather generator routine (*WXGEN*) and the best regression models (*REG*) (see section 5), on the water balance modeling is assessed using SWAT. Six meteorological stations and the Penman-Monteith potential evapotranspiration calculation procedure were used during this simulation. The efficiency of runoff modeling (*NSE*) increased from 0.71 to 0.75 and from 0.70 to 0.72 at calibration and validation level, respectively, when *REG* was used instead of *WXGEN* (data not shown). About 20 mm to 60 mm and 120 mm to 180 mm higher *AET* and *PET*, respectively, were modeled by the SWAT weather generator (*WXGEN*) in comparison with the regression method (Table 6-5).

Table 6-5 Simulated evapotranspiration using different station densities and missing data filling methods

| *AET/PET* | **Two stations** | | **Four stations** | | **Six stations** | |
|---|---|---|---|---|---|---|
| | *WXGEN* | *REG* | *WXGEN* | *REG* | *WXGEN* | *REG* |
| *AET* | 623 | 605 | 599 | 637 | 672 | 649 |
| *PET* | 1170 | 1130 | 1250 | 1372 | 1384 | 1258 |

***AET = actual evapotranspiration (mm), PET = potential evapotranspiration (mm). All combinations were treated using Penman-Monteith PET calculation method.***

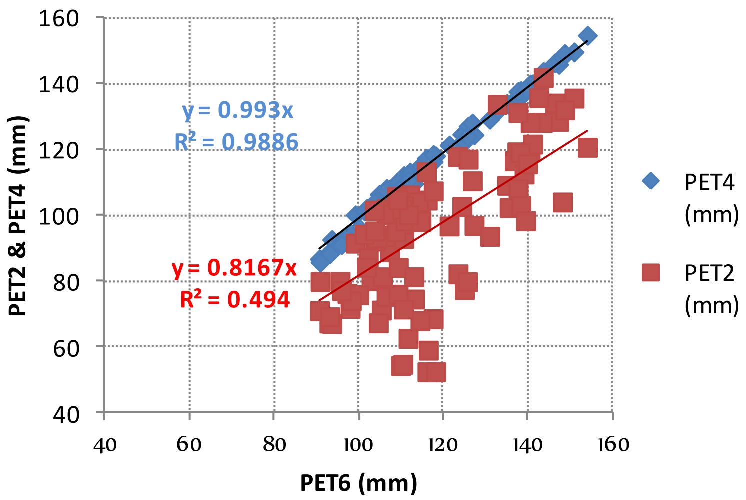


Figure 6-9 *PET* relationships using different climate station densities (mm/month).

***AET = actual evapotranspiration (mm), PET = potential evapotranspiration (mm). Numbers with AET and PET are number of stations used. All combinations were treated using Penman-Monteith PET calculation method.***

Higher *AET* and *PET* values were observed when two meteorological stations were used as compared to four and six stations (Figure 6-9). Using four and six meteorological stations gave almost identical values for all months, while *PET* values were low when only two meteorological stations were used.

Table 6-6 illustrates the annual water balance modeled using two, four and six stations. It shows both the average quantity of the water balance components as well as the statistical significant differences of simulated values at 95% level of significance. A significant difference was observed for surface runoff (*SUR_Q*) and potential evapotranspiration (*PET*) of the water balance components between modeled results using two stations and the other station densities. Higher values were observed for rainfall (*RF*), surface runoff (*SUR_Q*), groundwater discharge (*GW_Q*), percolation to the soil layers (*PERCO*) and river discharge (*YLD*), while lower values were observed for actual and potential evapotranspiration (*AET* and *PET*), respectively, during simulation using two stations as compared to modeled values using four and six meteorological stations.

Table 6-6 Annual water balance (mm) using different station densities

| | **Rainfall** | ***SUR_Q*** | ***LAT_Q*** | ***GW_Q*** | ***AET*** | ***PET*** | ***YLD*** |
|---|---|---|---|---|---|---|---|
| Two stations | 1,549 | 326* | 86 | 483 | 589 | 1,147* | 759 |
| Four stations | 1,448 | 261 | 77 | 409 | 655 | 1,398 | 738 |
| Six stations | 1,433 | 209 | 86 | 419 | 670 | 1,408 | 707 |
| Sig. | 0.29 | 0.00 | 0.63 | 0.17 | 0.08 | <0.01 | 0.85 |

* The mean difference is significant at the 0.05 level.

***RF = rainfall, SUR_Q = surface runoff, LAT_Q = lateral flow, GW_Q = groundwater flow, AET = actual evapotranspiration, PET = potential evapotranspiration, YLD = water yield (all in mm). All combinations were treated using Penman-Monteith PET calculation method.***

## 6.6 Discussion

This study gave better calibration results than other similar studies for the area. Setegn et al. ($2009_a$) achieved a p-factor of 0.79 and an r-factor of 0.77 for the *Gumara* watershed. This indicates that the same percentage of observation in the present study was captured at 95%PPU within a very wide 95%PPU band in the same watershed. Setegn et al. ($2009_a$) used only one meteorological station (*Debre tabor*) with a coarse sub-watershed discretization, soil data, and 90-m resolution DEM. Therefore, some prediction uncertainty might originate in uncertain input data. In an earlier study, Setegn et al. (2008) concluded that the sub-watershed discretization had a limited impact on flow prediction when only using data from one meteorological station. However, it was impossible to capture additional meteorological stations without further fine sub-watershed discretization. Schuol et al. (2008) studied the water availability at the sub-watershed, country and continental level for Africa and gained a p-factor from 0.41 to 0.60 and an r-factor from 0.64 to 0.80 for the Blue Nile of Ethiopia at the monthly level, which is a lower performance than in this study. The reason for the better modeling performance in the present study may be due to fine meteorological, soil and land-use data. In addition, careful data screening was carried out on the base runoff-rainfall relation prior to calibration.

In addition to a lower uncertainty obtained in this study, the model efficiency resulted in a performance level comparable with that of other studies. Setegn et al. (2008), Asres and Awulachew (2010) and Easton et al. (2010) presented 0.62, 0.76 and 0.87 *NSE* values for the *Gumara* watershed, respectively, at the monthly level. All studies used different approaches for SWAT modeling, which showed poorer performance than the modeling in this study. In addition to coarse databases used in the studies, the areas assigned for the watershed were different. Asres and Awulachew (2010) and Easton et al. (2010) used 1464 $km^2$ and 1286 $km^2$, respectively, while the area was 1369 $km^2$ in this study. The difference in watershed area might be from locating the watershed outlet in a different place. Ground control points were taken to delineate the water divide at the outlet in this study to obtain more accurate results than in the other studies.

There were two reasons for achieving better modeling performance by using regression models (*REG*) rather than by using the SWAT weather generator (*WXGEN*) for filling missing data. Firstly, *WXGEN* could not consider spatial attributes to fill the missing data of a given station with data from its neighbor. It rather filled the missing value at a given time from another time data of the same station. Secondly, data were missing for months and years in the study area so the *WXGEN* approach could not be used effectively. Therefore, better modeling performance confirmed the advantage of using both spatial and temporal regression techniques to fill missing data.

Overestimated stream flow using two meteorological stations might be due to the higher rainfall observed at the upstream of the watershed (*Debre Tabor station*) than at the other stations. Cho et al. (2009) observed the same trend of increasing simulated stream flow as the level of watershed delineation decreased.

Low modeling performance was observed during low flow situations. This is because of the weakness of SWAT in addressing soil moisture (saturated excess flow) for runoff formation. The curve number (*CN*) routine for calculating runoff only addresses the infiltration excess runoff (Easton et al. 2010). However, a higher share of the runoff is generated from the saturated excess rather than from the infiltration excess in Ethiopian highland watersheds (Derib 2005; Lue et al. 2008; White et al. 2011; Easton et al. 2010). Therefore, most small rainfall events generated different runoff amounts that varied from 0 to 50 mm.

Different spatial trends of water balance components (with small differences in statistical modeling performances) were achieved when different station density was used. Good statistical performance of stream flow modeling at the watershed outlet using two stations was at the expense of the accuracy of the spatial distribution of the water balance in the watershed. It is possible to use modeling results with low station density for runoff management at the outlet of the watershed with relatively better confidence than water resources management within the watershed. However, Setegn et al. ($2009_b$), Asres and Awulachew (2010) and Easton et al. (2010) used data from less than three stations for the *Gumara* watershed for identifying hotspot areas of severe soil erosion. Such studies for spatial details need fine spatial data with distributed hydrological models (Bormann & Diekkrueger 2003). For a detailed watershed management study, the use of six meteorological stations has shown better practical significance than the statistical modeling performance presented in this study.

## 6.7 Conclusions

In this study, calibration of SWAT with different model setups was performed. The modeling setups were based on potential evapotranspiration (*PET*) calculation methods (Penman-Monteith and Hargreaves), missing data filling methods (*WXGEN* and spatial and temporal regression models), and three levels of meteorological station density (two, four and six stations). Very good modeling performance was observed with 65% (95%), ±5 (±5) and 0.3 (0.06), at daily (monthly) levels for *NSE, PBIAS* and *RSR*, respectively, using Penman-Monteith *PET* calculation methods and six stations.

The Hargreaves *PET* calculation procedure uses only maximum and minimum daily air temperature, which could be measured at most meteorological stations in the area. However, the Penman-Monteith procedure also needs solar radiation, relative humidity and wind speed data, which were hard to find at all climatic stations. The Hargreaves procedure showed comparable SWAT modeling performance compared to the Penman-Monteith. Therefore, Hargreaves method can be widely used for future water resource management by increasing the climate stations that can measure air temperature and rainfall. It is also possible to use climatic data from Class 3 stations that have been excluded in past studies. As a recommendation, the Meteorological Agency of Ethiopia can use elementary schools and health centers that have been established in every small administration unit (*Kebele*) of the country to install Class 3 stations. Installation of automatic and manual recording stations can improve data quality by minimizing personal errors as well as data missing due to failure of automatic instrumentation.

Missing data handled by the SWAT weather generator (*WXGEN*) and regression models using neighboring stations gave comparable modeling performance. *WXGEN* gave values of 0.94, 2.5%, 0.07 and regression models 0.96, -5%, 0.05 for *NSE, PBIAS, RSR*, respectively, at the monthly level. Regression models led to better performance than *WXGEN*. In addition, regression models have a background that is more practical, since the spatial correlation of climatic variables between stations is not considered within *WXGEN*. For further SWAT applications, it is recommended to incorporate the spatial regression routine.

Meteorological station density played a crucial role in the SWAT hydrological modeling. Similar statistical modeling performance was observed using two, four and six meteorological stations for the *Gumara* watershed in the Blue Nile Basin, Ethiopia. However, the spatial distribution of the water balance components, which is very important for water resources management, was very variable. Understanding of spatial dynamics is very important for decision making regarding water resources in addition to temporal flow modeling performance at the outlet of a watershed. This study shows the influence of spatially distributed climatic data on SWAT. Considering spatially distributed climatic data is crucial under the conditions of the monsoon climate as in the study area.

# 7 WATER BALANCE AND WATER AVAILABILITY UNDER LAND-USE AND LAND MANAGEMENT SCENARIOS

## 7.1 Summary

Land-use scenarios were used to identify water flow shift and water availability in the *Gumara* watershed, Ethiopia. Basic water requirements in 2001 and 2050 were used to identify water scarcity at a seasonal level. Results show that watershed management practices decrease the surface runoff and increase the groundwater flow without significantly altering the average annual water yield at the outlet of the watershed. The state of existing rainfed production system will not maintain the basic human and ecosystem water demands in 2050.

## 7.2 Introduction

Sufficient quality and quantity of available water is fundamental for life (Jefferies et al. 2012). Accessibility of this resource is affected by the spatial and temporal distribution of fresh water. About 30% of the world population suffers from lack of water availability (IWMI 2007) and water scarcity has become one of the main challenges of life. Population growth is among the expected factors that will increase the level of water scarcity in the future (Jefferies et al. 2012). The Blue Nile Basin (known as Abbay in Ethiopia) is the least managed sub-watershed with high and erratic rainfall of 800 to 2,200 mm per year with dry spells that reduce crop yields and sometimes lead to total crop failure (Erkosa et al. 2009).

Agriculture is the backbone of the economy and the livelihoods of Ethiopia. It supports about 85% of the population in terms of employment and livelihoods; 50% of the country’s gross domestic product (GDP) generates about 88% of the export earnings, and supplies around 73% of the raw material requirements of agriculture-based domestic industries (MEDaC 1999). However, agriculture in this area is rainfed and is highly vulnerable to droughts and dry spells, and rainfall productivity is low. Based on the Agricultural Census Survey of Ethiopia, Diao and Pratt (2007) calculate that 37% of the rural population lives in food-deficit areas. Water shortage that is related to the erratic seasonal rainfall is one of the main sources of this problem. Due to the rainfall variability and other related factors, the country had to import 0.62 million tons of grain per year during 1995 to 2004 to feed 7 million people. It has made the country the first food aid recipient in Sub-Saharan Africa (Walker and Wandschneider 2005). The imported commercial and food aid accounts for 0.3 $km^3$/year virtual water (Hoekstra and Hung 2002).

The government of Ethiopia is, therefore, trying to develop the water resources, and the Blue Nile Basin is one of the development corridors of the country (World Bank 2008; McCartney et al. 2010). The *Gumara* Irrigation Project (*GIP*) (MoWR 2008) is one of many development activities under feasibility evaluation. Outside the *Gumara* watershed, many water resource development studies have been performed along the Blue Nile Basin for irrigation and hydropower projects, the first one being in 1964 (USBR 1964; WAPCOS 1990; MoWR 1998; MoWR 2008).

Downstream countries have opposed water development in Ethiopia as it may hamper their 'historical' right to use the Nile water. It is not the interest of Egypt to share the Nile flow with upstream riparian countries especially Ethiopia, as they assume that Ethiopia has ample green water from rainfall (Arsano 2007). However, the net green water resource for Ethiopia could not been determined since this water can be recycled and double counted again through evaporation and cooling process of the hydrological cycle. In addition, the Ethiopian population is increasing, and drought occurrence and climate change are becoming an increasing challenge for the existing rainfed agriculture. Information on water availability and scarcity is limited in Africa (Wallace and Gregory 2002) especially at meso- and micro-watershed levels and on seasonal or monthly scales. As explained by Smakhtin et al. (2005) after comparison of spatial patterns on maps, an increasing number of sub-watersheds show a higher magnitude of water stress when considering ecosystem water requirements. Schoul et al. (2008) recommend performing detailed spatially distributed studies for African countries like Ethiopia.

This study was carried out on the head water of the Blue Nile to identify the water availability status in 2001 and 2050 considering the demographic and water development options.

## 7.3 Objectives

The objectives of this study were:

1. To model the water balance components in different land-use and land management scenarios, and
2. To identify the effect of land-use and demographic changes on the water availability status at seasonal scales.

## 7.4 Materials and methods

### 7.4.1 Study area

The study was performed in the *Gumara* watershed in the Blue Nile Basin of Ethiopia, which is located at 37˚38' to 38˚ 11' E longitude and 11˚ 35' to 11˚ 54' N latitude (Figure 2-1). The study focuses on an area of 1520 km$^2$ in the watershed after calibration on the 1360 km$^2$ gauged part. The watershed is tributary of Lake *Tana,* which is considered the source of the Blue Nile. It is located in food-secure districts (*woredas*; Fogera*, Farta, Dera and Iste* (see Section 10-2 or Appendix 2) in the south *Gondor* administrative zone (FEWS NET 2008). The watershed is also a food balance area where the production is similar to the average cereal equivalent production per household at country level (Diao and Pratt 2007). The climate of the area is of a tropical highland monsoon type with a single rainy season between June and September (Alemayehu et al. 2009). The average annual rainfall 1992 to 2001 was 1444 mm. In the middle and upstream parts, the topography is highly rugged and dissected, while the downstream part is flat with gentle slopes and plain topography. About 87% of the watershed is intensively cultivated. Rice, tef, maize, wheat and barley are the main crops grown. Overgrazed bush or shrubland, grassland, and forest/wood land are other land-cover types (WWDSE 2007). Haplic luvisol, Chromic luvisol, Lithic leptosol, Eutric vertisol, Eutric fluvisol and Chromic cambisol are the common soil types found in the watershed (FAO classification system; Asres and Awulachew 2010).

### 7.4.2 SWAT model development

The SWAT model was applied to the *Gumara* watershed using 1992 to 1995 climate and hydrometric data for calibration and 1998 to 2001 for validation (see section 6). Sub-watersheds and hydrological response units (HRU) discretization was based on a 30-m resolution DEM as well as on land-use and soil data. During calibration, 37 sub-watersheds with 113 HRUs were derived on the 1360 $km^2$ gauged part of the *Gumara* watershed. Daily meteorological data from six stations were used. Missing data were filled using different methods as described (see section 5). The model was fitted very well for the measured river discharge giving 0.75 Nash-Sutcliffe efficiency (*NSE*), 6 percent bias (*PBIAS*), and 0.3 root mean square error (*RMSE*) to observation standard deviation (*SRS*) values (see section 6.5.1). After calibration, scenarios were computed for the 1520 $km^2$ watershed area using 328 sub-watersheds and 917 HRUs.

### 7.4.3 Land-use scenario development

Land-use scenario development was done using field survey data of the author in 2008 and 2009, scanned maps from the feasibility study of *Gumara* Irrigation Project (*GIP*) from the library of the Ministry of Water Resources of Ethiopia (MoWR 2008), and information from the land-use policy of the country. Two additional land-use scenarios were developed: land-use up to 2008 and land-use planned by the government to be implemented in the near future (explained further down). Five land-use types were identified in the watershed, i.e., cultivated land (87% of the area), grazing bush-rangelands (7%), pasture (4%), mixed forest woodlands (3%) and water (0.09%) (Figure 7-2). Cultivated lands were fine-tuned with respect to three farming systems identified by Haileslassie et al. ($2009_a$) for SWAT modeling. Small-scale irrigation covered 213.8 ha (0.14% of the watershed) in 2009. The farming systems have different tillage, planting and harvesting schedules, which were identified during the field surveys in 2008 and 2009.

Mixed forestlands are composed of native and exotic tree types. Most of these forests are concentrated along riversides, in steep rugged landscapes and in churchyards. Some plantation forestlands can be found at the upstream of the watershed. Bush rangeland partly covers the steep hillsides (Table 7-1). It is the feed source for livestock grazing during the main rainy season, since the cultivated lands are covered by crops.

Figure 7-1 Hillside bushland (July 2009)

The second land-use scenario is based on the *Gumara* Irrigation Project. A dam is planned on one of the tributaries of the *Gumara* River known as *Kinti-Gumara* covering a 3.51 $km^2$ inundated area on the full reservoir level. The stored water will then irrigate about 14,000 ha land at the downstream side of the watershed. Details of this irrigation project plan study were compiled in five independent volumes of reports (MoWR 2008) with detailed watershed development activities. This plan will change the land-use such that cultivated land will decrease from 87% to 78% of the watershed, and bush rangeland from 7% to 5%. On the other hand, the area covered by the water body will increase from 0.1% to 0.8% and forest from 2.5% to 4.3% (Figure 7-2 and Table 7-1). Irrigated land coverage will increase from 0.14% to 8%. These changes result from the inundation of the area under the dam reservoir and some watershed development plans to safeguard the environment and the dam.

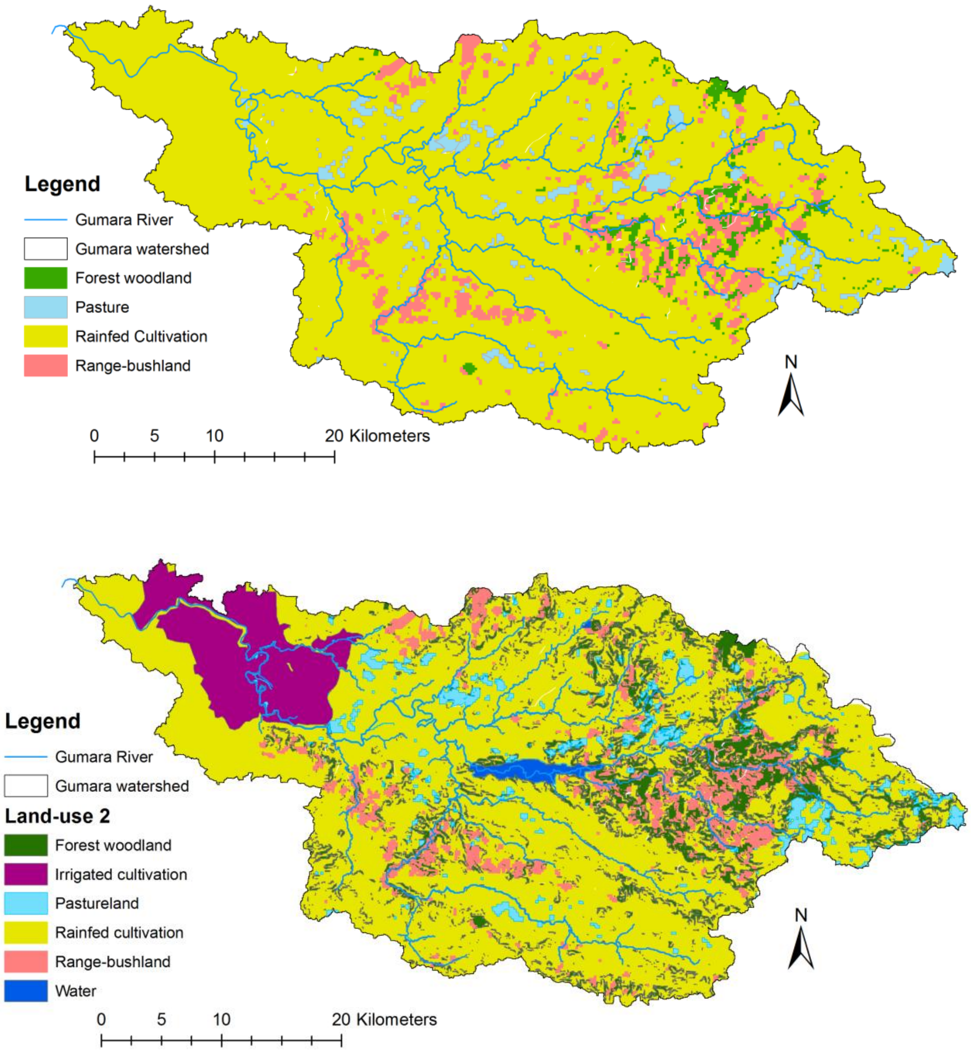


Figure 7-2 Land-use map of *Gumara* watershed

**Without (top) and with (bottom) watershed treatment and planned *Gumara* Irrigation Project (Compiled from field survey, *Gumara* Irrigation Project feasibility study (WoWR 2008) and farming system classification from Haileslassie et al. 2009$_a$).**

Watershed development and land-use policy in the country aims at reducing land degradation and related production and productivity loses. Therefore, the water balance assessment was carried out with and without considering some land management practices for the above land-use change scenarios. The land management practices are dependent on the steepness of the slopes. Slope categories were taken from Federal Democratic Republic of Ethiopia Rural Land Administration and Land-Use Proclamation No. 456/2005. Under Part 3 of Article 13 it is stated that land with slopes between 31% and 60% can only be used for annual crops if bench terraces are constructed. Slopes above 60% cannot be used for farming or free grazing but can be used for trees for wood production, perennial plants and forage production for cut-and-carry animal feeding (Federal Negaritgazeta 2005).

Table 7-1 Land-use area (in %) for three scenarios

| **Land-use** | ***$LU_1$*** | ***$LU_2$*** | ***$LU_3$*** |
|---|---|---|---|
| Rainfed cultivation | 86.4 | 69.8 | 77.3 |
| Irrigation cultivation | 0.3 | 8.1 | 0.3 |
| Forest woodland | 2.5 | 11.9 | 11.9 |
| Pasture | 3.8 | 4.3 | 3.6 |
| Range-bush land | 6.8 | 5.1 | 6.8 |
| Water | 0.1 | 0.8 | 0.1 |
| Total | 100.0 | 100.0 | 100.0 |

***$LU_1$ is baseline land-use scenario, $LU_2$ is land-use with Gumara irrigation project, and $LU_3$ is watershed management practices***

Table 7-2 Reservoir parameters used in SWAT modeling

| **Name** | **Definition** | **Value** |
|---|---|---|
| *MORES* | Month the reservoir became operational (1-12) | Nov |
| *IYRES* | Year the reservoir became operational | 1992 |
| *RES-ESA* (ha) | Reservoir surface area at the emergency spill level | 351 |
| *RES-EVOL* ($10^4$ $m^3$) | Reservoir volume at the emergency spill level | 5969 |
| *RES-PSA* (ha) | Reservoir surface area at the principal spill level | 236 |
| *RES-PVOL* ($10^4$ $m^3$) | Reservoir volume at the principal spill level | 3400 |
| *RES-VOL* ($10^4$ $m^3$) | Initial reservoir volume | 5969 |
| *RES-K* (mm $hr^{-1}$) | Hydraulic conductivity of the reservoir bottom | 1.0062 |

| Months of the year | | | | | | | | | | | |
|---|---|---|---|---|---|---|---|---|---|---|---|
| **1** | **2** | **3** | **4** | **5** | **6** | **7** | **8** | **9** | **10** | **11** | **12** |
| Average daily outflow of the month from the reservoir ($m^3s^{-1}$) (RESOUT) | | | | | | | | | | | |
| 4.23 | 6.18 | 4.22 | 0.19 | 0.05 | 0.05 | 1.45 | 0.32 | 2.17 | 0.32 | 0.24 | 2.76 |
| Average daily removal of the month from the reach ($m^3s^{-1}$) (WRCH) | | | | | | | | | | | |
| 4.17 | 6.13 | 4.17 | 0.14 | 0.00 | 0.00 | 1.16 | 0 | 1.85 | 0.00 | 0.00 | 2.66 |

***Source: MoWR 2008: 90-92***

Terraces with 12-m slope length have to be installed for the 30-60% slope ranges, and parallel contouring is demanded for the 15-30% slope ranges. Land units that have slopes more than 60% were delineated as forest land in this study. The above information was incorporated to develop land-use scenarios using the ArcGIS 9.3 interface. Thus, 3 land-use scenarios were developed and used as inputs for SWAT to see their effect on the water balance of the watershed. The initial curve numbers of the newly developed land-uses were selected from the corresponding hydrologic conditions (see Appendix 10.1). Parameters calibrated for the existing land-use is assumed to have the same effect on water flows as in the land-use scenarios.

### 7.4.4 Water stress indices development

Many indices have been developed to evaluate water availability and water stress in the past decades. Most of them were calculated using the ratio of water demand and water available (equation 7.1) based on human water requirements (Falkenmark 1989; Gleick 1996), water withdrawal (Raskin et al. 1997), environmental water requirement (*EWR*) (Smakhtin et al. 2005), and water footprint (Hoekstra et al. 2009; Hoekstra and Mekonnen 2011). The International Water Management Institute (CA 2007) used physical and economical water scarcity for countries with respect to the proportion of water withdrawn from the total blue water and the infrastructure used for accessing the water resources.

$$WSI = \frac{\text{Water demand}}{\text{Water available}} \tag{7.1}$$

Different approaches using water stress indices (*WSI*; Equation 7.1) are based on assumptions on the demand and the available water components. A recent study on water stress index development using the water footprint (divided into green, blue, grey water scarcity) considers the volume of fresh water used for the whole chain of the given product (Hoekstra et al. 2009). These authors recommended correcting errors in previous water stress indices development. One of these errors was caused by ignoring return water. Another error is when total river discharge is considered as available water, since a fraction of the runoff has to be used to maintain the environment. The third error is when water stress indices are developed on an annual level, since water availability is highly variable within the year. Falkenmark (1989) recommends 1700 $m^3$/capita per annum as a threshold for basic human water requirements, while above this value there is no water stress.

**Water availability**

Green water comprises most of the available water for the existing rainfed cultivation, forest cover and grazing lands in the watershed. The blue water, which is mainly the river discharge from the streams of the watershed, has not been accessible until now except for about 0.03% of the watershed that uses springs, river diversions, and hand-dug wells (see section 4 and Eguavoen et al. 2012). The inaccessibility is due to technological limitations and the transboundary water barriers to borrow the technology from elsewhere around the world.

FAO (1986) defines the green water (part of the rainfall that is available for plant growth) as effective rainfall (mm per unit time day, month or growing season; Equation 7.2):

$$Effective\ rainfall = (Total\ rainfall) - (Runoff) - (Evaporation) - (Deep\ percolation) \qquad (7\text{-}2)$$

It is the part that is stored in the root zone after a rainfall event and that is ready for uptake by plant roots or stored as the soil moisture available for plant growth. The amount of the effective rainfall is affected by the climate and the soil factors like soil texture and structure, and the depth of the root zone.

The evaporation part represents water evaporated from stagnated water and bare soil after rainfall events. The evaporation cannot be avoided since it occurs at the pre-germination and early germination stage of cultivation activities (Rost et al. 2009). It is difficult to separate this unproductive evaporation from the productive transpiration in SWAT as seen in the water balance accounting (see section 3.4). Rost et al. (2009) used a reduction factor of 0.85 to consider this unproductive rainfall component of the actual evapotranspiration. Therefore, actual evapotranspiration simulated using SWAT is used as available green water for the existing rainfed production considering the reduction factor for the unproductive evaporation. This factor is considered during categorization of the water stress index development. The 20% rule of a presumptive standard for environmental flow protection (Richter et al.

2011) was used to establish the environmental flow requirement. This rule proposed that 80% of the natural runoff be allocated for environmental flow with 20% as available blue water.

Productive cultivated land, pasture and wood lands cover 99% and small-scale irrigation 0.1% of the watershed (Figure 7-2 and Table 7-1), i.e., almost the whole of the watershed is covered by productive land-use classes. The following water balance components are defined as available water options in this study based on the land-use scenarios developed (see section 7.4.3). Average actual evapotranspiration (*AET*) in 1992 to 2001 with factor of reduction as a green water, green water plus 20% river flow and green water plus all river discharge were used as different options of available water depending on the land-use scenarios.

**Water demand**

In this study, population data were used to quantify water demand for each water-scarcity land unit (WSLU) in the dry and wet seasons using data as given in Table 7-3. WSLU were formed by overlaying HRU and population density data on the smallest administrative units (known as *Kebele*), which have an average size of 24 $km^2$. Rainfed agricultural activities starting from sowing to early harvesting occur in the period from June to October. These months were considered as wet season and the rest of the year as dry season. Most of the food and feed production of the year was in the wet season. All agricultural water demands were distributed equally over these months. Domestic and economic (industrial) water needs were also distributed equally over all months of the year. Livestock drinking water demand was calculated from the water need for different cattle types in different seasons and distributed over both seasons according to the data. As observed during the field work in 2008 and 2009, the small rainfall events during the dry season are very important to supplement livestock feed. These rainfall events make the crop aftermath palatable and also make the grass- and bushlands green for a short period of time. 30% of the animal feed production needs were distributed equally over the dry months of the year.

Table 7-3 Input data for basic water requirement calculation

| Output | Input | Quantity | Units | Source |
|---|---|---|---|---|
| **Domestic** | | **18** | **$m^3$/c/y** | **Calculated** |
| | Drinking | 5 | l/c/d | Gleick (1996) |
| | Bathing | 15 | l/c/d | Gleick (1996) |
| | Food preparation | 10 | l/c/d | Gleick (1996) |
| | Sanitation | 20 | l/c/d | Gleick (1996) |
| | Population | | | MoWRs database |
| **Agricultural** | | **1103** | **$m^3$/c/y** | **Calculated** |
| | **Cereal production** | **401** | **$m^3$/c/y** | **Calculated** |
| | Energy requirement | | Kcal/c/d | FAO (2004) |
| | Cereal equivalent | 4.04 | Kcal/gm | FAO (2003) |
| | Water productivity | 0.6 | Kg/$m^3$ | Haileslassie et al. ($2009_b$) |
| | **Livestock** | **698** | **$m^3$/c/y** | **Calculated** |
| | Drinking (dry/wet) | (30/4) | l/TLU/d | Duguma et al. ($2012_b$) |
| | Feed from grass | 1557 | $m^3$/TLU/y | Tulu et al. ($2009_b$) |
| | Population | 0.64 | TLU/c | Haileslassie et al. ($2009_b$) |
| **Industrial*** | | **4** | **$m^3$/c/y** | **Calculated** |
| | Per cent of agricultural water need | 1 | % | FAO (2013) |
| **Total** | **2001** | **1125** | **$m^3$/c/y** | **Calculated** |

****Industrial water need in 2050 was assumed to be 10% of the agricultural water need. TLU stands for Tropical Livestock Units representing 250 kg life weight.***

Of the animal feed, 30% was left as crop residue (Haileslassie et al. $2009_b$) and was not included in the livestock feed calculation, since it was already considered in the cereal production water demand. The remaining 70% was considered to be supplemented using grass production that needs 1557 $m^3$ water per TLU per year (Tulu et al. 2009). Livestock population (TLU/c) was derived from human population and livestock per hectare data stated by Haileslassie et al. ($2009_b$; Table 7-3). According to these data, the amount of the basic water requirement is 1125 $m^3$/c/y, which is lower than the 1700 $m^3$/c/y threshold value given in Falkenmark (1989). About 98 % (1103 $m^3$/c/y) is attributed to agriculture where 62% is from livestock. The big water share for livestock indicates how livestock is important part of the system.

Figure 7-3 shows the population density ($km^{-2}$) of the *Gumara* watershed for 2001. The population of the country is estimated to increase from 65,891,874 in 2001 (World fact sheet 2001) to 174,800,000 in 2050 (Population Reference Bureau 2010). This national population growth rate was applied on the study *Kebele* and town levels to compute the local population in 2050. The steep and fragile areas of the watershed were less populated as compared to the upstream and downstream plain areas. The average rural and town population densities are 266 and 4730 $km^{-2}$, respectively.

These values are higher than the national (114), regional (122) and zonal (159) averages (CSA 2011).

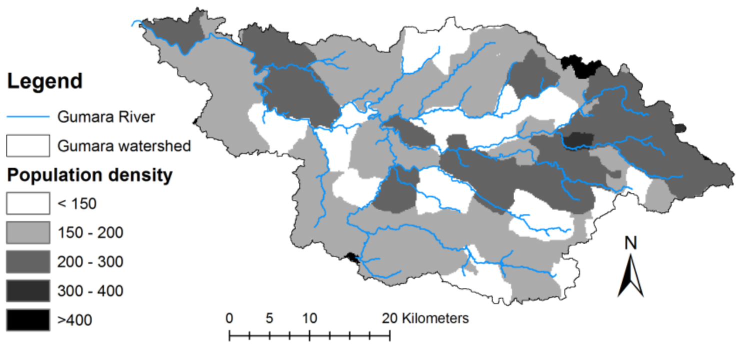


Figure 7-3 Population density (per $km^2$) of the *Gumara* watershed for 2001.

***(Source: Ministry of Water Resources of Ethiopia)***

**Water stress indices**

Although different water availability and water demand definitions are given in studies, categorization for defining the water stress level is fairly similar. The most frequently used categories used to identify the level of scarcity are 30%, 60% and 100% of the available water. Smakhtin et al. (2005) categorized the following water stress indices (WSI) using long-term mean annual runoff and considering environmental flow.

1. WSI > 1: *overexploited* (current water use is tapping into *EWR*)-environmentally water scarce basins.
2. 0.6 ≤ WSI < 1: *heavily exploited* (0 to 40% of the utilizable water is still available in a basin before *EWR* are in conflict with other uses)-environmentally water stressed basins.
3. 0.3 ≤ WSI < 0.6: *moderately exploited* (40% to 70% of the utilizable water is still available in a basin before EWR are in conflict with other uses).
4. WSI < 0.3: *slightly exploited.*

However, using these categories for rainfed agriculture and when all river discharge is diverted leads to wrong conclusions, since they were designed for blue water scarcity considering environmental flow. Considering the erratic nature of the rainfall in the area and the unproductive evaporation components in the available green water, a water demand exceeding 60% of the actual evapotranspiration is considered as highly scarce rainfed sub-watershed in this study.

The different scenarios that were used to develop water stress indices are listed in Table 7-4. Two land-uses and three water availability status were used for the population of 2001 and 2050 to develop 8 water stress scenarios.

Table 7-4 Water stress indices scenarios

| Scenario No. | Code | Scenario No. | Code |
|---|---|---|---|
| 1 | $LU_1$_ $G_N$01 | 5 | $LU_2$_ $G_NE_{WR}$01 |
| 2 | $LU_1$_ $G_N$50 | 6 | $LU_2$_ $G_NE_{WR}$50 |
| 3 | $LU_2$_ $G_N$01 | 7 | $LU_2$_ $G_NY_{LD}$01 |
| 4 | $LU_2$_ $G_N$50 | 8 | $LU_2$_ $G_NY_{LD}$50 |

***$LU_1$ is existing land-use practice, $LU_2$ is land-use considering Gumara irrigation project (GIP). Water availability is $G_N$ (green water), $G_NY_{LD}$ (green water plus water yield) and $G_NE_{WR}$ (green water plus 20% of water yield that considers environmental water requirement-$E_{WR}$). Total water needed was calculated based on the population in 2001 and 2050 indicated as 01 and 5o, respectively.***

### 7.4.5 Assumptions and limitations

Computing land-use and demographic change scenarios was performed using the following assumptions. Different HRU discretization used for model calibration and scenario development results in the same water balance and water availability modeling values. The basic water requirement for domestic and agriculture per capita per year in 2001 was assumed to be the same in 2050, and industrial water demand was assumed to be 1% and 10% of the agricultural demand in 2001 and 2050, respectively. The availability of groundwater recharge was not considered. The effect of climate change on water balance and water availability was not included in this study.

## 7.5 Results

### 7.5.1 Water balance shift due to land-use changes

The annual water balance of the *Gumara* watershed using six meteorological stations and the Penman-Monteith potential evapotranspiration methods for the 328 sub-watersheds is shown in Figure 7-4 for the period 1992 to 2001 with and without the *Gumara* Irrigation Project (*GIP*). About 95 % of the annual rainfall left the watershed through river discharge or yield (*YLD*; 752 mm)) and *AET* (648 mm). The remaining 5% was stored in the deep groundwater. This storage was about 61 mm (92 $Mm^3$) per annum. River discharge and *AET* accounted for 51% and 44% of the annual rainfall, respectively, under the existing land-use conditions. A shift from river discharge and groundwater storage to *AET* was observed due to *GIP* and watershed treatment methods. Watershed management and the planned irrigation project shifted an additional 99 mm (151 $Mm^3$) of the annual yield to *AET*. However, 106 mm (161 $Mm^3$) water was additionally evapotranspired due to *GIP*. The balance was filled from deep groundwater recharge. Therefore, groundwater storage was decreased by 4 mm (7 $Mm^3$) when watershed treatment and *GIP* were implemented in the model.

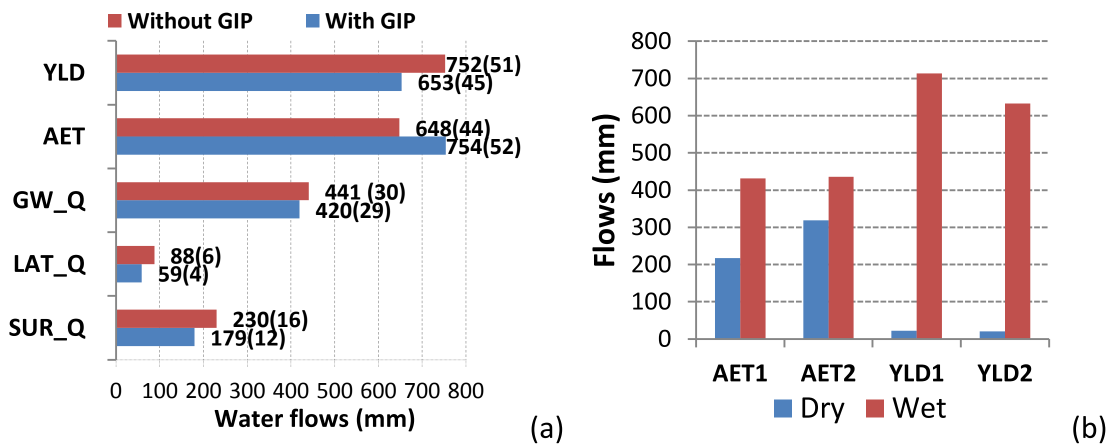


Figure 7-4 Annual water flows without and with *Gumara* irrigation project (*GIP*): (a) annual (b) seasonal.

***Values are average of 1992 to 2001. Numbers in brackets are percent annual rainfall covered by each component. (YLD is total river discharge through the outlet of the watershed, AET is actual evapotranspiration, GW_Q is groundwater flow, LAT_Q is lateral flow, and SUR_Q is surface water flow to the channel. The numbers 1 and 2 indicate land-use scenarios without and with Gumara irrigation project).***

Figure 7-5 shows the monthly time series of *AET* and *YLD* with and without *GIP* land-use scenarios. The effect of *GIP* in different parts of the hydrograph is illustrated on a monthly scale. The rising limb and the peak of the hydrograph were regulated due to *GIP*. Evapotranspiration increases during the dry period using *GIP*. An additional 154 $Mm^3$ water is evapotranspired in the dry season based on 130 $Mm^3$ *YLD* regulation during the wet season. The difference of 24 $Mm^3$ in the *AET* is from the rainfall in the dry season. Both Figure 7-4 and Figure 7-5 show that the natural *YLD* was altered without affecting the 20% presumptive standard for environmental flow requirements.

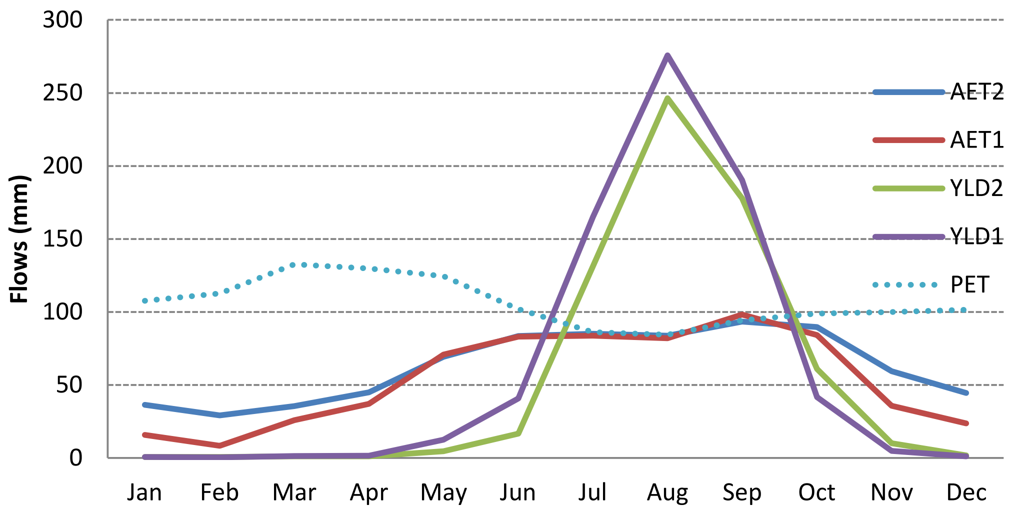


Figure 7-5 Average monthly discharge at the outlet of the watershed with and without *Gumara* irrigation project.

***(YLD is total discharge through the outlet of the watershed, AET is actual evapotranspiration, and PET is potential evapotranspiration. The numbers 1 and 2 indicate land-use scenarios without and with Gumara irrigation project)***

### 7.5.2 Spatial patterns of water flow shifts

Figure 7-6 shows the patterns of the water balance components with and without the *Gumara* irrigation project (*GIP*). Watershed treatment practices like contouring of land units with slopes between 15% and 30%, terracing of slopes steeper than 30%, and afforestation of hillsides steeper than 60% led to differences in surface and groundwater flows. These land management practices decreased surface runoff by 49% on average, and increased groundwater and lateral flows by 27% and 20%, respectively.

An effect of watershed management practices can be seen on surface and groundwater flows. However, there was also a small effect on *AET* and *YLD*. Only 1.8% and -1.2% changes were observed for *AET* and *YLD*, respectively, due to the watershed management interventions (results not shown here) at the watershed level. As shown in Figure 7-6, average annual *YLD* and *AET* values were more dependent on climatic data (see section 6.5.4) than on land treatment practices, except in the irrigated and reservoir area. However, the watershed management interventions modify the surface and groundwater flow components even though this results only in a small effect on total *YLD*. Higher *YLD* was observed from sub-watersheds covered by the *Wanzaye* and *Debre Tabor* meteorological stations (see section 6.5).

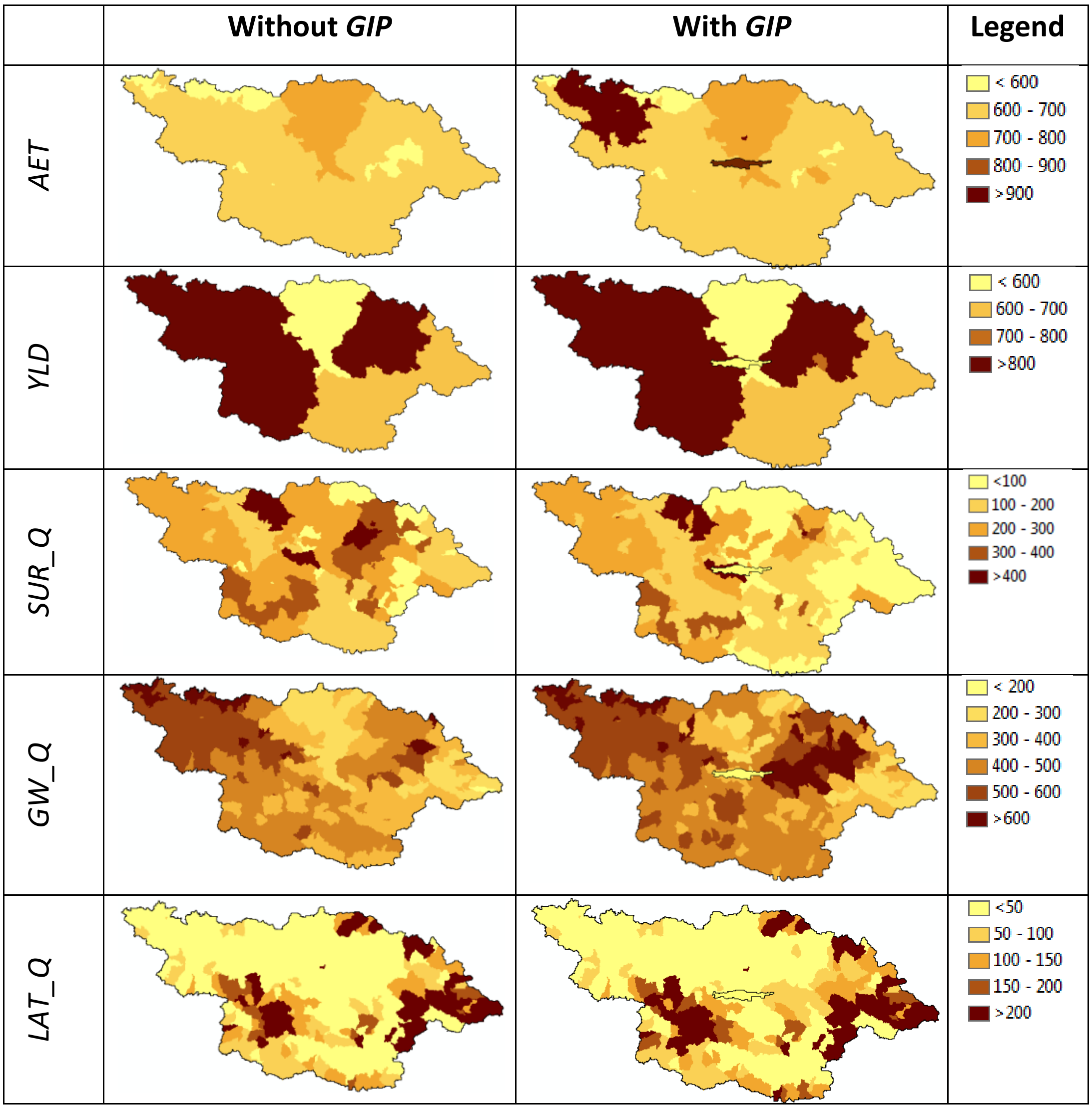


Figure 7-6 Water balance components (mm $y^{-1}$) without and with *Gumara* irrigation project (*GIP*) and watershed management interventions.

***(AET is actual evapotranspiration, YLD is discharge through the outlet of the watershed, SUR_Q is surface water flow, GW_Q is groundwater flow, and LAT_Q is lateral flow through the soil layer).***

The reservoir was planned at a position where it could trap the higher *YLD* produced from upstream steep slopes and high rainfall from sub-watersheds covered by the *Debre Tabor* station. Annual evaporation from the open water surface of the reservoir is about 1492 mm. An annual average *AET* increment by 73 mm (varies from 0 to 962 mm) and *YLD* decrement by 74 mm (varies from 0 to 784 mm) at watershed level (results not shown here) was observed where the variations were observed in some sub-watersheds due to land management interventions and *GIP*.

### 7.5.3 Water availability and scarcity

Available water was categorized in three groups in this study: Green water (approximated by part of actual evapotranspiration), green water plus 20 % of the river flow (*YLD)* and green water plus all the river flow. Figure 7-7 shows the water stress indices of the existing land-use scenario using green water as available water during dry and wet seasons as well as at an annual level in 2001 and 2050 under basic water requirement conditions.

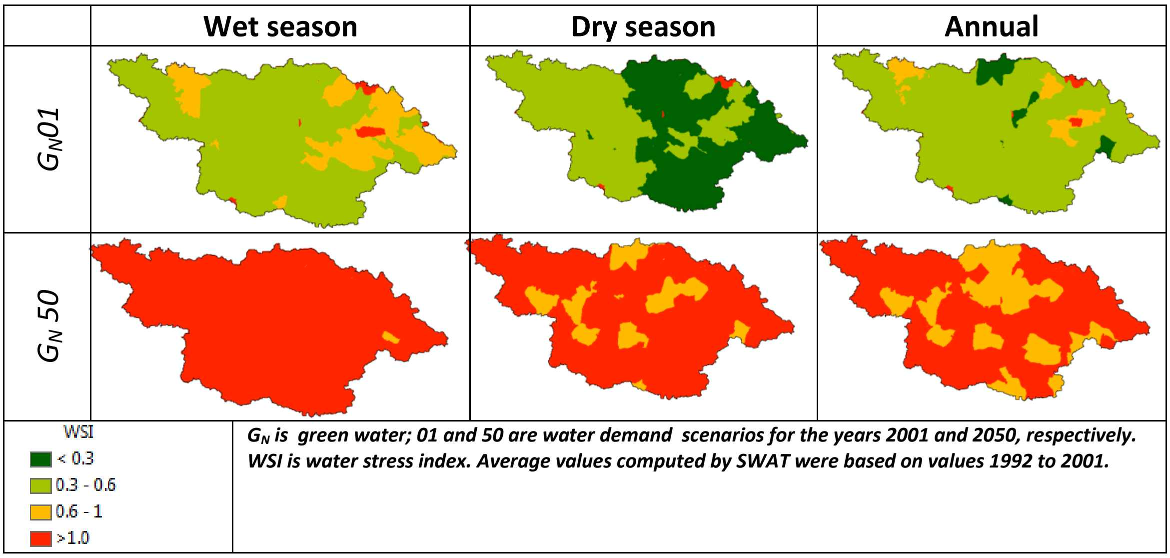


Figure 7-7 Water stress index (*WSI*) using land-use data of 2009.

Most of the sub-watersheds belong to the class with a *WSI* lower than 0.6 under the current rainfed agriculture during the wet season. Water is highly scarce (*WSI*>0.6) at the upstream part of the watershed during this season. However, green water is not scarce in this area during the dry season (*WSI*<0.3). This shows that the green water from the existing crop, pasture and wood lands can fulfill the basic water demand of the watershed in both wet and dry seasons. All the sub-watersheds will be under extremely water scarce conditions (*WSI* >1.0) in 2050 if the current rainfed land-use activities are continued with the existing low water productivity.

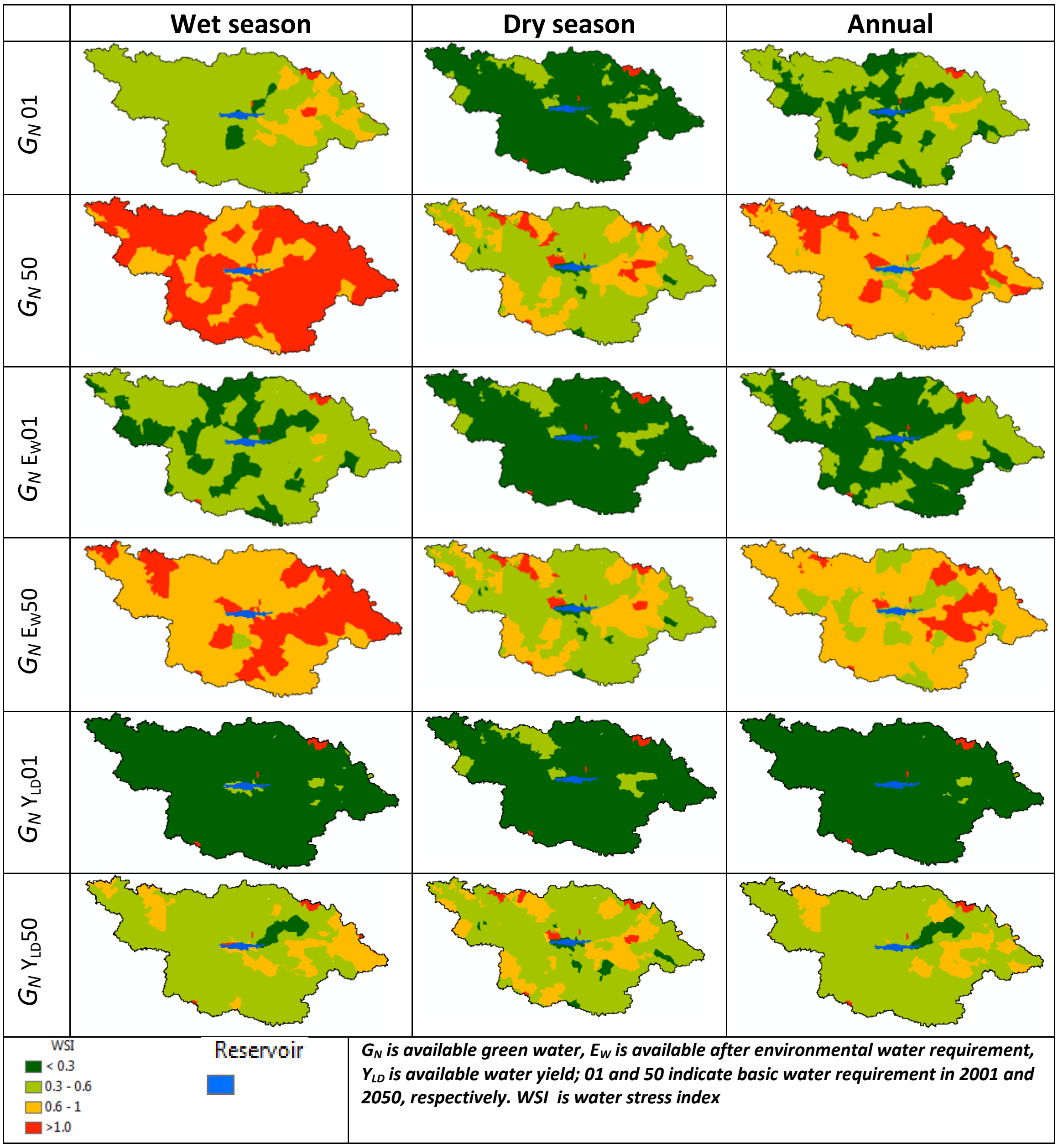


Figure 7-8 Water stress indices (*WSI*) based on planned irrigation project and watershed management interventions

The spatial distribution of water stress indices based on watershed management and the planned irrigation project interventions is shown in Figure 7-8. The water stress level is improved when blue water is withdrawn in addition to the green water to fulfill the basic water needs of the population. The addition of 20% of the *YLD* to the green water improved water availability and decreased the water stress index from moderately exploited (0.3<*WSI*<0.6) to slightly exploited (*WSI*<0.3) for some of the sub-watersheds. In this case, much of the available water (40% to 70%)

was still there for other water needs beyond the basic water requirements in 2001. However, most of the sub-watersheds will still be overexploited (*WSI*>1) in 2050 if only green water is used. The watershed will be environmentally water scarce in 2050 and the contribution of the watershed to downstream livelihoods will be limited.

## 7.6 Discussion

### 7.5.4 Impact of watershed management interventions on water balance

Slight differences in the watershed area and flow simulation results were simulated as compared to the results of the *GIP* feasibility study carried out by MoWR (2008). The total size of the sub-watersheds at the diversion and the dam were quantified as 1166 $km^2$ and 385 $km^2$ in the feasibility study, respectively, while the values were 1152 $km^2$ and 381 $km^2$ in this study. The annual water yield was 662 mm and 664 mm at the dam and diversion sites, respectively, in the feasibility study and 710 mm and 827 mm in this study. Potential evapotranspiration (*PET*) was 1391 mm for the *Gumara* irrigation command area in the feasibility study and 1316 mm in this study. These differences can be explained by the use of a different DEM, other meteorological data, and a different model discretization in this study. This shows that meteorological data refining (see section 5) plays a role in designing water resources. However, measurement and interpolation errors and their propagation to the final model results always exist. The amount of water evaporated from the water surface of the reservoir was about 1492 mm per annum. This was lower than the evaporation from the surface of Lake *Tana* that was estimated at about 1675 mm (SMEC 2008). A higher reservoir evaporation value (1818 mm/year) (MoWR 2008) was simulated in the *GIP* feasibility study as compared to the 1492 mm in this study. This *PET* difference were because the meteorological data from the *Bahir Dar* station were used in the *GIP* feasibility study, which is located in a relatively warm climate and far away from the watershed.

Water flow shift from one component of the water balance to another due to watershed management intervention and the *GIP* was observed. This shift was not only from water yield to *AET*, but also from deep groundwater recharge to *AET*. This may be due to the lower seepage occurring on the lined irrigation canals compared to the natural river and the revap flow due to the well maintained vegetation covers during the watershed management. Such vegetation together with afforestation of the steep slopes increases actual evapotranspiration and decreases groundwater recharge. Micro-basin water harvesting structures has shown good land-cover and increased biomass production by minimizing discharge in the north-east Ethiopia (Derib et al. 2009). Shrubland was considered the best choice for minimizing runoff and soil erosion in China as compared to alfalfa pastureland (Wei et al. 2007). The authors suggest grassland and woodland for runoff and soil erosion management rather than large-scale alfalfa plantations. Around the study area, legume trees, alfalfa, napier and vetiver grasses were proposed and used (Gebreslassie et al. 2009). However, careful selection of crops and trees has to be done with respect to environmental benefits and water productivity optimization.

### 7.5.5 Water availability and demand

Green water is the only available water for the existing rainfed agricultural system in the study area. Based on the experience of the author and field observations, the most productive green water was that of the wet season. The *AET* during the dry season was lost through unproductive evaporation, since the land is bare and there is almost no production of food and feed during this season. This is for two reasons. The first and most important reason is the small rainfall amount and duration and the resulting low soil moisture (green water), which was not enough to supply the required *AET* for food and feed production in the dry season. The second reason was that the farmers had no additional technology such as irrigation infrastructure and low-water-demanding crops in the dry season. However, the contribution of the existing small amount of available blue water from rivers, springs and wells for domestic uses and livestock drinking was not considered in the green water analysis.

Environmental water requirement was considered as the second option for calculating water availability. Using the 20% rule of presumptive standard for environmental flow protection (Richter et al. 2011), 20% of the *YLD* was added to the green water, and this sum was considered as available water. However, in practice this presumptive standard is difficult to implement in the existing Nile hydropolitics. The standard can minimize about 10.5 $km^3$ of the water from Nile flow at Aswan if it is implemented on the whole Ethiopian Blue Nile watershed. The sum of green water and *YLD* was the other option used to calculate available water for each sub-watershed.

Water availability and water stress status on seasonal scales resulted in practical implications of how water and watershed management strategies can be derived. Hoekstra and Mekonnen (2011) estimated blue water scarcity on monthly levels. However, the results in their study showed similar monthly values within a given season, so that seasonal scale can address most of the practical variability of the water resources availability and water scarcity status. A monthly level water stress analysis requires agricultural water demand data at a monthly level. This is only possible with a detailed study of crop water requirements. This was done neither by Hoekstra and Mekonnen (2011) nor in this study. However, seasonal analysis can provide equivalent information to that based on a monthly scale saving modeling time and resources. Nevertheless, a monthly scale analysis can address the impact of water stress in the dry spells during the growing season.

The contribution of *YLD* to the water stress status was smaller during the dry season as compared to the wet season in the watershed. This is due to the low *YLD* occurring in this season. However, shifting 6% of the rainfall from annual *YLD* to the productive evapotranspiration, *GIP* and associated watershed management interventions made another 2% evaporated annual rainfall productive in the dry season in the irrigation command area. It played a role in increasing water availability for the community without compromising the environmental flow. This indicates that water flow regulation structures are important to make water available so that the unproductive green water in the dry season can be shifted to productive transpiration using supplemental irrigation. Although the contribution of river *YLD* for available water was low during the dry season, water stress level was seen to be better than in the wet season. This is because the annual agricultural water need was assigned for the productive wet season so that less water was needed during the dry season. Green water was shown to be enough to satisfy the basic water need in 2001 based on the existing rainfed agricultural production conditions. However, observations and informal discussions during the field study showed that the productivity of this green water was not enough to sustain life due to rainfall variability and late entering and early onset of the rainfall in the growing season.

After satisfying the environmental requirements, the available green and blue water will not be sufficient to fulfill the basic water requirements of the area in 2050. The results of this study show that it is possible to satisfy the basic needs using all the environmental water in 2050. However, the watershed is situated in a position to sustain downstream life from the nearby Lake *Tana* to the Mediterranean Sea. Therefore, actions have to be taken at both local and basin levels. Some of the key issues to increase green water productivity are to mitigate the problems associated with intra-seasonal dry spells with supplemental irrigation, maximize infiltration, minimize unproductive evaporation, increase soil-water holding capacity, maximize root depth, and maximize the water-uptake of crops (Rockström et al. 2003). Selection of short-maturing dry season food/feed materials can make evaporation water beneficial for the livelihoods in the sub-watersheds.

### 7.5.6 Implications for the Nile Basin water

In addition to the physical water stress, Nile water is now in a more political tension than ever. The Ethiopian highland contributes about 86 % of the Nile flow at the Aswan High Dam while the country is using less than 5% of its total internal renewable water (FAO AQUASTAT 2005) and 3% of the Blue Nile runoff (Mason 2004). The largest user of this flow, Egypt, is dependent to 98% on the Nile water. However, it contributes almost nothing, which means that the livelihoods of the Egyptians are totally dependent on the blue water of the Nile that comes from the upstream countries. Egypt and Sudan agreed to use the Nile flow in 1929 and 1959, but the agreements are not binding for all the riparian countries in the Nile basin.

Ethiopia gains 936 $km^3$ annual rainfall and discharges 122 $km^3$ (14%) of this rainfall, where 90% of this flow is transboundary (FAO AQUASTAT database;

http://www.fao.org/nr/water/aquastat/countries_regions/ Cited 12/08/2013; see section 2). Per capita, 14,200 (5,300) $m^3$ and 1,800 (698) $m^3$ rain and river flow water, respectively, are calculated for 2001 (2050). The effective rainfall that accounts for a total 814 $km^3$ with 12,300 (4,600) $m^3$ per capita in 2001 (2050) is a very large amount as compared to Egypt's total water availability of 68.3 $km^3$ with 979 (504) $m^3$ per capita in 2001 (2050). However, as can be observed at the head water of the Blue Nile, about 53% of the annual rainfall is directed to river flow, and the green water is not enough to support the basic water needs in the future if the existing rainfed water productivity does not improve. This indicates that there are some sources and sinks of river flow in the Blue Nile. For example, the study concerning the Lake *Tana* basin (15,096 $km^2$) showed that about 30% of the rainfall is discharged through the outlet (Setegn et al. 2008). Another modeling study carried out by Engida (2010) in the same basin using 8 sub-watersheds (area varies from 103 $km^2$ to 15,120 $km^2$) showed variation of discharge contribution from 24% to 60% of the annual rainfall. Green and blue water management has to be designed based on these difference. The rainfed agricultural system is not productive enough to support future life due to the large discharge contribution, low green water productivity and high population density.

The integral understanding of the global and the regional water balancing on different time scales calls for another way of thinking to alleviate the consumptive water scarcity and the existing hydro-political stress. Even watershed management and blue water withdrawal can improve water availability in the area; it will not solve the water stress in the society and the environment in the future. As recommended by many studies (e.g., Waterbury and Whittington (1998); Whittington 2004; Mason (2004); Arsano (2007); Martens (2011)), basin-wide integration and efficient water use in the Nile Basin can benefit the local livelihoods and environment. Non-water-consumptive uses like hydropower production, fishery and tourism can benefit the local livelihoods while the environmental water is not negatively affected. An extensive Blue Nile water development project in Ethiopia, the "Grand Ethiopian Millennium Dam Project (GERDP)", started in April 2011 on the Blue Nile River. It is designed to generate 6000 MW electric power making 74 $km^3$ in a reservoir covering 1680 $km^2$

(EEPC, Ethiopian Electric Power Corporation 2013). The project is non-water consumptive, since it is designed only for power generation. As it is located in a sparsely populated (19 persons $km^{-2}$ (CSA 2011); (see Appendix 0; Figure 10-2)) and inaccessible river valley area, it will attract human life after completion so that the green water burden of the densely populated highland and cities will be alleviated to a certain extent. Fish production, navigation and tourism and business activities related to the stored water may be livelihood means for the community. There is also a chance to use the generated power to develop the groundwater of the Ethiopian lowlands outside the Nile basin for irrigation and drinking water infrastructure. Ethiopia has ample potentials and diversity of non-water consumptive alternatives without appreciably harming the water share of the downstream users.

The political will of the riparian countries to use diversified water development corridors in different parts of the Nile Basin has been a challenge for decades. An initiative, the 'Nile Basin Initiative', was formed in 1999 to smoothen the political tensions so that the riparian countries can be benefited from cooperative investments and equitable water sharing. The initiative has developed capacity, regional institutions, and networks based on a shared vision and equitable utilization of water resources. Promising advancement has been shown like signing of the Cooperative Framework Agreement (CFA) by six out of the ten riparian countries (Salman 2013; NBI http://www.nilebasin.org/newsite/).

### 7.5.7 Uncertainties regarding water availability and demand quantification

Reliability of calculations of water availability and water scarcity depends on the quality of the underlining data (Hoekstra and Mekonnen 2011; Brown and Heuvelink 2005). Generally, model uncertainty is lower in physically based models like SWAT as compared to empirical and conceptual models (Giertz et al. 2006). In this study, data quality of the SWAT outputs for water availability was improved by using smaller hydrological response units as compared to other studies of the area. Soil data were improved by using a recent detailed study in the watershed (MoWR 2008). More data from the climate stations were considered by using the best missing data filling methods among the selected approaches (see section 5). The recent 30-m resolution DEM from ASTER and fine soil and climatic data used made it possible to use a fine HRU delineation. The combined effect of the above data quality efforts results in acceptable error measures of river discharge modeling: 0.49 r-factor and 0.8 p-factor on a daily scale, and 65% (95%), $\pm$5 ($\pm$5) and 0.3 (0.06), on daily (monthly) levels for *NSE, PBIAS* and *RSR*, respectively (see section 6.5). Errors in climatic variables interpolation were discussed (see section 5). However, uncertainty sources from inverse water balance modeling still exist. Sharp changes in water balance components at the border of sub-watersheds are caused by the structure of the SWAT model. Improving SWAT structures to spatial interpolation of point climate data needs further research to improve water availability data quality with respect to the scale limit to rugged topographical features affecting the local climate. Furthermore, water scarcity information quality can be improved by decomposing water availability through different crops with high green-water productivity and livestock management activities, since about 98% of the basic water requirement is caused by agriculture. Partitioning and averaging each component of human basic water needs for the population of the smallest administrative units is the additional quality of this research to increase our understanding at the local level. However, the effect of dry spells on the rainfed agriculture within a growing season was not addressed but may receive increasing importance due to climate change.

## 7.7 Conclusions

The water availability status with and without the Ethiopian government plan for the *Gumara* watershed with an area of 1520 $km^2$ was modeled at the head water of the Blue Nile Basin. The hydrological model Soil and Water Assessment Tool (SWAT) was applied at a very fine discretization. Livestock is not only the direct source of human food but also a component of production and household assets. Therefore, the water requirement of livestock was systematically included in the per capita basic water requirement considering the local mixed crop-livestock agricultural production system. Finally, the water scarcity status was identified on spatial and seasonal scales for 2001 and 2050 population scenarios. The water availability was partitioned into three options to consider rainfed and irrigation productions as well as environmental water flows.

The watershed management interventions modified the hydrological balance, especially the ratio of surface runoff to subsurface and groundwater flows. This can increase the residence time of water in the watershed that favors the rainfed agricultural production. The planned reservoir was designed to retain the discharge from the highly contributing sub-watersheds. The dam and diversion structures were modeled to minimize the natural flow of the main stream within acceptable ranges that favor environmental flow. Both watershed management interventions and proposed irrigation project increased water availability in the watershed. The aggregated water availability per capita is 1125 $m^3$ per annum: 98% is for agriculture and 62% of this portion was used by livestock. High spatio-temporal variations of water scarcity were simulated in the watershed. The green water of the rainfed production supports the basic water requirement during the growing season using the existing land-use and 2001 basic water requirement scenarios. This result could not address the effect of dry spells of the growing season on the rainfed productivity that is increasingly challenging the livelihoods in the area. Additional exploitation of the river flow (blue water) improved the water stress status. However, the green water of the existing land-use and climatic conditions will not support the basic water requirements of the population in 2050 assuming the current population growth rate of the country for the area in 2001. In 2050, water flow will be highly exploited to affect the environment and the downstream uses.

The current land-use and rainfed production system will not withstand demographic pressure. In addition, more and more intensive use of the blue water will exploit the environmental flow in 2050 and affect the downstream life of this transboundary water. In addition to family planning, improving green water productivity by using supplemental irrigation and appropriate food and feed materials and management systems, basin-wide cooperation of water use like hydropower development, tourism and fish production can improve the local water stress shown in this study. As advised by many studies, these options may also improve the existing physical and political water stress at the Nile Basin level.

# 8 GENERAL SUMMARY AND PERSPECTIVES

Ethiopia suffers from economic and technological water scarcity that makes difficult to increase the productivity of available water. In depth understanding of the water balance and water availability at different scales and for different scenarios is important for future intervention to alleviate the scarcity. As part of this basin-wide and national concern, this study examines the water balance and water availability on farm and watershed scales at different scenarios. Therefore, the study was carried out to attain the following objectives: (1) to evaluate water use and water productivity of a small-scale irrigation scheme, (2) to evaluate methods for filling gaps in climatic data, (3) to adopt Soil and Water Assessment Tool (SWAT) hydrological model for modeling river discharge using different modeling setups, and (4) to simulate water demand and water stress status for a period up to 2050 using different land-use and demographic scenarios. The *Gumara* watershed (1520 km$^2$), a tributary of Lake *Tana* of the Blue Nile in Ethiopia, was selected for this study.

- **A case study on small-scale irrigation scheme to investigate water balance and water productivity.**

After mapping small-scale irrigation schemes in the Gumara watershed, in-depth field measurements (water flow through canals, water application on the field, and biomass of grain, crop residue and grass) and close observation (effect of water logging and water shortage) were taken on a 90 ha scheme during the irrigation season in 2009. Farmlands, canal network, drainage basins and wetlands were mapped using geographical information system (*GIS*), satellite images and field measurements. Before selection and distribution of sampling plots in the scheme, classification of irrigation system (as pumped and gravity), canals (as main, secondary and field) and land-use (as cropland, drainage basin, wetland and grasslands) were performed. High water loss was observed during water conveyance and water application while there was water shortage to irrigation farms at the downstream side of the scheme. The water loss and shortage varies along crop types, location of field in the scheme and cost related to pumping. Some irrigation farmlands were out of production due to water logging resulted from canal overflow especially during night irrigation. Therefore, water and land productivity was very low as compared to the results of other studies. The water application of the farmers did not match the water requirement of the crops. Night storage to solve problems associated with night irrigation, proper irrigation scheduling and empowering farmers to manage irrigation water are some of the recommendation to improve the diverted water productivity.

- **Compare and evaluate missing data filling methods to increase the number of climate station for hydrological modeling.**

Climatic variables, especially rainfall and temperature, are the forcing factors for hydrological flows. Climatic data are very important particularly for data demanding and most used Penman-Monteith evapotranspiration method in hydrological modeling. However, gaps in climatic data are one of the constraints to have detailed spatial water balance analysis in the Blue Nile basin. In this study, gaps climatic data (rainfall, temperature, relative humidity and solar radiation) in a given station was tried to fill using neighboring station data. This approach was used in SWAT water flow modeling to compare its effect on model performance with SWAT weather generation (*WXGEN*) routine. The *WXGEN* used only within a station relationship to fill missing data that is not practical for stations with long and continuous gap in climatic data. Four deterministic daily rainfall estimation methods were selected. The statistical performance of estimation showed comparable results with similar studies done elsewhere. Multiple regression models were developed to fill missing data of daily minimum and maximum temperature data. These models perform well for maximum temperature for most of the stations. However, the low performance was observed for minimum air temperature. Relative humidity and solar radiation data of stations were derived from minimum and maximum daily air temperature data. Some parameters were optimized based on seasonal categorization of the area that resulted in better results as compared to without seasonal categorization. It should be important to derive additional relationship of climatic variables with some topographical features like altitude. In this case, more stations data at a bigger spatial scale should be considered. As proposed by Oregon State University and Technical University of Delft with a project called Trans-African Hydro-Meteorological Observatory (*TAHMO*) to install weather stations every 30 km (available on http://tahmo.info/about-tahmo), elementary schools and health centers can be used to install more climate stations. The approach used in this study can be, then, used for the future to extrapolate the newly installed stations in the watershed using long-term data of the existing stations.

- **Assess the effect of different modeling setups on SWAT modeling performance.**

Data availability and the way to develop the model setup could have significant effect on the performance of a hydrological model. The study explores the effect of different model setups on river flow modeling. Number of climate stations used varied (two, three and six) according to their data availability and proximity to the watershed after filling missing data using different methods. Two stations (one in the watershed and the other outside) had frequently been used on academic and water resources planning studies for the watershed. Different meteorological stations with varying proximity to the study watershed were used to evaluate their relative performances on hydrological modeling. Selection of representative climate stations and their density affect the performance SWAT model adaptation. Four and six stations have given better efficiency of water flow modeling than frequently used *Bahir Dar* and *Debre Tabor* stations. The performance of stations density is explained not only increasing modeling efficiency of estimating river discharge at the outlet of the watershed from 60% to 70%, but also, each water balance component is differently distributed in the watershed. Penman-Monteith and Hargreaves methods of calculating potential evapotranspiration methods have given comparable modeling performances. The approach to update and use local climate data has given better hydrological modeling results. However, uncertainties from non-uniqueness of model parameter, measurement error in class-three stations and errors propagated from filling gaps in climate data are still there in the results. Further research should consider effect of interpolation of climatic data for each sub-watershed delineated.

The spatial interpolation can be based on the relation with relief and altitude especially for rainfall and temperature data.

- **Assess the effect of different scenarios on water balance and availability.**

Spatial and temporal water availability status can be used to derive development and policy interventions. In this part of the study, land-use scenarios were developed to evaluate water balance and water availability based on the results of the case study, missing data handling and calibration of SWAT. Both green and blue water availability options were considered to analyze the water stress status with respect to the basic water requirement of the area in 2001 and 2050. Watershed treatment options decreased surface runoff. This surface runoff was shifted to lateral flow, groundwater flow and evapotranspiration increasing by 8%, 10% and 0.2%, respectively. Watershed treatment and planned *Gumara* Irrigation Project (*GIP*) decreased surface runoff, lateral flow and groundwater flow by 19%, 33% and 4%, respectively. Spatial basic water requirement was quantified using literature values and the population distribution. The aggregated basic water requirement per capita is 1125 $m^3$ per annum of which 98% is for agriculture. High variation of water scarcity was observed on spatial and temporal distributions. Evapotranspired water from the existing rein fed production is enough for the demand in 2001 while it will not support the basic water requirement of the population in 2050. In 2050, water flow will be highly exploited to affect the environment and the downstream uses. However, the existing low water productivity wheat crop is used for this analysis. Increasing water productivity, non-consumptive water uses development and green water management options may improve the blue water stress on the Nile Basin level. Further modeling research that address climatic change and different crop production is crucial.

# 9 REFERENCES


Abbaspour, KC, CA Johnson, and MT van Genuchten (2004) Estimating Uncertain Flow and Transport Parameters Using a Sequential Uncertainty Fitting Procedure. Vadose Zone J 3:1340-1352.

Abbaspour, KM (2011) SWAT-CUP4: SWAT Calibration and Uncertainty Programs - A User Manual. Swiss Federal Institute of Aquatic Science and Technology, (eawag).

Akkuzu, E, HB Unal and BS Karatafi (2007) Determination of water conveyance loss in the menemen open canal irrigation network. Turk J Agric 31:11-22

Alamirew, D (2006) Modelling of Hydrology and Soil Erosion of Upper Awash River Basin. PhD Dissertation, University of Bonn.

Alemayehu, T, M McCartney and S Kebede (2009) Simulation of water resource development and environmental flows in the Lake Tana Sub basin. In: Awulachew, SB, T Erkossa, V Smakhtin and A Fernando (Comps.) (2009) Improved water and land management in the Ethiopian highlands: its impact on downstream stakeholders dependent on the Blue Nile. Intermediate Results Dissemination Workshop held at the International Livestock Research Institute (ILRI), Addis Ababa, Ethiopia, 5-6 February 2009. Colombo, Sri Lanka.

Allen, RG (1986) A Penman for all seasons. J Irrig Drain E-ASCE 112(4): 348-368.

Allen, RG, LS Pereira, D Reas and M Smith (1998) *Crop evapotranspiration: guidelines for computing crop water requirements*, FAO irrigation and drainage paper 56. FAO- Food and Agriculture Organization of the United Nations, Rome.

Allen, RG, ME Jensen, JL Wright, and RD Burman (1989) Operational estimates of evapotranspiration. Agron J 81:650-662.

Allen, RJ and AT DeGaetano (2001) Estimating missing daily temperature extremes using an optimized regression approach. Int J Climatol 21:1305-1319.

Amede, T, S Tarawali and D Peden (2011) Improving water productivity in crop-livestock systems of drought-prone regions: Editorial comment. Exp Agr 47 (S1):1–5.

Andersen, J, J Refsgaard and K Jansen (2001) Distributed hydrological modeling of the Senegal River basin-model construction and validation. J Hydrol 247: 200-214.

Anderson, MP and WW Woessner (1992) Applied ground water modeling. Academic Press, Inc., San Diego.

Arnold, JG, R Srinivason, RR Muttiah and JR Williams (1998) Large Area Hydrologic Modeling and Assessment Part I: Model Development. J Am Wat Res 34(1): 73-89.

Arsano Y (2007) Ethiopia and the Nile Dilemmas of National and Regional Hydropolitics. PhD Dissertation. Swiss Federal Institute of Technology

Asres, MT and SB Awulachew (2010) SWAT based runoff and sediment yield modelling: A case study of the *Gumera* watershed in the Blue Nile basin. Ecohydrology and Hydrology 10(2-4):191-200.

Awulachew, SB, AD Yilma, M Loulseged,W Loiskandl, M Ayana, and T Alamirew (2007) Water Resources and Irrigation Development in Ethiopia. Colombo, Sri Lanka: International Water Management Institute. 78p. (Working Paper 123)

REFERENCES


Awulachew, SB, DJ Merrey, AB Kamara, B Van Koopen, De Vries, F Penning and E Boelle (2005) Experiences and opportunities for promoting small-scale/micro irrigation and rainwater harvesting for food security in Ethiopia. International Water Management Institute. (Working Paper 98)

Awulachew, SB, M McCartney and TS Steenhuis (2008) A review of hydrology, sediment and water resource use in the Blue Nile Basin. Colombo, Sri Lanka: International Water Management Institute. (Working Paper 131)

Ayoade, J. O. (1983). Introduction to Climatology for the Tropics. John Wiley and Sons, New York.

Bakry, MF and AM Awad (1997) Practical estimation of seepage losses along earthen canals in Egypt. Water Resour Manag 11: 197–206.

BCEOM (Egis Bceom International) (1998) Abbay river basin integrated development master plan. Ministry of Water Resources, Addis Ababa, Ethiopia.

Bekele S and K Tilahun (2007) Regulated deficit irrigation scheduling of onion in a semiarid region of Ethiopia. Agr water manage 89:148 – 1 52

Beven, K and J Freer (2001). Equifinality, data assimilation, and uncertainty estimation in mechanistic modelling of complex environmental systems using the GLUE methodology. J Hydrol 249(1-4): 11-29.

Beven, RL (1985) Distributed hydrological models, In: MG Anderson and TP Burt (Eds) Hydrological Forcasting, Wiley, Chichester, UK. 405-435.

Block, PJ, K Strzepek and B Rajagopalan (2007) Integrated Management of the Blue Nile Basin in Ethiopia: Hydropower and Irrigation Modeling. International food policy research institute, 2033 K Street, NW, Washington DC, USA. http://www.ifpri.org/sites/default/files/publications/ifpridp00700.pdf accessed on 23/5/2011 Cited 27 Jun 2010.

Bormann, H and B Diekkrueger (2003) Possibilities and limitations of regional hydrological models applied within an environmental change study in Benin (west Africa), Phys Chem Earth 28(33-36):1323-1332.

Bormann, H and B Diekkrueger (2004) A conceptual hydrological model for Benin (West Africa): validation, uncertainty assessment and assessment of applicability for environmental change analyses, Phys Chem Earth 29(11-12):759-768.

Bormann, H, B Diekkrüger and O. Richter (1999) Effects of spatial data resolution on the calculation of regional water balances. In: B Diekkrüger, MJ Kirkby and U Schröder (ed.) Regionalization in Hydrology: HAHS-AISH P 254:193-202.

Brown, J D and G B M Heuvelink (2005) Assessing uncertainty propagation through physically based models of soil water flow and solute transport, in: Encyclopedia of Hydrological Sciences, Andersen, M (ed.), John Wiley & Sons, Ltd.

CA (Comprehensive Assessment of Water Management in Agriculture) (2007) Water for Food, Water for Life: A Comprehensive Assessment of Water Management in Agriculture. London: Earthscan, and Colombo: International Water Management Institute.

Chaplot, V, A Saleh and DB Jaynes (2005) Effect of the accuracy of spatial rainfall information on the modeling of water, sediment, and $NO_3$–N loads at the watershed level. J Hydrol 312(1-4):223-234.

Chaubey, I, AS Cotter, TA Costello and TS Soerens (2005) Effect of DEM data resolution on SWAT output uncertainty. Hydrol Process 19:621–628.

Cho, J, D Bosch, R Lowrance, T Strickland and G Vellidis (2009) Effect of spatial distribution of rainfall on temporal and spatial uncertainty of SWAT output. ASABE 52(5):1545-1555.

Chow, VT, DR Maidment, and LW Mays (1988) Applied Hydrology. McGraw-Hill, New York.

Clemmens, AJ, MG Bos, and JA Replogle (1984) Portable RBC flumes for furrows and earthen channels. ASABE 27:1016–1021.

CSA (Central Statistics Authority) (2003) Ethiopian agricultural sample enumeration, 2001/2002 results for Amhara region, statistical reports on area and production of crops, part II B. Addis Ababa, Ethiopia.

CSA (Central Statistics Authority) (2011) Population Size by Sex, Area and Density by Region, Zone and Wereda, Addis Ababa, Ethiopia.

De Silva, RP, NDK Dayawansa and MD Ratnasiri (2007) A comparison of methods used in estimating missing rainfall data. J Agr Sci *3*(2):101-108.

Deneke, TT (2011) Institutional implications of governance of local common pool resources on livestock water productivity in Ethiopia. Exp Agr 47(S1): 99-111.

Derib, SD (2005) Rainfall-runoff processes at a hill-slope watershed: case of simple models evaluation at Kori-Sheleko Catchments of Wollo, Ethiopia. M.Sc. Dissertation, Wageningen University.

Derib, SD, T Assefa, B Berhanu and G Zeleke (2009) Impacts of micro-basin water harvesting structures in improving vegetative cover in degraded hillslope areas of north-east Ethiopia. Rangeland J 31(2):259-265.

Descheemaeker, K, T Amede and A Haileslassie (2009) Livestock and water interactions in mixed crop-livestock farming systems of sub-Saharan Africa: Interventions for improved productivity. Colombo, Sri Lanka: International Water Management Institute. (Working Paper 133).

Diao, X and AN Pratt (2007) Growth Options and Poverty Reduction in Ethiopia – an economy-wide model analysis. Food Policy 32:205 -228.

Dingman, SL (1994) Physical hydrology. Prentice-Hall, Inc., Englewood Cliffs, NJ.

Dooge, JCI (1968) The hydrologic cycle as a closed system. International Association of Scientific Hydrology. Bulletin 13 (1):58-68.

Duguma, B, A Tegegne and BP Hegde (2012) The effect of location and season on free water intake of livestock under field condition in *Ginchi* watershed area, Ethiopia. World J Agr Sci 8 (1): 38-42.

Easton, ZM, DR Fuka, ED White, AS Collick, BB Ashagre, M McCartney, SB Awulachew, AA Ahmed and TS Steenhuis1 (2010) A multi basin SWAT model analysis of runoff and sedimentation in the Blue Nile, Ethiopia. Hydrol Earth Syst Sci 14:1827-1841.

EEPC (Ethiopian Electric Power Corporation) (2013) Grand Ethiopian Renaissance Project progress report http://www.hidasse.gov.et/c/document_library/get_file?p_l_id=11731&folderId=11740&name=DLFE-202.pdf Cited 23 Jun 2013.

Eguavoen, I, SD Derib, TT Deneke, M McCartney, BA Otto and SS Billa (2012) Digging, damming or diverting? Small-scale irrigation in the Blue Nile basin, Ethiopia. Water Alternatives 5(3): 678-699.

Eijkelkamp. Operating Instructions 13.17.02 RBC Flume. Hog Flume Software. http://www.eijkelkamp.com/Portals/2/Eijkelkamp/Files/Manuals/M2-131702e%20RBC-Flume.pdf Cited 22 Dec 2008.

Eischeid, JK, CB Baker, T Karl and HF Diaz (1995) The quality control of long-term climatological data using objective data analysis. Journal Appl Meteor 34:2787-2795.

Engida, A (2010) Hydrological and suspended sediment modeling in the Lake Tana Basin, Ethiopia. PhD Dissertation, Université de Grenoble.

EPLAUA (Environmental Protection, Land Administration and Use Authority) (2006) Ecological significances, threats and management options of Lake Tana-associated wetlands. Bahir Dar, Ethiopia.

Erkossa, T, AS Bekele, A Haileslassie, YA Denekew (2009) Impacts of improving water management of smallholder agriculture in the Upper Blue Nile Basin. In: AS Bekele, T Erkossa and SVF Ashra (Comps.). Improved water and land management in the Ethiopian highlands: its impact on downstream stakeholders dependent on the Blue Nile. Intermediate Results Dissemination Workshop held at the International Livestock Research Institute, Addis Ababa, Ethiopia.

EWNHS (Ethiopian Wildlife and Natural History Society) (1996) Important bird areas of Ethiopia, First inventory. Addis Ababa. www.worldlakes.org/lakedetails.asp?lakeid=8568 Cited 17 Feb 2008.

Falkenmark (1989) The massive water scarcity threatening Africa-why isn't it being addressed. Ambio 18(2): 112-118.

FAO (1978) Effective rainfall in irrigated agriculture. FAO Irrigation and Drainage Paper 25, Rome, Italy.

FAO (1986) Irrigation Water Management. Training manual No. 3 Food and Agriculture Organization of the United Nations, Via delle Terme di Caracalla, Rome, Italy.

FAO (2003) Food energy - methods of analysis and conversion factors. FAO Food and nutrition paper 77. Food and Agriculture Organization of the United Nations, Rome, Italy. http://www.fao.org/docrep/006/Y5022E/y5022e04.htm Cited 20 Feb 2013.

FAO (2004) Food and nutrition technical report series; human energy requirements, report of a joint FAO/WHO/UNU expert consultation: 17-24 October 2001. FAO, Rome.

FAO (2009) CROPWAT 8.0 for Windows. Rome, Italy. http://www.fao.org/nr/water/infores_databases_cropwat.html Cited 8 Feb 2009.

FAO (2013) Country Fact Sheet: Ethiopia. Aquastat, http://www.fao.org/nr/water/aquastat/data/factsheets/aquastat_fact_sheet_eth_en.pdf Cited 22 Feb 2013.

FAO (Food and Agriculture Organization) (1993) Agro-ecological land resources assessment for agricultural development planning-a case study of Kenya resources data base and land productivity. Technical Annex 5, Rome, Italy. ftp://ftp.fao.org/agl/aglw/fwm/Manual3.pdf Cited 23 Feb 2013.

FAO AQUASTAT (2005) Irrigation in Africa in figures: Ethiopia – AQUASTAT Survey 2005 http://www.fao.org/nr/water/aquastat/countries_regions/ETH/CP_ETH.pdf Cited 18 Jul 2013.

Faulkner, JW, T Steenhuis, NV de Giesen, M Andreini and JR Liebe (2008) Water use and productivity of two small reservoir irrigation schemes in Ghana's upper east region. Irrig drain 57: 151–163

Federal Negaritgazeta (2005) Federal Democratic Republic of Ethiopia rural land administration and land-use proclamation. Addis Ababa. P. 3134-3144.

FEWS NET (2008) ETHIOPIA Food Security Update. Famine Early Warning Systems Network and World Food Programme, FEWS NET Washington, DC. http://reliefweb.int/sites/reliefweb.int/files/resources/47D0640C5B43A3C08525740900651DEF-Full_Report.pdf Cited 24 Sep 2013.

Gassman, PW, MR Reyes, CH Green and JG Arnold (2007) The soil and water assessment tool: historical development, applications, and future research directions. ASABE 50(4):1211-1250.

Gebreselassie, Y, T Amdemariam, M Haile and C Yamoah (2009) Lessons from upstream soil conservation measures to mitigate soil erosion and its impact on upstream and downstream users of the Nile River. Upstream-Downstream Project in the Blue Nile Intermediate Results Dissemination Workshop held on 5-6 February 2009, International Water Management Institute (IWMI), Nile Basin and East Africa Office, Addis Ababa.

Giertz, S, B Diekkrueger, and G Steup (2006) Physically-based modeling of hydrological processes in a tropical headwater catchment (West Africa) - process representation and multi-criteria validation. Hydrol Earth Syst Sc 10:829–847.

Gleick, PH (1996) Basic water requirements for human activities: Meeting basic needs. Water Int 21: 83-92.

Grey, D and C Sadoff (2006) Water for growth and development. A theme document of the 4th World Water Forum. Mexico City, Mexico. 56 pp.

Gupta, HV, S Sorooshian, and PO Yapo (1999) Status of automatic calibration for hydrologic models: Comparison with multilevel expert calibration. J Hydrol Eng 4(2):135-143.

Haileslassie, A, D Peden, S Gebreselassie, T Amede and K Descheemaeker ($2009_b$) Livestock water productivity in mixed crop–livestock farming systems of the Blue Nile basin: Assessing variability and prospects for improvement. Agr Syst 102: 33-40.

Haileslassie, A, D Peden, S Gebreselassie, T Amede, A Wagnew and A Taddesse ($2009_a$) Livestock water productivity in the Blue Nile Basin: assessment of farm scale heterogeneity. Range J 31:213–222.

Hargreaves, GH and ZA Samani (1982) Estimating potential evapotranspiration, J Irrig Drain E-ASCE 108(3):25-230.

Hargreaves, GH and ZA Samani (1985) Reference crop evapotranspiration from temperature. App Eng Agric 1:96-99.

Hoekstra, AY and MM Mekonnen (2011) Global water scarcity: monthly blue water footprint compared to blue water availability for the world's major river basins, Value of Water Research Report Series No. 53, UNESCO-IHE, Delft, The Netherlands.

Hoekstra, AY and PQ Hung, PQ (2002) Virtual water trade: Quantification of virtual water flows between nations in relation to international crop trade. National Institute for Public Health and Environment. Research report No. 11. IHE Delft, the Netherlands.

Hoekstra, AY, AK Chapagain, MM Aldaya, and MM Mekonnen (2009) Water Footprint Manual. Enschede: The Water Footprint Network.

Hooghoudt, SB (1940) Bijdrage tot de kennis van enige natuurkundige grootheden van de grond. Versl. Landbouwkd Onderz 46: 515-707.

Hulme, M, R Doherty, T Ngara and M New (2005) Global warming and African climate change: a reassessment. Cambridge University Press, Cambridge, 338 pp.

IPMS (Improving productivity and market success) (2005) Fogera Woreda Pilot Learning Site Diagnosis and Program Design http://www.ipms-ethiopia.org/content/files/Documents/PLS-DPD/Fogera.pdf accessed on 2/12/2010. Cited 16 Feb 2007.

Jefferies, D, I Muñoz, J Hodges, VJ King, M Aldaya, AE Ercin, LM Canals and AY Hoekstra (2012) Water Footprint and Life Cycle Assessment as approaches to assess potential impacts of products on water consumption. Key learning points from pilot studies on tea and margarine. J Clean Prod 33: 155-166.

Jensen, ME, RD Burman and RG Allen (eds) (1990) Evapotranspiration and irrigation water requirements. ASCE Manuals and Reports on Engineering Practice No. 70, ASCE, N.Y. 332 pp.

Johnston, R and M McCartney (2010) Inventory of water storage types in the Blue Nile and Volta river basins. Colombo, Sri Lanka: International Water Management Institute. 48p. (IWMI Working Paper 140).

Kebede S, Y Travi, T Alemayehu, V Marc (2006) Water balance of Lake Tana and its sensitivity to fluctuations in rainfall, Blue Nile Basin, Ethiopia. J Hydrol 316(1–4): 233–247.

Kim, TW, and H Ahn (2009) Spatial rainfall model using a pattern classifier for estimating missing daily rainfall data. Stoch Env Res Risk A 23:367–376.

King, J and MP McCartney (2007) Dams, ecosystems and livelihoods. Int J Ser Prog Wat Res 5(3): 167-168.

Kloezen, WH and C Garcés-Restrepo (1998) Assessing irrigation performance with comparative indicators: The case of the Alto Rio Lerma Irrigation District, Mexico. International Water Management Institute. (Research Report 22), Colombo, Sri Lanka

Kotsaiantis, S, A Kostoulas, S Lykoudis, A Argiriou and K Menagias (2006) Filling temperature values in weather data banks. In: 2nd IEE International Conference on Intelligent Environments, 5-6 July, 2006, Athens, Greece. PP:327-334.

Krause, P, DP Boyle and F Base (2005) Comparison of different efficiency criteria for hydrological model assessment. Adv Geosci 5:89–97

LakeNet (2004) Lake Tana Symposium. Bahir Dar University, Ethiopia. http://www.worldlakes.org/uploads/Lake_Tana_Symposium24Sep04_drb.pdf Cited 24 Feb 2007.

Lam, N.S., (1983). Spatial interpolation methods: a review. Am Cartographer 10(2): 129-139.

Lambiso, R (2005) Assessment of design practices and performance of small-scale irrigation structures in South Region, M.Sc. Dissertation, Arbaminch University.

Lane, LJ (1983) Transmission Losses (Chapter 4). p.19-1–19-21. *In:* Soil Conservation Service. National engineering handbook, section 4: hydrology. U.S. Government Printing Office, Washington, D.C.

Latron, J, M Soler, P Llorens and F Gallart (2008) Spatial and temporal variability of the hydrological response in a small Mediterranean research catchment. Hydrol Proces 22:775-787

Legesse, D, CV Coulomb and F Gasse (2003) Hydrological response of a chatchment to climate and land use change in Tropical Africa: case study South Central Ethiopia. Int J Hydrol 275:67-85.

Levine, G (1982) Relative water supply: An explanatory variable for irrigation systems. Technical Report 6. Ithaca, New York: Cornell University

Li, J and AD Heap (2008) A review of spatial interpolation methods for environmental scientists. Geoscience Australia, Record 2008/23, 137 pp.

Liersch, S (2003a) The program dew.exe and dew02.exe user's manual. http://www.brc.tamus.edu/swat/manual_dew.pdf Cited 23 Apr 2010.

Liersch, S (2003b) The program pcpSTAT user's manual. http://www.brc.tamus.edu/swat/manual_pcpSTAT.pdf Cited 23 Apr 2010.

Liu, BM, AS Collick, G Zeleke, E Adgo, ZM Easton and TS Steenhuis (2008) Rainfall-discharge relationships for a monsoonal climate in the Ethiopian highlands. Hydrol Process 22(7):1059–1067.

Marquardt, DW (1970) Generalized inverses, ridge regression and biased linear estimation. Technometrics 12:591–612.

Martens, AK (2011) Impacts of Global Change on the Nile Basin Options for Hydropolitical Reform in Egypt and Ethiopia, IFPRI Discussion Paper 01052, International Food Policy Research Institute (IFPRI).

Mason, S A (2004) From Conflict to Cooperation in the Nile Basin: Interaction Between Water Availability, Water Management in Egypt and Sudan, and International Relations in the Eastern Nile Basin, Conflict Sensitive Interviewing and Dialogue Workshop Methodology. PhD Dissertation, Swiss Federal Institute of Technology.

Matzarakis, A (1995). Human-biometeorological assessment of the climate of Greece. PhD Dissertation, University of Thessaloniki.

McCartney, M, T Alemayehu, A Shiferaw SB Awulachew (2010) Evaluation of current and future water resources development in the Lake Tana Basin, Ethiopia. Colombo, Sri Lanka: International Water Management Institute (IWMI) Research Report 134).

McCartney, MP, Y Ibrahim, Y Seleshi and SB Awulachew (2009) Application of the Water Evaluation and Planning Model (WEAP) to simulate current and future water demand in the Blue Nile. In: Improved water and land management in the Ethiopian highlands: Its impact on downstream stakeholders dependent on the Blue Nile. Intermediate Results Dissemination Workshop 5-6 February, 2009, Awulachew, SB, Ergossa, T; Smakhtin, V; Fernando, A (eds.) Addis Ababa, Ethiopia: IWMI, pp. 78-88.

MCE (Metaferia Consulting Engineers) (2001) Assessment of experiences and opportunities on medium and large scale irrigation in Ethiopia. Addis Ababa, Ethiopia.

MEDaC (Ministry of Economic Development and Co-operation) (1999) Survey of the Ethiopian Economy: Review of Post-Reform Developments, 1992/93-1997/98, Addis Ababa, Ethiopia.

Miles, J and M Shevlin (2001) Applying Regression & Correlation. SAGE Publications, London.

MoFED (Ministry of Finance and Economic Development) (2006) A plan for accelerated and sustained development to end poverty (PASDEP), (2005/06-2009/10), volume I. Addis Ababa, Ethiopia.

Molden, D, K Frenken, R Barker, C de Fraiture, B Mati, M Svendsen, C Sadoff and CM Finlayson (2007) Trends in water and agricultural development. In: Water for food, Water for life: A Comprehensive Assessment of Water Management in Agriculture. Molden, D (Ed) Earthscan/IWMI, 2007, p.11

Molden, DJ and Gates, TK (1990) Performance measures for evaluation of irrigation water delivery systems. J Irrig Drain Engin 116 (6): 804–823.

Molden, DJ, R Sakthivadivel, CJ Perry, C de Fraiture, and WH Kloezen (1998) Indicators for comparing performance of irrigated agricultural systems. International Water Management Institute. (Research Report 20), Colombo, Sri Lanka

Monteith, JL (1965) Evaporation and the environment. In: The state and movement of water in living organisms, XIXth Symposium. Soc Exp Biol 205-234. Swansea, Cambridge University Press.

Moriasi, DN, JG Arnold, MW Van Liew, RL Bingner, RD Harmel and TL Veith (2007) Model evaluation guidelines for systematic quantification of accuracy in watershed simulations. Transactions of the ASABE 50(3): 885−900.

Morid, S, AK Gosain and AK Keshari (2002) Solar radiation estimation using temperature-based, stochastic and artificial neural networks approaches. Nord Hydrol 33(4): 291-304.

MoWR (Ministry of Water Resources) (1998) Abbay River Basin Integrated Development Mater Plan Project: Phase 2, vol. VI, Water Resources Development, Part 2, Large Irrigation and Hydropower Dams. Report, MOWR, Addis Ababa, Ethiopia.

MoWR (Ministry of Water Resources) (1999) Water Resource Management Policy (WRMP), Addis Ababa: Ethiopia. Ministry of Water Resources. 2002. Water Sector Development Program (WSDP), Addis Ababa, Ethiopia.

MoWR (Ministry of Water Resources) (2002) Water Sector Development Program (WSDP), Addis Ababa, Ethiopia.

MoWR (Ministry of Water Resources) (2007) Lake Tana Sub-basin Four Dam Projects: Ribb dam project. Ministry of Water Resources of Ethiopia. Addis Ababa.

MoWR (Ministry of Water Resources) (2008) Gumara Irrigation Project Feasibility Study Report. Ministry of Water Resources, Addis Ababa, Ethiopia.

NAS (1996) Lost Crops of Africa: Volume I: Grains. National Academy Press, National Academy of Sciences, Washington, USA. ISBN: 0-309-58615-1, 408 pages.

Nash, JE and JV Sutcliffe (1970) River flow forecasting through conceptual models, Part I. A discussion of principles J Hydrol 10:282–290.

NBI (Nile Basin Initiative) (2001) Nile Basin Initiative Shared vision program 2001: report on Nile River Basin: transboundary environmental analysis. United Nations Development Programme World Bank and Global Environment Facility

Neitsch, SL, JG Arnold, JR Kiniry, JR Williams, and KW King (2002) Soil and Water Assessment Tool User's Manual, Version 2000. Temple, Tex.: USDA-ARS Grassland. Soil and Water Research Laboratory.

Neitsch, SL, JG Arnold, JRKiniry and JR Williams (2011) Soil and Water Assessment Tool theoretical documentation version 2009. Texas Water Resources Institute, Techinical Report No. 409. Texas A&M University.

Neter, J, W Wasserman and M Kutner (1996) Applied linear statistical models. Chicago, London: Irwin, 4th edition.

Nicks, AD (1974) Stochastic generation of the occurrence, pattern, and location of maximum amount of daily rainfall. *In:* Proc. Symp. Statistical Hydrology, 154-171, Aug-Sept 1971. Tucson, AZ. U.S. Dept. of Agriculture. Misc. Publ. No. 1275. US Gov. Print Office, Washington, DC.

Peden, D, G Tadesse and AK Misra (2007) Water and livestock for human development. *In*: 'Water for Food, Water for Life: A Comprehensive Assessment of Water Management in Agriculture'. (Ed. D. Molden.) 485–514. International Water Management Institute: Colombo.

Perry, CJ (1996) The IIMI water balance framework: A model for project level analysis.. International Irrigation Management Institute (IIMI). (Research Report 5), Colombo, Sri Lanka

Phillips, DL, J Dolph and D Marks (1992) A comparison of geostatistical procedures for spatial analysis of precipitations in mountainous terrain. Agric Forest Meteor 58:119-141.

Population Reference Bureau (2010) World Population data sheet http://www.prb.org/Publications/Datasheets/2010/2010wpds.aspx Cited Aug 2013.

Presti, RL, B Emanuele and P Giuseppe (2010) A methodology for treating missing data applied to daily rainfall data in the Candelaro River Basin (Italy). Environ Monit Assess 160:1-22

Ramesh, SV and V Chandramouli (2005) Improved weighting methods, deterministic and stochastic data-driven models for estimation of missing precipitation records. J Hydrol 312:191–206

Raskin, P, P Gleick, P Kirshen, G Pontius, and K Strzepek (1997) Water futures: Assessment of long-range patterns and prospects. Stockholm, Sweden: Stockholm Environment Institute.

Richter, BD, MM Davis, C Apse and C Konrad (2011) A presumptive standard for environmental flow protection. River Res Applic 28:1312–1321.

Rockström, J, J Barron and P Fox (2003) Water productivity in rain-fed agriculture: Challenges and opportunities for smallholder farmers in drought-prone tropical agroecosystems. CAB International. IN: Water Productivity in Agriculture: Limits and Opportunities for Improvement. (eds) JW Kijne, R Barker and D Molden http://www.iwmi.cgiar.org/publications/CABI_Publications/CA_CABI_Series/Water_Productivity/Unprotected/0851996698ch9.pdf 4/21/2013 Cited 13 Sep 2013.

Rost, S, D Gerten, H Hoff, W Lucht, M Falkenmark and J Rockström (2009) Global potential to increase crop production through water management in rainfed agriculture. Environ Res Lett 4 044002 (9pp)

Salini and Mid-day (2006) Environmental impact assessment for Beles multipurpose project. Addis Ababa, Ethiopia: Ethiopian Electric and Power Corporation.

Salman, MAS (2013) The Nile Basin Cooperative Framework Agreement: a peacefully unfolding African spring? Water Int 38(1):17-29

Sangrey, DA, KOH Williams, and JA Klaiber (1984) Predicting ground-water response to precipitation. ASCE J Geotech Eng 110(7): 957-975.

Santhi, C, JG Arnold, JR Williams, WA Dugas, R Srinivasan and LM Hauck (2001) Validation of the SWAT model on a large river basin with point and nonpoint sources. J Am Water Resour Assoc 37:1169–1188.

Schuol, J, KC Abbaspour, H Yang, R Srinivasan, and AJB Zehnder (2008) Modeling blue and green water availability in Africa. Water Resour Res 44(W07406):1-18.

SCS (Soil Conservation Service Engineering Division) (1986) Urban hydrology for small watersheds. U.S. Department of Agriculture, Technical Release 55.

SCS (Soil Conservation Service) (1972) National Engineering Handbook Section 4, Hydrology. USDA-SCS, Washington, DC, USA.

Setegn, SG, R Srinivasan and B Dargahi (2008) Hydrological modelling in the Lake Tana Basin, Ethiopia using SWAT model. Open Hydrology J 2: 49-62.

Setegn, SG, R Srinivasan, AM Melesse, and B Dargahi ($2009_a$) SWAT model application and prediction uncertainty analysis in the Lake Tana Basin, Ethiopia. Hydrol Process 24(3): 357-367.

Setegn, SG, R Srinivasan, B Dargahi and AM Melesse ($2009_b$) Spatial delineation of soil erosion vulnerability in the Lake Tana Basin, Ethiopia. Hydrol Proces 23:3738-3750.

Sharplay, AN and JR Williams (Eds) (1990) EPIC-Erosion Productivity Impact Calculator, 1. Model documentation. U.S. Department of Agricultural Research Service, Tech. Bull. 1768.

Sing, VP (1994) Elementary hydrology. Prentice Hall of India: New Delhi.

Singh, J, HV Knapp and M Demissie (2004) Hydrologic modeling of the Iroquois River watershed using HSPF and SWAT. ISWS CR 2004-08. Champaign, Ill.: Illinois State Water Survey. Available at: http://www.isws.illinois.edu/pubdoc/CR/ISWSCR2004-08.pdf Cited 8 Sep 2012.

Skogerboe, GV, RS Bennett and WR Walker (1973) Selection and installation of cutthroat flumes for measuring irrigation and drainage water. Colorado State University Experimental Station, Fort Collins Technical Bulletin 120.

Sloan, PG and ID Moore (1984) Modeling subsurface stormflow on steeply sloping forested watersheds. Water Resour Res 20(12): 1815-1822.

Smakhtin, V, C Revanga, and P Doll (2005) Taking into account environmental water requirements in global-scale water resources assessments. IWMI The Global Podium. http://podium.iwmi.org/podium/Doc_Summary.asp Cited 23 Jun 2010.

SMEC (Snowy Mountains Engineering Corporation) (2008) Hydrological Study of the Tana-Beles sub-basins, main report. Addis Ababa, Ethiopia: Ministry of Water Resources.

Smedema, LK and DW Rycroft (1983) Land drainage-planning and design of agricultural drainage systems, Cornell University Press, Ithica, N.Y.

SPSS Inc. (2007) SPSS for Windows, Version 16.0. (Statistical Package for the Social Sciences Released 2007) Chicago, SPSS Inc.

Tabios, GQ and JD Salas (1985) A comparative analysis of techniques for spatial interpolation of precipitation. Water Resour Bull 21(3):365-380.

Tang, WY, AHM Kassim and SH Abubakar (1996) Comparative studies of various missing data treatment methods-Malaysian experience. Atmos Res 42:247-262.

Teegavarapu, RSV and V Chandramouli (2005) Improved weighting methods, deterministic and stochastic data-driven models for estimation of missing precipitation records. J Hydrol 312:191–206.

Tessema, SM (2006) Assessment of Temporal Hydrological Variations due to Land use Changes using Remote Sensing/GIS: A Case Study of Lake Tana Basin. http://www.lwr.kth.se/Publikationer/PDF_Files/LWR_EX_06_21.PDF Cited 3 Feb 2008.

Thornthwaite, CW (1948) An approach toward a rational classification of climate. Geogr Rev 38:55-94.

Tulu M, E Boelee, and G Taddesse (2009) Estimation of livestock, domestic use and crop water productivity of SG-2000 water harvesting pilot project in Ethiopia In: Proceedings of the CGIAR challenge program on water and food 2nd international forum, Addis Ababa, Ethiopia, November 10-14, 2008. Colombo.

Turner, B (1994) Small-scale irrigation in developing countries. Land Use Policy 11(4): 251–261.

UN Water (2006) Water: A shared responsibility. World Water Development Report 2. Case study: Ethiopia. www.unesco.org/water/wwap accessed on 21/2/2011 Cited 19 Mar 2011.

Unal, HB, S Asik, M Avci, S Yasar and E Akkuzu (2004) Performance of water delivery system at tertiary canal level: a case study of the Menemen Left Bank Irrigation System, Gediz Basin, Turkey. Agr Water Manage 65: 155–171.

USBR (United States Bureau of Reclamation) (1964) Land and Water Resources of the Blue Nile Basin. Main Report, United States Department of Interior Bureau of Reclamation, Washington, D.C.

Vincent, L (1994) Lost chances and new futures: interventions and institutions in small-scale irrigation. Land Use Policy 11(4): 309–322.

Vincent, L (2003) Towards a smallholder hydrology for equitable and sustainable water management. Nat Resour Forum 27: 108–116.

von Grebmer, K, H Fritschel, B Nestorova, T Olofinbiyi, RP Lorch and Y Yohannes. (2008) Global Hunger Index: The Challenge of hunger. Bonn: Welthungerhilfe; Washington: IFPRI; Dublin: Concern Worldwide, 40p.

Wale, AT, HM Rientjes, ASM Gieske, and HA Getachew (2009) Ungauged catchment contributions to Lake Tana's water Balance. Hydrol Process 23:3682-3693.

Walker, DJ and T Wandschneider (2005) Local Food Aid Procurement in Ethiopia: A case study report for EC-PREP (UK Department for International Development), Natural Resources Institute, University of Greenwich, Chatham Maritime , Kent ME4 4TB , UK.

Wallace, JS and PJ Gregory (2002) Water resources and their use in food production systems. Aquat Sci 64: 363–375.

Wang, X and AM Melesse (2006) Influences of potential evapotranspiration estimation methods on swat's hydrologic simulation in a northwestern Minnesota watershed. ASABE 49(6):1755-1771.

WAPCOS (Water and Power Consultancy Service) (1990) Preliminary water resources development master plan for Ethiopia, vol. VII, Annex J: Hydropower, Ethiopia Valleys Development Studies Authority Report, WAPCOS, India.

Waterbury, J and D Whittington (1998) Playing chicken on the Nile? The implications of microdam development in the Ethiopian highlands and Egypt's New Valley Project. Nat Resour Forum 22(3):166-163.

WCD (World Commission on Dams) (2000) Dams and Development: a new framework for decision-making. The report of the World Commission on Dams. London, UK: Earthscan Publications, Thanet Press.

Wei, W, L Chen, B Fu, Z Huang, D Wu and L Gui (2007) The effect of land uses and rainfall regimes on runoff and soil erosion in the semi-arid loess hilly area, China. J Hydrol 335: 247-258.

Weisberg, S (2005). Applied Linear Regression, 3rd ed. John Wiley and Sons, Hoboken, New Jersey.

White, ED, ZM Easton, DR Fuka, AS Collick, E Adgo, M McCartney, SB Awulachew, Y Selassie and TS Steenhuis (2011) Development and application of a physically based landscape water balance in the SWAT model. Hydrol Process 25(6):915-925.

Whittington, W (2004) Visions of Nile basin development. Water policy 6:1-24.

WHO-UNICEF (2010). Joint program for water supply and sanitation: Ethiopia 2008 estimates http://www.wssinfo.org/datamining/tables.html Cited 14 Jan 2012.

Williams, JR (1995) The EPIC model. In: Computer Models of Watershed Hydrology, 909-1000. V P Singh (ed.) Highlands Ranch, Colo.: Water Resources Publications.

Woldemariam, M (1972) An introductory geography of Ethiopia. Berhanena Selam, H.S.I. Press, Addis Ababa.

World Bank (2006) Ethiopia: Managing water resources to maximize sustainable growth: World Bank Agriculture and Rural Development Department, Washington, DC, USA.

World Bank (2008) Project appraisal document on a proposed credit in the amount of SDR 27.4 million (US$45 million equivalent) to the Federal Republic of Ethiopia for a Tana & Beles integrated water resources development project. Washington DC, USA.

World fact sheet (2001) https://www.cia.gov/library/publications/the-world-factbook/index.html Cited 15 June 2013.

WWDSE (Water Works Design and Supervision Enterprise) (2007) Catchment Development Plan, Gumara Irrigation Project. Ministry of water resources, Addis Ababa.

Yang, J, P Reichert, KC Abbaspour, J Xia and H Yang (2008) Comparing uncertainty analysis techniques for a SWAT application to the Chaohe basin in China. J Hydrol 358(1-2):1-23.

Yilma, AD and SB Awulachew (2009) Characterization and Atlas of the Blue Nile Basin and its Sub basins. In: Awulachew, SB; Erkossa, T; Smakhtin, V; Fernando, A (ed.) Improved water and land management in the Ethiopian highlands: its impact on downstream stakeholders dependent on the Blue Nile. Intermediate Results Dissemination Workshop held at the International Livestock Research Institute (ILRI), Addis Ababa, Ethiopia, 5-6 February 2009. Summary report, abstracts of papers with proceedings on CD-ROM. Colombo, Sri Lanka: International Water Management Institute (IWMI).

Zinn, KE, MT Zinn, M Ozdemir and JF Harper (2010) Temperature stress and plant sexual reproduction: uncovering the weakest links. J Exp Bot 61(7):1959–1968.

# 10 APPENDICES

## 10.1 Appendix 1 Initial runoff curve numbers (CN2) for cultivated and non-cultivated agricultural lands (SCS 1986)

Table 10-1 Runoff curve numbers for cultivated agricultural lands[1]

| ------------Cover description---------------------- | | | Curve numbers for hydrologic soil group | | | |
|---|---|---|---|---|---|---|
| Cover type | Treatment [2] | Hydrologic condition[3] | A | B | C | D |
| Fallow | Bare soil | — | 77 | 86 | 91 | 94 |
| | Crop residue cover (CR) | Poor | 76 | 85 | 90 | 93 |
| | | Good | 74 | 83 | 88 | 90 |
| Row crops | Straight row (SR) | Poor | 72 | 81 | 88 | 91 |
| | | Good | 67 | 78 | 85 | 89 |
| | SR + CR | Poor | 71 | 80 | 87 | 90 |
| | | Good | 64 | 75 | 82 | 85 |
| | Contoured (C) | Poor | 70 | 79 | 84 | 88 |
| | | Good | 65 | 75 | 82 | 86 |
| | C + CR | Poor | 69 | 78 | 83 | 87 |
| | | Good | 64 | 74 | 81 | 85 |
| | Contoured & terraced (C&T) | Poor | 66 | 74 | 80 | 82 |
| | | Good | 62 | 71 | 78 | 81 |
| | C&T+ CR | Poor | 65 | 73 | 79 | 81 |
| | | Good | 61 | 70 | 77 | 80 |
| Small grain | SR | Poor | 65 | 76 | 84 | 88 |
| | | Good | 63 | 75 | 83 | 87 |
| | SR + CR | Poor | 64 | 75 | 83 | 86 |
| | | Good | 60 | 72 | 80 | 84 |
| | C | Poor | 63 | 74 | 82 | 85 |
| | | Good | 61 | 73 | 81 | 84 |
| | C + CR | Poor | 62 | 73 | 81 | 84 |
| | | Good | 60 | 72 | 80 | 83 |
| | C&T | Poor | 61 | 72 | 79 | 82 |
| | | Good | 59 | 70 | 78 | 81 |
| | C&T+ CR | Poor | 60 | 71 | 78 | 81 |
| | | Good | 58 | 69 | 77 | 80 |
| Close-seeded or broadcast legumes or rotation meadow | SR | Poor | 66 | 77 | 85 | 89 |
| | | Good | 58 | 72 | 81 | 85 |
| | C | Poor | 64 | 75 | 83 | 85 |
| | | Good | 55 | 69 | 78 | 83 |
| | C&T | Poor | 63 | 73 | 80 | 83 |
| | | Good | 51 | 67 | 76 | 80 |

[1] Average runoff condition, and $I_a$=0.2S

[2] Crop residue cover applies only if residue is on at least 5% of the surface throughout the year.

[3] Hydraulic condition is based on combination factors that affect infiltration and runoff, including (a) density and canopy of vegetative areas, (b) amount of year-round cover, (c) amount of grass or close-seeded legumes, (d) percent of residue cover on the land surface (good ≥ 20%), and (e) degree of surface roughness.

Poor: Factors impair infiltration and tend to increase runoff.

Good: Factors encourage average and better than average infiltration and tend to decrease runoff.

Table 10-2 Runoff curve numbers for other agricultural lands[1]

| ------------- Cover description------------ | | Curve numbers for hydrologic soil group | | | |
|---|---|---|---|---|---|
| **Cover type** | **Hydrologic condition** | **A** | **B** | **C** | **D** |
| Pasture, grassland, or range—continuous forage for grazing[2] | Poor | 68 | 79 | 86 | 89 |
| | Fair | 49 | 69 | 79 | 84 |
| | Good | 39 | 61 | 74 | 80 |
| Meadow:-continuous grass, protected from grazing and generally mowed for hay. | — | 30 | 58 | 71 | 78 |
| Brush:-brush-weed-grass mixture with brush the major element[3] | Poor | 48 | 67 | 77 | 83 |
| | Fair | 35 | 56 | 70 | 77 |
| | Good | 30[4] | 48 | 65 | 73 |
| Woods:-grass combination (orchard or tree farm)[5] | Poor | 57 | 73 | 82 | 86 |
| | Fair | 43 | 65 | 76 | 82 |
| | Good | 32 | 58 | 72 | 79 |
| Woods[6] | Poor | 45 | 66 | 77 | 83 |
| | Fair | 36 | 60 | 73 | 79 |
| | Good | 30[4] | 55 | 70 | 77 |
| Farmsteads:-buildings, lanes, driveways, and surrounding lots. | — | 59 | 74 | 82 | 86 |

1 Average runoff condition, and $I_a = 0.2S$.
2 *Poor:* <50%) ground cover or heavily grazed with no mulch.
*Fair:* 50 to 75% ground cover and not heavily grazed.
*Good:* > 75% ground cover and lightly or only occasionally grazed.
3 *Poor*: <50% ground cover.
*Fair:* 50 to 75% ground cover.
*Good:* >75% ground cover.
4 Actual curve number is less than 30; use CN = 30 for runoff computations.
5 CN's shown were computed for areas with 50% woods and 50% grass (pasture) cover. Other combinations of conditions may be computed from the CN's for woods and pasture.
6 *Poor:* Forest litter, small trees, and brush are destroyed by heavy grazing or regular burning.
*Fair:* Woods are grazed but not burned, and some forest litter covers the soil.
*Good:* Woods are protected from grazing, and litter and brush adequately cover the soil.

*Initial CN2 values for land-cover change and surface treatment scenarios model calibration were selected from this table (section 6.4.2). The hydrologic conditions of the cultivated agricultural and pasture lands were observed "poor". However, the hydrologic conditions of bushlands (brush) and forestlands (woods) were fair.*

## 10.2 Appendix 2. Watershed, irrigation and demographic maps.

Figure 10-1 Gumara watershed with planned irrigation infrastructures (dam, canal network and command area).

***Sources: Base map has downloaded from www.arcgis.com free database and the irrigation plan was taken from MoWR (2008).***

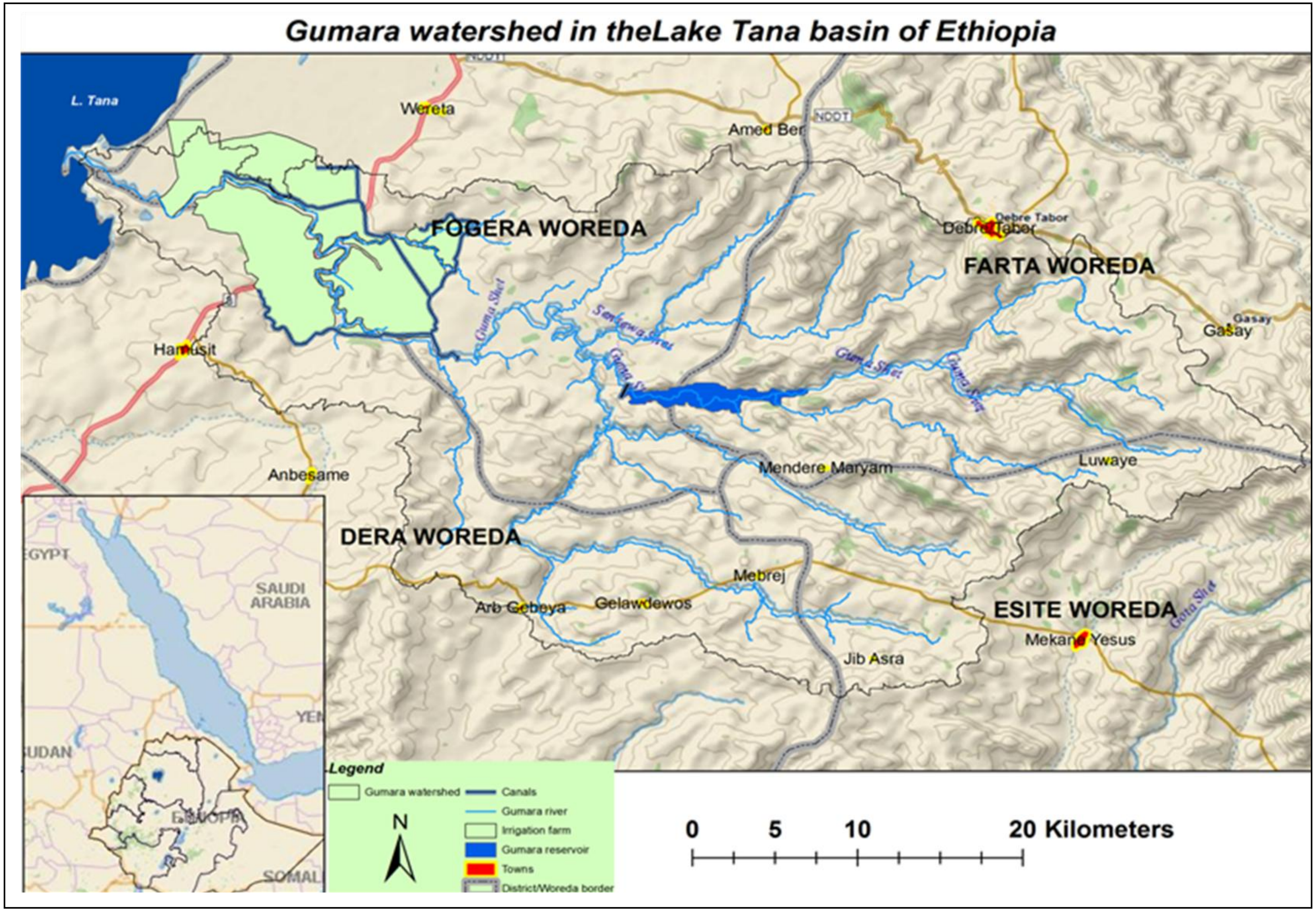
Gumara watershed in theLake Tana basin of Ethiopia
L. Tana
Wereta
Amed Ber
FOGERA WOREDA
Debre Tabor
FARTA WOREDA
Gasay
Hamusit
Anbesame
Mendere Maryam
Luwaye
DERA WOREDA
Mebrej
Arb Gebeya
Gelawdewos
ESITE WOREDA
Mekane Yesus
Jib Asra
EGYPT
SAUDI ARABIA
SUDAN
ETHIOPIA
Legend
Gumara watershed
Canals
Gumara river
Irrigation farm
Gumara reservoir
Towns
District/Woreda border
N
0 5 10 20 Kilometers

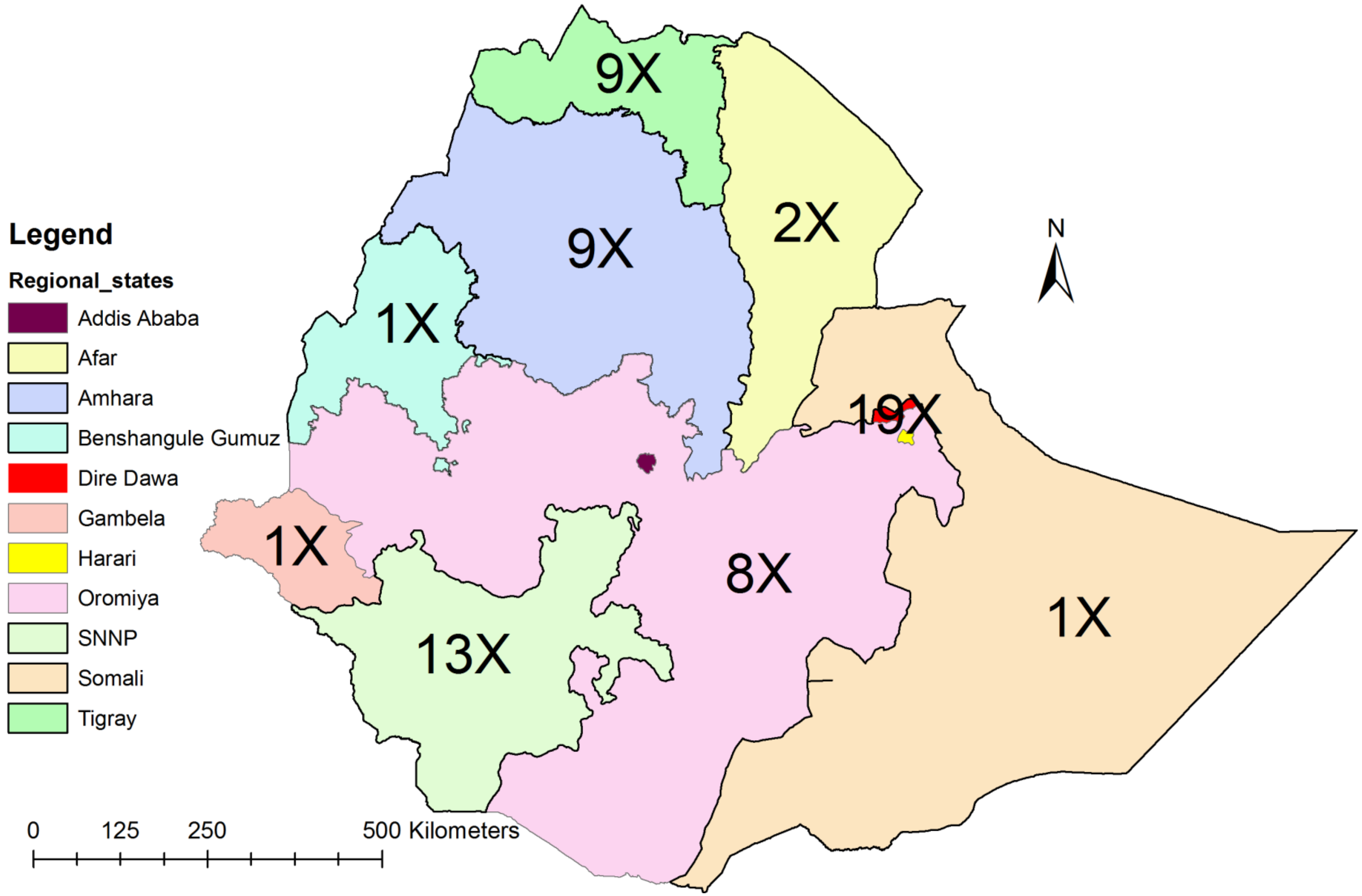


Figure 10-2 National regional states and city administrations maps of Ethiopia and their relative population density (per km$^2$)

***Addis Ababa and Dire Dawa are city administrations while the rest are regional states. The figures with a multiple of "X" indicate the relative population densities where the value of "X" is 15 persons per km$^2$. (Sources: Data from Ministry of Water Resources of Ethiopia and CSA (2011)***

## ACKNOWLEDGEMENT

**“ስለማይነገር ስጦታው  እግዚአብሔር ይመስገን።”**

**2ኛ ቆሮ.9፥15**

Glory to the Almighty!!!

I am sincerely grateful to Prof. Dr. Bernd Diekkrüger, University of Bonn, Germany, for his supervision. Without his scientific and unreserved assistance, it would have been very difficult to get this dissertation to the final stage. I am also very thankful to Prof. Dr. Paul Vlek and Dr. Bernhard Tischbein for their comments, encouragement and for giving me their precious time to shape my work at the starting stage of my study. Friendly coordination and support by Dr. Manfred Denich, Dr. Günther Manske, Ms. Rosemarie Zabel, Ms. Maike Retat-Amin, Ms. Sabine Aengenendt-Baer, and Ms. Doris Fuß (Center for Development Research, ZEF, Bonn University) were the most encouraging and feel-at-home ingredients of working at ZEF. I would like to thank Mss. Margaret Jend for language editing and fine tuning the first drafts of this dissertation. I thank the German Federal Ministry for Economic Development Cooperation (Bundesministerium für Wirtschaftliche Zusammenarbeit-BMZ) for the financial support, the International Water Management Institute (IWMI) and Amhara Region Agricultural Research Institute (ARARI) for providing me with materials and facilitating my field work. I would also like to acknowledge the National Meteorological Agency and Ministry of Water Resources of Ethiopia for providing secondary data. The Basic Educational Campaign Program of the Mengistu Haile-Mariam military regime is of special importance on my way to science. Without this program, it would have been completely impossible for me to start my education at all.

I would like to extend my sincere appreciation to Dr. Seleshi Awulachew, Dr. Tilahun Amede, Dr. Amare Hailesilassie, Dr. Girma Tadesse, Dr. Katrien Descheemaeker, Dr. Enyew Adgo, Dr. Yihenew Gebreselassie, Dr. Biru Yitaferu, Fisseha Werede, Asmare Wubet, Abebe Getu, Mesenbet Yibeltal, Mesfin Yibre, Kefelegn Nigussie, Ahmed Amedin, Hirut Yirgu, Besufekad Tadesse, Solomon Ewnetu, Habtamu Tensae, Aklilu Yirgu, and Ato Teferi, and to all others who facilitated field data collection and shared their experience.

Thank you all my friends Dr. Aymar Bossa, Dr. Lulseged Temam, Dr. Seid Nuru, Dr. Joe Hill, Dr. Sewmehon Demissie, Dr. Tilaye Teklewold, Dr. Dessie Salilew, Dr. Tigist Abebe, Dr. Adane Girma, Dr. Tilahun Derib, Dr. Asfaw Kebede, Adefirs Worku, Philipp Baumgartner, Jeroen Spauwen, Patrik, Tigist Araya, and all Ethiopian mates in Germany and The Netherlands. You made my life pleasant especially by your discussions about our countries and the world, which have given me extra-curricular knowledge for my life. Encouragement and paternal treatment by Dr. Moges Mekonnen and his family from Frankfurt played an indirect and important role in my study. Dr. Moges, Ambelye and Birhane, I remember your contribution at the start of my education under the big oak tree in my birth village.

Words can’t explain the respect and love I have for my lovely wife, Hiwot Yirgu Astemir for her treatment, comments and encouragement. My two lovely baby girls, Meklit and Etsubdink, thanks for coming - it is time for us to play together.

My mother, Zewdie Gashu Kinde, deserves all I have. Her paternal care both as a dad and as a mom alone in a rural and harsh poverty life in Ethiopia created my personality and education on a firm foundation. Mami, your long term-stock for me is now lucrative. Mam, live safe and long!